A COMPARISON OF THREE TECHNIQUES FOR THE DETERMINATION OF DEFORMATION PROPERTIES OF ROCK

by

NORMAN IAN NORRISH

B.A.Sc., University of British Columbia, 1971

A THESIS SUBMITTED IN PARTIAL FULFILMENT OF

THE REQUIREMENTS FOR THE DEGREE OF

MASTER OF APPLIED SCIENCE

in the Department

of

Mineral Engineering

We accept this thesis as conforming to the

required standard

THE UNIVERSITY OF BRITISH COLUMBIA

April, 1974

In presenting this thesis in partial fulfilment of the requirements for an advanced degree at the University of British Columbia, I agree that the Library shall make it freely available for reference and study. I further agree that permission for extensive copying of this thesis for scholarly purposes may be granted by the Head of my Department or by his representatives. It is understood that copying or publication of this thesis for financial gain shall not be allowed without my written permission.

Department of Mineral Engineering

The University of British Columbia
Vancouver 8, Canada

Date April 19, 1974.

ABSTRACT

Laboratory and *in situ* testing programmes to determine the deformation behaviour of three rock types have provided an opportunity for a comparison of three testing techniques.

To aid future standardization, procedures and equipment for the laboratory testing, Goodman Jack testing and plate loading tests are presented in detail.

Laboratory tests and plate loading tests show that the gneiss and schist rock types are well differentiated on the basis of deformation modulus. The ratio of average modulus for gneiss to schist is 2.0 from the laboratory testing and 5.6 for the plate loading tests. The Goodman Jack modulus values are similar for all rock types, the ratio of gneiss to schist being 1.3. Similarly the laboratory and plate loading tests show a wide range of values while the jack tests exhibit a very narrow range. The modulus results for the schist conform to the anticipated scale effect while the gneiss tests do not. It is concluded that the partial correlation between the three testing techniques reflects the need to quantify important factors such as rock quality and *in situ* stresses and to incorporate these factors into valid interpretive formulae.

Anisotropy investigations for the laboratory and plate loading tests are consistent. The schist is approximately twice as rigid loaded parallel to the foliation than when loaded perpendicular to it. Anisotropy investigations with the Goodman Jack are qualitative only

without very detailed geologic information at the test locations.

Permanent deformations of the rock are consistent for the three testing methods and reflect the volume of rock influenced as well as the rock quality at the test location.

ACKNOWLEDGEMENTS

For providing equipment and facilities, the author would like to thank the Mineral Engineering Department of the University of British Columbia. Thanks are especially due Mr. J.B. Evans, Department Head, and Dr. I. Weir-Jones, programme supervisor.

The author also thanks the professional engineering group that contributed data and reviewed the draft thesis.

TABLE OF CONTENTS

Chapter | Page

Chapter Page

LIST OF TABLES

LIST OF FIGURES

Figure | Page

Figure Page

CHAPTER I

INTRODUCTION

A knowledge of deformation properties is required for engineering projects founded upon or excavated within rock. The deformation properties are used either to predict rock movement under prototype loading or to develop finite element models for the project site.

For most engineering materials Young's Modulus, also known as the modulus of elasticity, is used as the characteristic deformation property. This modulus is applicable to materials which are homogeneous, isotropic and elastic. Unfortunately, rock with its geologic defects such as fractures and joints is very seldom homogeneous, isotropic or elastic. Thus, the modulus of deformation has been defined to include both the elastic deformation of the rock substance and the deformation due to rock defects. [Kruse, 1]

The deformation modulus, due to its inclusive definition, suffers an intrinsic problem in its determination, namely the scale effect. That is, tests which influence a smaller volume of rock tend to have larger modulus values. The reason being that small scale tests do not influence a representative sample of the more deformable rock defects. [Stagg and Zienkiewicz, 2] Deformation modulus values can vary by greater than 100% depending on the testing method. [Bukovansky, 3]

This thesis examines the problem of variation in modulus results due to testing method. This is accomplished by critically examining the results of three testing methods:

1. Laboratory tests carried out on samples of rock core,
2. Goodman Jack tests,
3. Plate loading tests.

The methods are compared on the basis of how they reflect the deformation behavior of distinct rock types. Conclusions are then reached on the relative merits of each method.

The equipment, procedures and theoretical formulation for each testing method are presented in detail. The reason for this is that testing methods in the field of rock mechanics have not been highly standardized. Thus any factors that can affect test results should at least be specified.

CHAPTER II

BACKGROUND TO TESTING PROGRAMMES

The *in situ* testing programmes in this report were carried out at the site of a proposed underground civil engineering project. Due to the considerable size of this project and because of the variations in load concentration, several testing programmes were carried out to determine the *in situ* rock behavior. The Goodman Jack programme, in which the writer participated, was carried out to determine deformation characteristics at a large, and therefore statistically representative, number of test locations. On the other hand, the plate loading tests were performed at fewer sites but the volume of rock tested it supposedly more representative of *in situ* rock behavior. The plate loading tests were carried out by an engineering firm.

The laboratory tests are the least representative of *in situ* rock behaviour due to the fact that rock defects are lost in the sampling process. In spite of this inherent disadvantage, laboratory tests are performed for a number of reasons. Firstly, the testing is convenient to perform. Secondly, control of test variables is more easily attained. The third reason, the most important from the viewpoint of this report, is that laboratory results establish an upper limit for the modulus results from the *in situ* testing. [Stagg and Zienkiewicz, 2]

CHAPTER III

DESCRIPTION OF TEST SITE

A. Introduction

As previously mentioned the *in situ* testing programmes were carried out at the site of a proposed underground complex. The principal excavation is to be several hundred feet in length. In addition several smaller chambers and tunnels are to be excavated.

The *in situ* tests were carried out in an exploratory drift at the project site. This drift had a length just over 2100 feet and its normal cross-section was 7 feet by 8 feet. Three larger chambers provided sites for portions of the testing programmes.

B. Geology of the Test Site

The rock sequence in the project area consists of regionally folded metamorphosed sediments dipping at 10 to 35 degrees. The principal rock types are medium to coarse crystalline quartz feldspar schists, quartzites,quartzite gneisses with some mica schists and minor marble beds. The principal rock types occur as interbedded units varying from 15 to 150 feet in thickness. In addition to the above four rock types, lenses and veins of pegmatite and quartz are common in the layered sequence and are generally comformable to the layering.

An examination of hand size rock specimens indicated the percentage mineral constituents as follows:

Quartzite Gneiss	Quartz Feldspar Schist	Pegmatite
quartz, 55 - 65%	quartz, 20-30%	quartz, 80-90%
feldspar, 20-25%	feldspar, 10-20%	muscovite, 10-20%
biotite, 5-10%	biotite, 30-40%	garnet, minor
garnet, minor to 5%	muscovite, 10-20%	
chlorite, very minor		

The quartzite gneiss samples were composed of uniform, medium sized mineral grains. In most samples preferential orientation of grains was not present, however, a small number of samples did contain faintly oriented micaceous minerals. Many gneiss samples contained chloritized bands and very few contained healed fracture planes. The pegmatite samples contained coarsely crystalline quartz and mica and displayed no visible structural features or fabric orientation. The foliation spacing in the schist measured 1/16 to 1/8 inch. The schist samples showed some deviation in mineral content but were selected in order that a representative sample of foliation angles could be tested.

For this thesis rock types identified in the field as quartzite and quartzite gneiss have been grouped together. It is recognized that this grouping is not strictly valid in the geologic sense as quartzite gneiss implies a foliated structure whereas quartzite

does not. Since in the rock core available, the only clue to foliated structure was the orientation of fine grained biotite, the presence of foliation was difficult to determine. To avoid a rather arbitrary division the single inclusive term quartzite gneiss was selected.

CHAPTER IV

REVIEW OF TESTING PROGRAMMES

A. Laboratory Testing Programme

1. Sample Preparation

The laboratory testing programme utilized samples of BX core. This core was obtained from holes drilled from the exploratory drift in conjunction with a separate testing programme. From the large footage of core available, samples were prepared that exhibited uniformity of each rock type. The core samples were divided into three basic rock types; quartzite gneiss, pegmatite and quartz feldspar schist.

The BX core was cut with a diamond saw to yield samples having a length to diameter ratio of 2:1. The sample ends were then ground parallel and flat using a "Blohm Simplex" surface grinder shown in Figure 1. This machine is capable of producing a surface which is flat to within 50 μ inches, well within the required end flatness standard. Parallelism of ends was assured by grinding both ends of a group of fourteen samples then regrinding the first end. After preparation the samples were dried at room temperature for at least two weeks. Samples were then measured three times for length and three times for diameter and weighed to the nearest 0.1 gram.

Figure 1

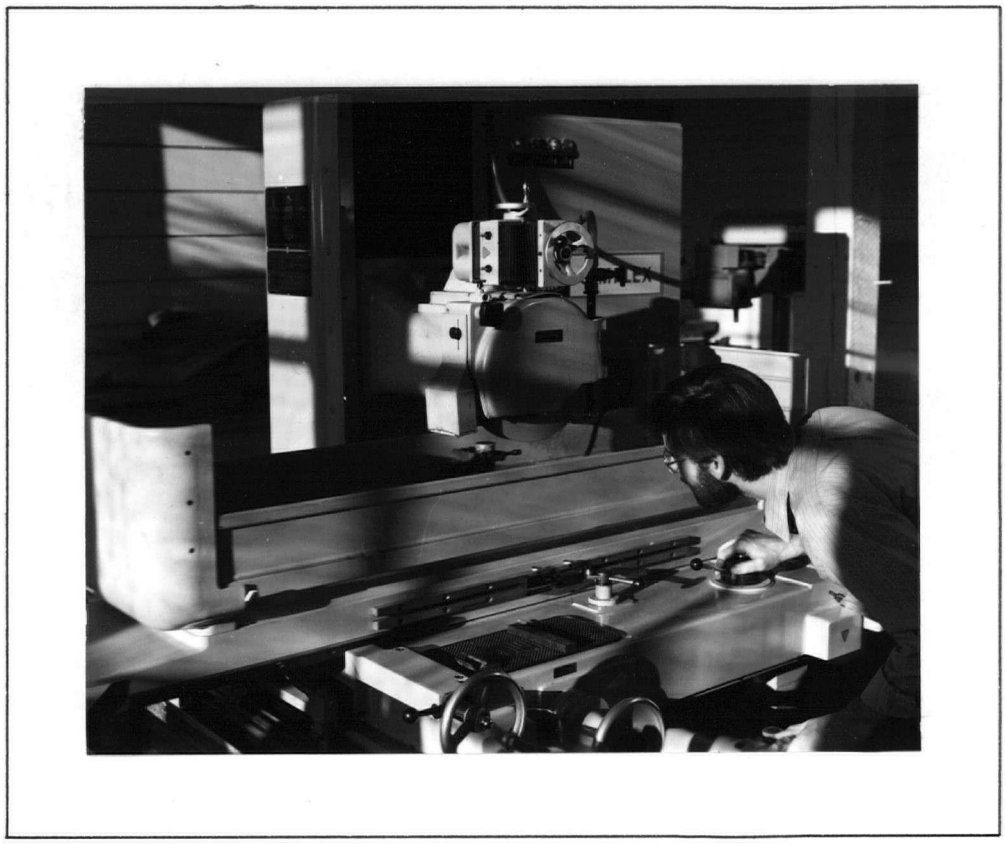

PREPARATION OF CORE SAMPLES USING "BLOHM SIMPLEX" SURFACE GRINDER

2. Load Measurement

Axial loads were applied to the samples using a hydraulic press as shown in Figure 2. This press can develop up to 250,000 pounds load but for this testing programme maximum loads were approximately 20% of capacity. The loads were measured with a 50,000 pound capacity, "Baldwin SR-4," load cell. The readout unit consisted of a "Doric" digital strain gauge transducer unit having a reading capacity of 20,000 units. The calibration of the testing assembly was carried out using a "Morehouse" proving ring mounted in series with the load cell as shown in Figure 3. The "Doric" transducer unit was adjusted to display a number of units equal to the accurately known mechanical load. Thus the "Doric" read directly in pounds. The load cell and "Doric" also showed linearity over the load range of the proving ring. The calibration proved to be extremely stable over the one month duration of the testing. Subsequent calibration checks carried out weekly indicated a maximum deviation of 10 pounds in 5000 pounds or 0.2%. The sensitivity of the hydraulic press controls and the load sensing system is illustrated by the fact that for weaker rock types it was possible to apply load increments as low as 40 pounds.

An additional feature of the "Doric" allowed the loading rate to be controlled quite accurately. The "Doric" was set to the track mode so that the load was sensed at a precise scan rate. By determining this scan rate and by adjusting the control valves of the press the desired loading rate could be achieved. For example, the scan rate of

Figure 2

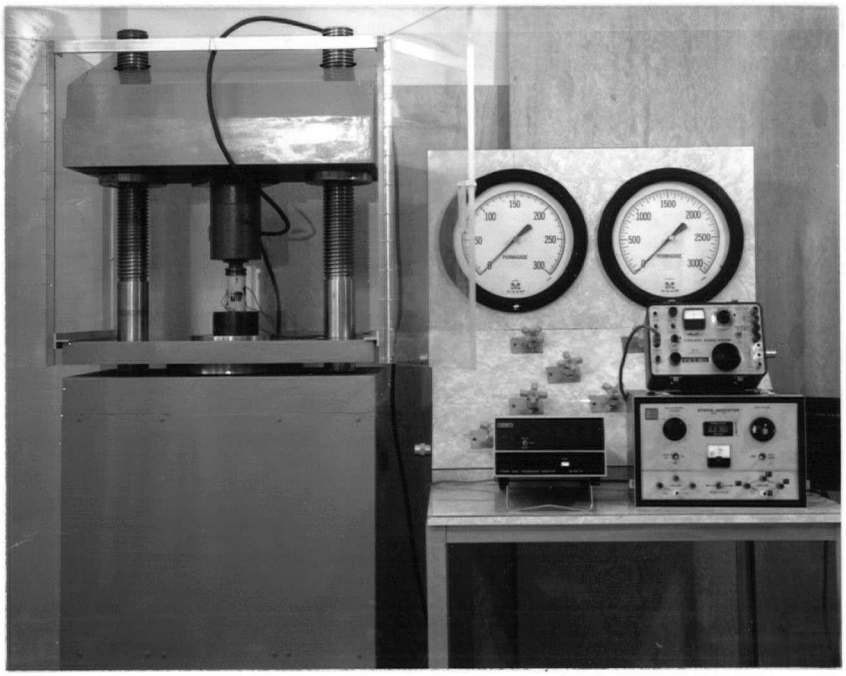

HYDRAULIC PRESS AND INSTRUMENTATION
FOR LABORATORY TESTING

Figure 3

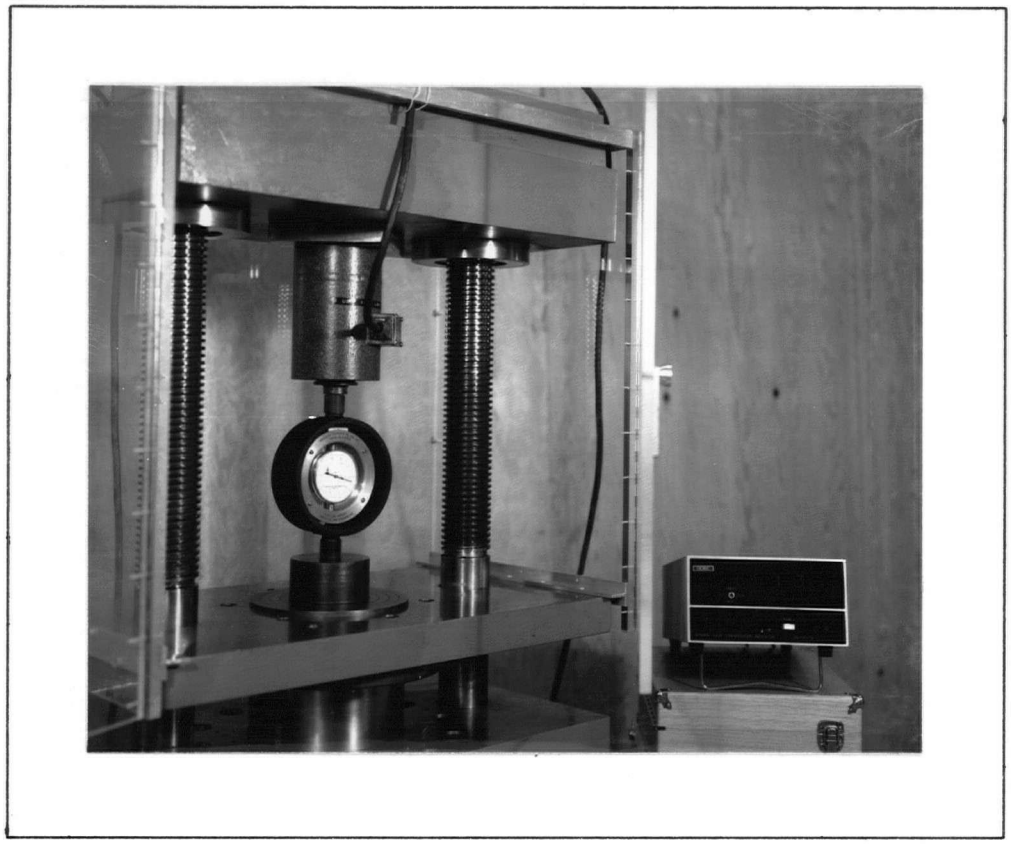

CALIBRATION OF LOAD CELL AND
READOUT UNIT

the "Doric" was 0.90 per second so that load jumps of 100 pounds corresponded to a stress rate of 60 pounds per square inch (psi)/ second for the BX core samples.

3. Strain Measurement

Strains were sensed by resistance type strain gauges. The specific brand was "Kyowa," type KFC-5-C1-11, the specifications of which are as follows:

type: foil	gauge factor: 2.12 ± 1.5%
gauge length: 5mm	thermal output: ±1.8 micro strains/ degree centigrade
resistance: 120.0 ± 0.3 ohms	

Due to the large number of gauges required, primary considerations in the choice of gauge type were their availability and cost. In spite of the low cost of these gauges they were considered satisfactory for the following reasons:

1. All testing was carried out under laboratory conditions, thus compensation for temperature extremes was unnecessary.
2. Strains were of relatively small magnitude (less than 1%).
3. Only 2 or 3 loading cycles were employed, therefore the fatigue life of the gauge was unimportant.

4. Heat dissipation was no problem since the gauge current would be 6.25 milli-amperes, far less than the 100 milli-ampere maximum for foil type gauges. [Dalley and Riley, 4]
5. The gauge length of 5 mm was considered sufficiently long,
   (a) to avoid the strain gauge being attached to a single rock grain, and
   (b) to avoid stability problems due to stress relaxation in the adhesive.

Two axial and two circumferential strain gauges were attached to the gneiss and pegmatite samples. Since these rock types were uniform and unfoliated the gauges were not oriented with respect to structural features. Figure 4 shows gauge installations on the various rock types. Because of the distinct foliation present in the schist samples four axial gauges were used in an attempt to detect directional movements. The position of these gauges with respect to the strike and dip directions of the foliation is illustrated in Figure 5.

The procedure for attaching the strain gauges to the rock samples was that given by Hardy [5] with some modifications. This procedure can be summarized as follows:

1. After cutting and grinding, samples dried at room temperature for not less than two weeks.
2. The samples were cleaned of all dirt and grease.
3. Positioning lines were drawn axially and circumferentially at mid-height to locate gauges.

Figure 4

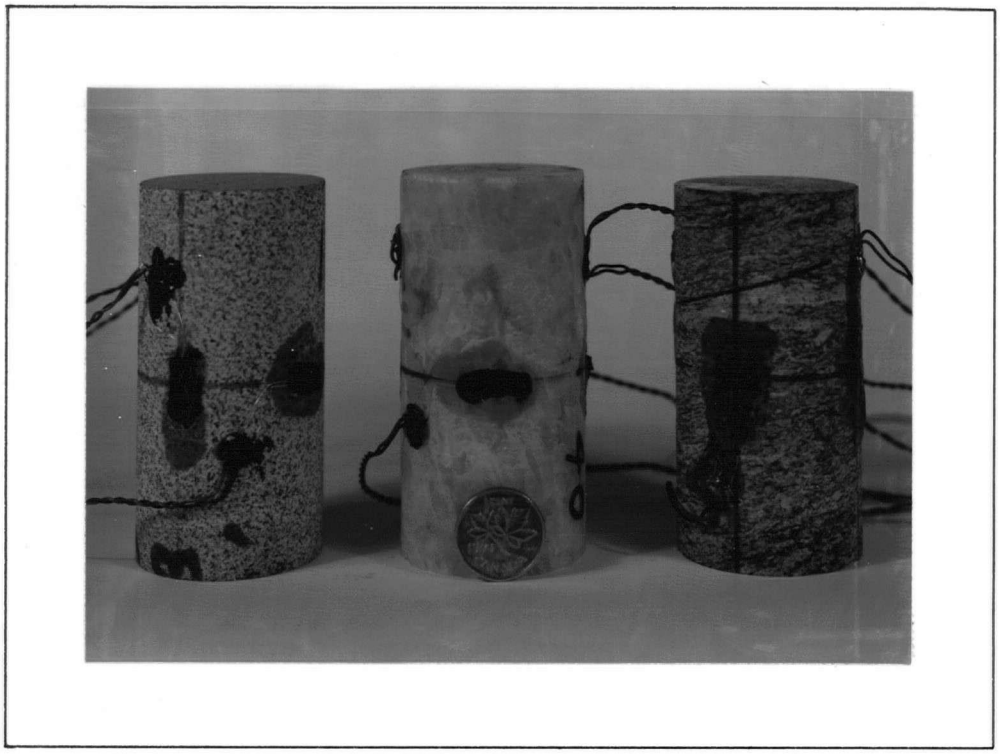

DEPLOYMENT OF STRAIN GAUGES FOR THE
THREE ROCK TYPES
From left to right; quartzite gneiss,
pegmatite, quartz feldspar schist

Figure 5

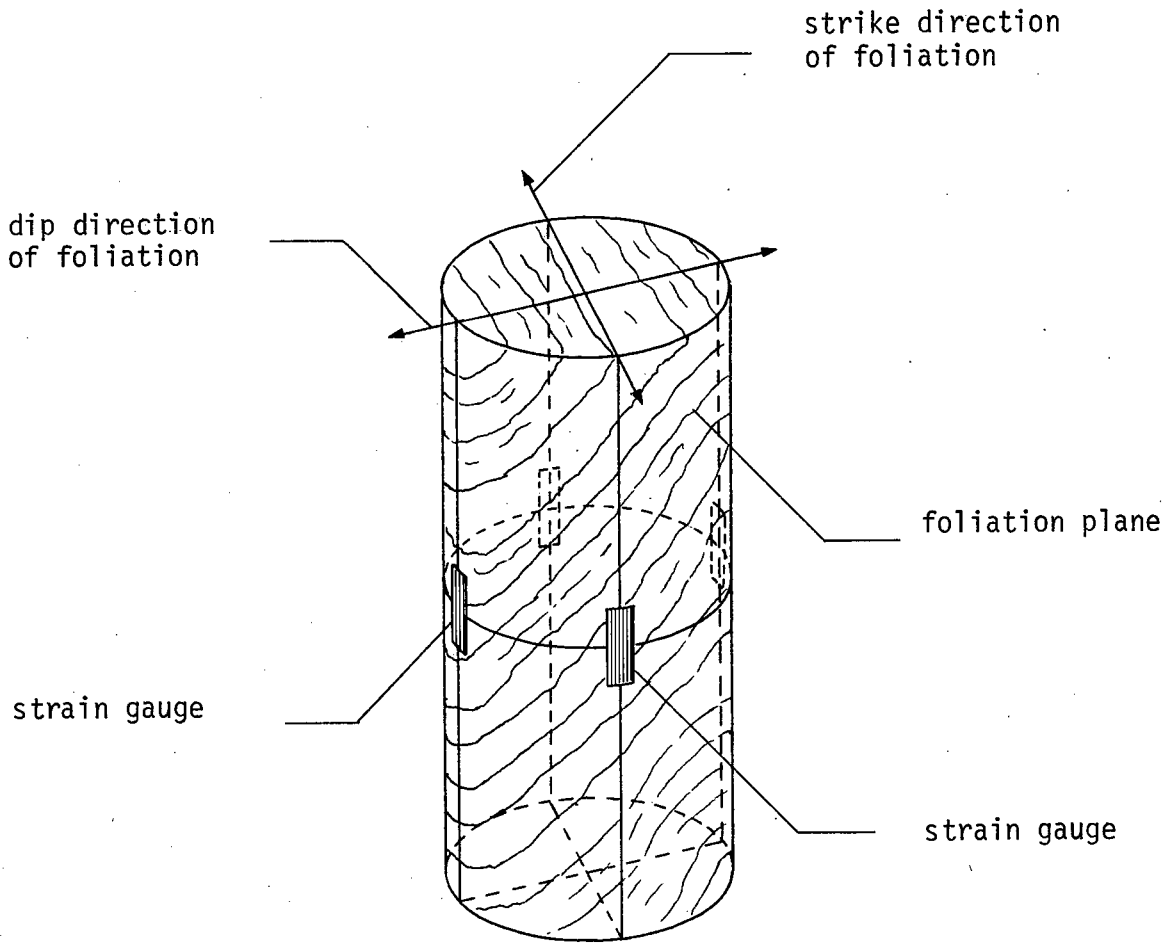

PLACEMENT OF STRAIN GAUGES RELATIVE TO STRIKE AND DIP DIRECTIONS FOR QUARTZ FELDSPAR SCHIST SAMPLES

4. The areas to which gauges were to be attached were thoroughly cleaned as follows: (a) acetone vigorously brushed in using a toothbrush, (b) final cleaning using tissue paper soaked in acetone.
5. The sample was allowed to dry until all traces of acetone had disappeared. (about 2 minutes)
6. Two strain gauges were removed from their packages, special care being taken not to touch the under side of the gauge.
7. The cement(Phillips-Type PR9244/04) was mixed and applied to two of the gauge positions on the rock sample.
8. The gauge was placed on the sample in the correct orientation. A piece of cellophane was placed over the gauge and any bubbles in the cement were removed by pressing with the thumb.
9. The sample, with its two attached gauges,was placed in a drying press consisting of wooden blocks, sponge rubber and a G-clamp.
10. The cement was allowed to set for 5 minutes with the sample in the gauge press. The sample was then withdrawn, the cellophane removed, and steps 5 to 10 repeated for the second set of gauges.
11. The sample was allowed to dry for an additional 24 hours to ensure complete cement curing.
12. Terminal tabs were cemented to the sample to provide a soldering point for attaching gauge lead wires and circuit lead wire.
13. After soldering leads was complete the continuity of the gauge circuit was checked using an ohmeter.

14. The gauges and solder joints were coated with a low modulus silicone rubber. There were several reasons for this precaution. Firstly, to protect the gauge installation from moisture in the air. Secondly, to firmly attach the lead wires to the sample to prevent any induced strain to the gauges. Finally, to prevent the lead wires from being pulled off.

The readout units for strains consisted of two commercial bridges that were calibrated to read strain directly in microinches per inch. The axial strains were read out on a "Budd Strain Indicator" while a "BLH Strain Indicator" was used for circumferential strains or axial strains in the dip direction in the case of schist samples. The strain gauge circuit for each set of gauges is illustrated in Appendix 1. The circuit indicates double the correct strain, the proof of which is also shown in Appendix 1. Thus,strains were detected to the nearest 0.5 microinch/inch.

Temperature fluctuations, though minimal under laboratory conditions, were compensated for in the strain gauge circuitry. Strain gauges were attached to a "dummy" rock sample in the same orientation as those on the test samples. These gauges were then connected as compensating gauges in the strain gauge circuit. A temperature change would cause equal thermal strains in the test and "dummy" samples assuming their coefficients of thermal expansion to be the same. However, due to the positions of the gauges in the circuit the electrical output of the test and "dummy" samples would be identical but of opposite sign. The electrical effect of the thermal strains was thereby cancelled.

4. Test Procedure

The test procedure for the laboratory rock testing can be summarized as follows:

1. The "Doric" was allowed to warm up until it showed the correct zero reading.
2. The sample was set in the press and connected to the bridge circuits. After a warmup period the zero readings were taken.
3. From previous strength testing programmes an estimate of the ultimate compressive strength was made.
4. The sample was then incrementally loaded to 75% of the estimated ultimate compressive strength. The load increments were chosen such that a complete load-unload cycle had 15 to 20 readings.
5. The maximum load and/or load increments were modified on second and subsequent loading cycles if warranted by the first cycle behaviour. For example, if the first cycle strain readings showed linearity then the maximum load and load increments would be increased on the second cycle.

Several problems arose in conjunction with the testing programme. The most important of these was that it was imperative that the testing be non-destructive in order that other workers could carry out further testing on the samples. Out of a total of 72 samples tested, 11 were broken, due mainly to overestimating the strength or to difficulties encountered when initiating low loading rates at sample loads above 30,000 pounds. A second problem involved loss of load due to leakage in the control valves of the press. This condition was most prevalent at low

loads on the unloading cycle and was overcome by synchronizing the strain readings with the drifting load.

5. Summary

When comparing the results of testing techniques it is desirable to make these comparisons with respect to the time required to carry out the testing. Appendix 2 presents a time study for each phase of the laboratory testing programme from the time the core is received at the laboratory. It is emphasized that these times are those encountered by this writer. The times required by a testing laboratory would undoubtably be less. From Appendix 2 it is seen that sample preparation and testing required 1 3/4 hours per sample.

Clarke [6] presented a table of items which should be specified for laboratory tests for deformation modulus. Based on that table, a summary of the test items utilized in the writer's test programme is presented in Table 1.

B. Goodman Jack Testing

1. Description of Equipment

The Goodman Jack, also referred to as the NX plate bearing device or bore hole jack, is a hydraulic jack designed to determine the load-deformation characteristics of rock. This is accomplished by applying a unidirectional load to a portion of the circumference of an NX bore hole by forcing apart rigid bearing plates.

The disassembled jack is shown in Figure 6. As can be seen, it consists of two steel plates which are forced apart by 12 race track-

TABLE 1

SUMMARY OF LABORATORY TESTING PROGRAMME

1. Length of Sample: average 3.200 inches
2. Diameter of Sample: average 1.600 inches
3. Shape of Sample:

   Cross-section: circular
   Vertical section: rectangular
   Symmetry: that of a right cyclinder

4. End Conditions:

   Platen: hardened steel
   Specimen: flat to within 0.001 inch
   Lubricant: none

5. Measurement of Load: load cell coupled to a digital readout unit
6. Rate of Loading:

   Gneiss, Pegmatite: 60 psi/sec
   Schist: 30 psi/sec

7. Number of Cycles: 2 (occasionally 3)
8. Test to Failure: no
9. Sensors:

   Resistance strain gauges
   Type: foil
   Length: 5mm
   Number: 4
   Placement: gneiss, pegmatite: 2 axial, 2 circumferential
   schist: 4 axial

10. Lateral Extension-Poisson's Ratio: measured circumferentially with strain gauges
11. Coordination of above with rock properties:

    Ratio gauge length to grain size: gneiss 10:1,
    pegmatite 2:1,
    schist 5:1
    Ratio sample size to grain size: gneiss 160:1,
    pegmatite 40:1,
    schist 80:1

12. Instrumentation:

    Accuracy: load:- 10 lb. in 5000 lb or 0.2%
    strain:- Tektronix Oscilloscope #549 used as standard
    Overall system checked using an aluminum sample.

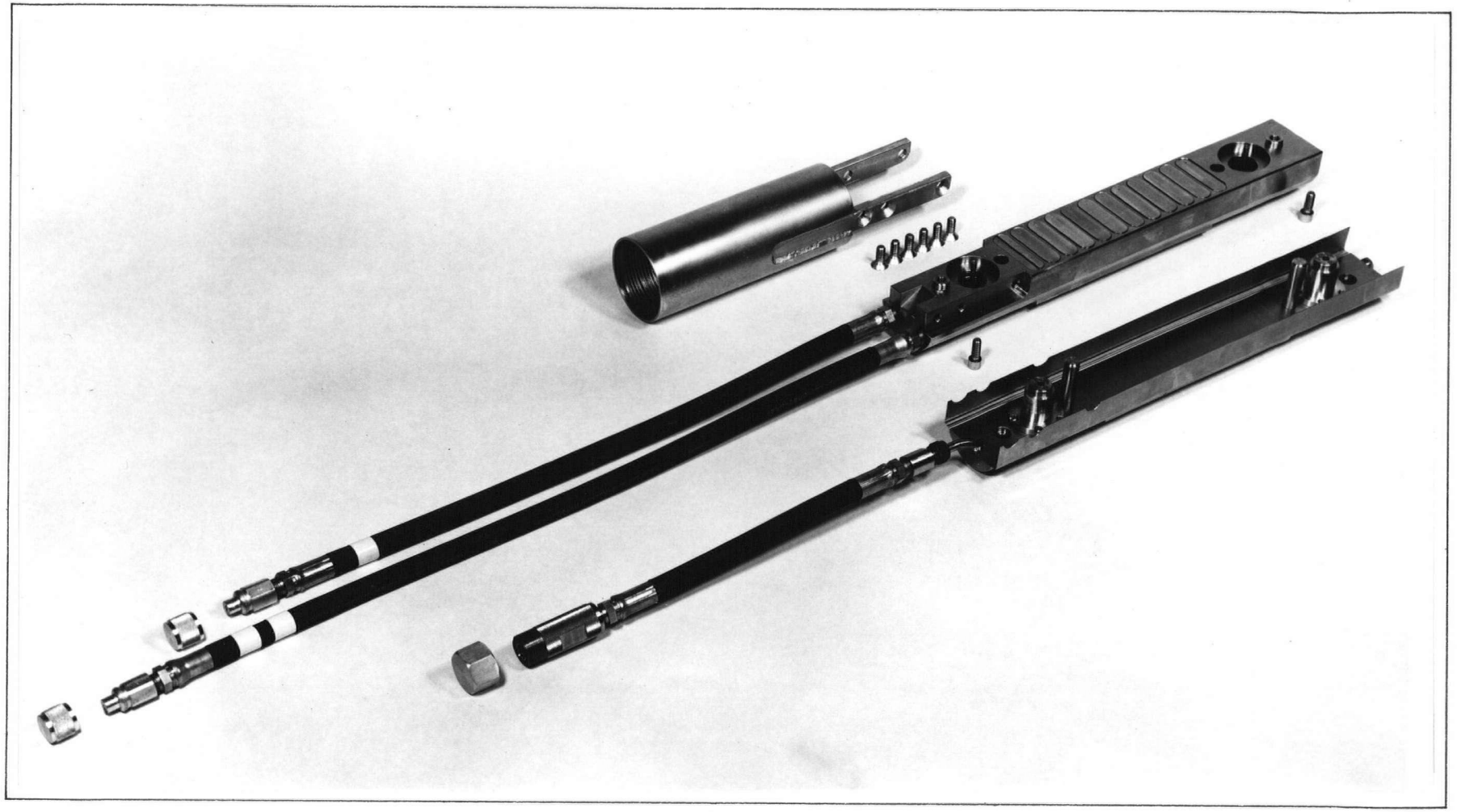

Figure 6

Disassembled Goodman Jack

shaped pistons. Two linear variable differential transformers (known as LVDTs) measure the diametral deformation at either end of the 8 inch long plates. The jack is collapsed by means of two return pistons. The jack's collapsed diameter is 2 3/4 inches, thereby providing one-quarter inch clearance in an NX bore hole.

Ancillary equipment used in conjunction with the Goodman Jack includes a portable transducer readout unit, hydraulic pump, pressure gauge, hydraulic hose and electrical cable. The transducer readout is calibrated by plotting readings on this unit versus the diameter of the jack. The hydraulic pump is hand operated to produce 10,000 psi line pressure. The assembled jack, transducer readout unit and hydraulic pump are shown in Figure 7.

The operating specifications of the jack are as follows. A maximum bydraulic line pressure of 10,000 psi produces a stress of 9,300 psi against the sides of the bore hole. This stress field is uniform and unidirectional and corresponds to a force of 158,000 pounds. [Tran, 7] The jack has a 0.5 inch extension range from 2.75 to 3.25 inches in diameter. The LVDTs have a linear range of 0.2 inches. This linear range can be adjusted to correspond to any portion of the jack extension range depending upon rock deformability. Under normal conditions the linear range of the LVDTs corresponds to jack diameters from 2.9 to 3.1 inches.

Bore hole test methods, such as the Goodman Jack, have several advantages. The principal advantage is that special underground test chambers need not be constructed.

Figure 7

Assembled Goodman Jack, Transducer Readout Unit and Hydraulic Pump

Most projects involve large exploratory drilling programs which provide appropriate test locations for deep investigation of undisturbed rock using bore hole methods. Further advantages of these methods are that they consist of relatively light equipment and are fast and economical to carry out. As a result many tests can be run and a statistical average employed.

Compared to other bore hole methods such as dilatometers, the Goodman Jack has two distinct advantages. Firstly, the jack can develop much higher compressive stresses; 9300 psi versus 2200 psi maximum for dilatometers. This means that the Goodman Jack can be used to determine the deformation modulus in very rigid rock. The second advantage is that the jack has directional loading capabilities while dilatometers supply a uniform internal pressure to a section of the bore hole. Thus, the jack can be oriented on specific geologic features assuming their intersection with the bore hole is accurately known. For example, the jack can be positioned so that it forces apart fractures or joints provided good bore hole data is available. The directional loading capability also means that the deformation modulus can be determined in several directions thereby providing information on the anisotropy of the rock.

2. Procedure

The Goodman Jack test procedure followed closely that recommended by the manufacturer, Slope Indicator Company. The principal modification involved the substitution of insertion rods for BX casing to insert the jack into the bore hole. The casing is recommended in

order to provide maximum protection for the jack, hydraulic hoses and electrical cables. The disadvantage of this system is that the casing weighs approximately 50 pounds per 10 foot section. Thus, for lengths of casing greater than 20 feet, a drill rig or similar system must be used to handle the load. In order to facilitate manual placement of the jack, light aluminum insertion rods were used. These rods weighed less than 5 pounds per 10 foot section. As a result, two men with a small hand winch could place and retrieve the jack at depths greater than 100 feet from the exploratory drift.

The actual testing procedure followed with the Goodman Jack can be summarized as follows:

1. Hydraulic hoses and electrical cables were connected.
2. The jack was inserted a short distance into the bore hole, loaded and retracted to ensure correct performance at depth.
3. The jack was then positioned at the correct depth and oriented with respect to the drift axis. (See Figure 8)
4. The jack was expanded using the hand pump until a hydraulic pressure of 1000 psi was reached. This base loading was the initial point of the load deformation data rather than the zero stress point because of the difficulty in determining the exact moment of jack-bore hole contact.
5. The jack pressure was increased in increments of 1000 psi to a maximum of 9500 psi. Readings for both deformation transducers were taken at each load increment. If, at any point during the loading cycle, these readings differed by more than 0.020 inches the jack was retracted and re-located.

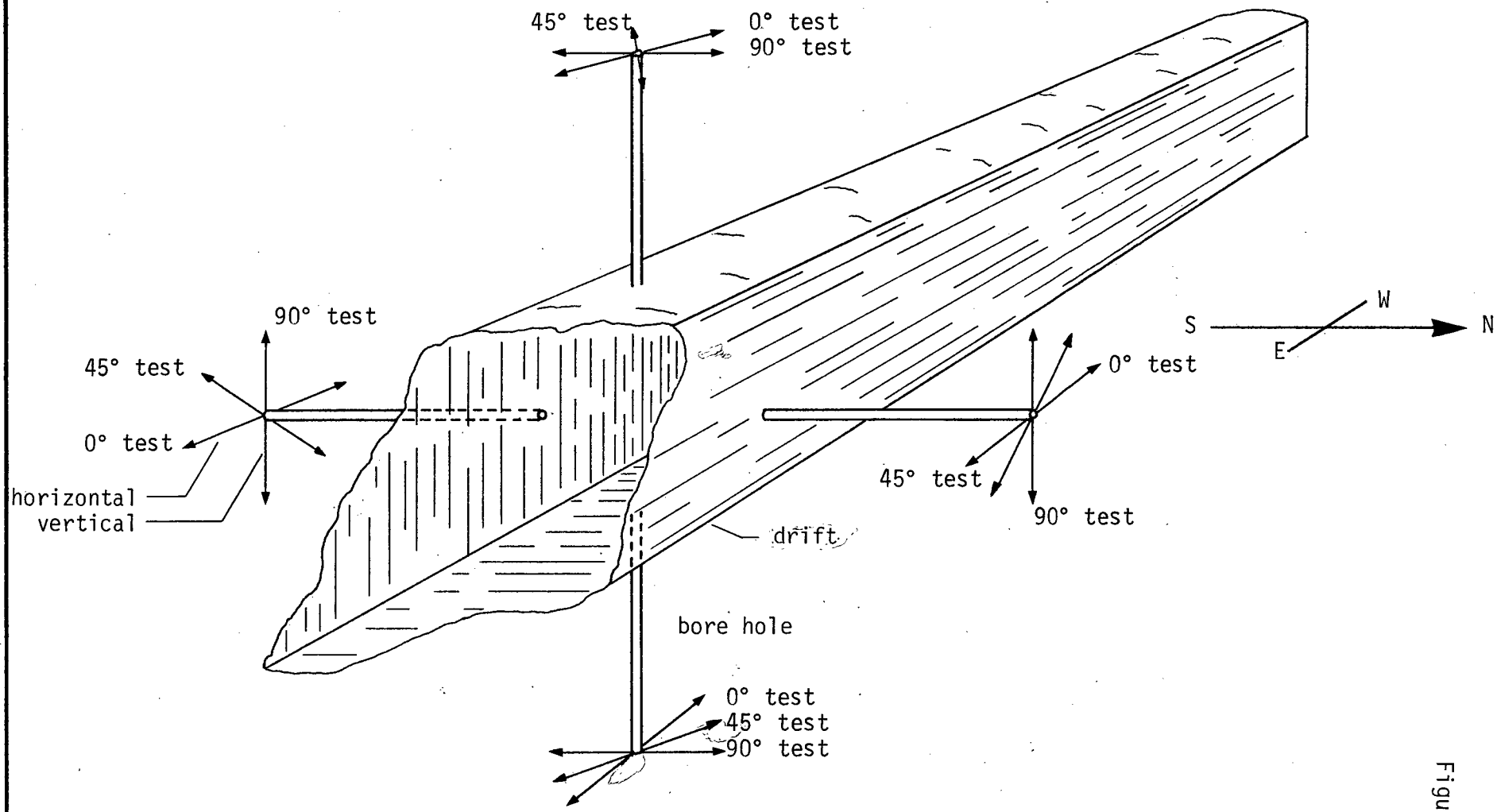

Figure 8

ORIENTATION CONVENTION FOR THE GOODMAN JACK

The reason for this precaution was that the difference indicated the jack was tilting due to non-uniform deformation of the rock. Excessive tilting could cause wear on the jack's guide pins or LVDT adapter or, in the extreme case, cause the jack to jam.

6. The jack pressure was then decreased in increments of 1000 psi to complete the unloading portion of the cycle. For most locations 2 or 3 load-unload cycles were performed. However, in some cases, inconsistent results necessitated 4 cycles.
7. After step 6 was completed the jack would be rotated and similar tests carried out at 90 degrees and 45 degrees to the first direction of loading.

The loading was controlled by how fast the operator could develop pressure with the hand pump. It is estimated that the loading rate was approximately 100 to 150 psi per second (rock pressure). The time required for a 2 cycle test for one orientation of jacking was approximately 10 to 20 minutes depending on the time necessary to locate the jack.

The main problem encountered in the Goodman Jack testing programme concerned the tendency of the jack to malfunction in the retract operation. This happened twice during the course of the programme with the result that the jack could not be readily retrieved from the bore hole. Possible causes for the malfunctioning include dislodged O-rings on the retract pistons, mud and rock chips entering the jack and failure to completely tighten the self-sealing hydraulic couplings.

In both cases, after considerable lost testing time, the jack was retrieved with the aid of a drill rig.

A second problem encountered, concerned the deformation transducers. During the course of disassembling the jack it was found that there was a small amount of play between the LVDTs and their mountings.This condition meant that when the direction of loading was reversed the initial jack deformation would be lost in the backlash of the LVDTs. The result was that the first pressure increment of loading or unloading exhibited an abnormally high deformation modulus. This effect is shown quite clearly on the load-deformation curves and it will be discussed later. It should be noted that this was a characteristic of the specific jack being used and probably is not an inherent feature of all Goodman Jacks.

C. Plate Loading Tests

1. Description of Equipment

Plate loading tests are performed to determine the *in situ* deformation characteristics of a rock mass. This is accomplished in one of two ways. One method, known as the cable jacking test, loads a plate on the surface. The load is supplied by hydraulic jacks, the reaction being provided by cables anchored at depth. [See Zienkiewicz and Stagg, 8] In the second method a hydraulic jack is used to separate the walls of a tunnel. The plate loading tests for this project utilized the latter method as is schematically shown in Figure 9. For a detailed study of tunnel plate loading tests see Wallace, Slebir, et al. [9].

Figure 9

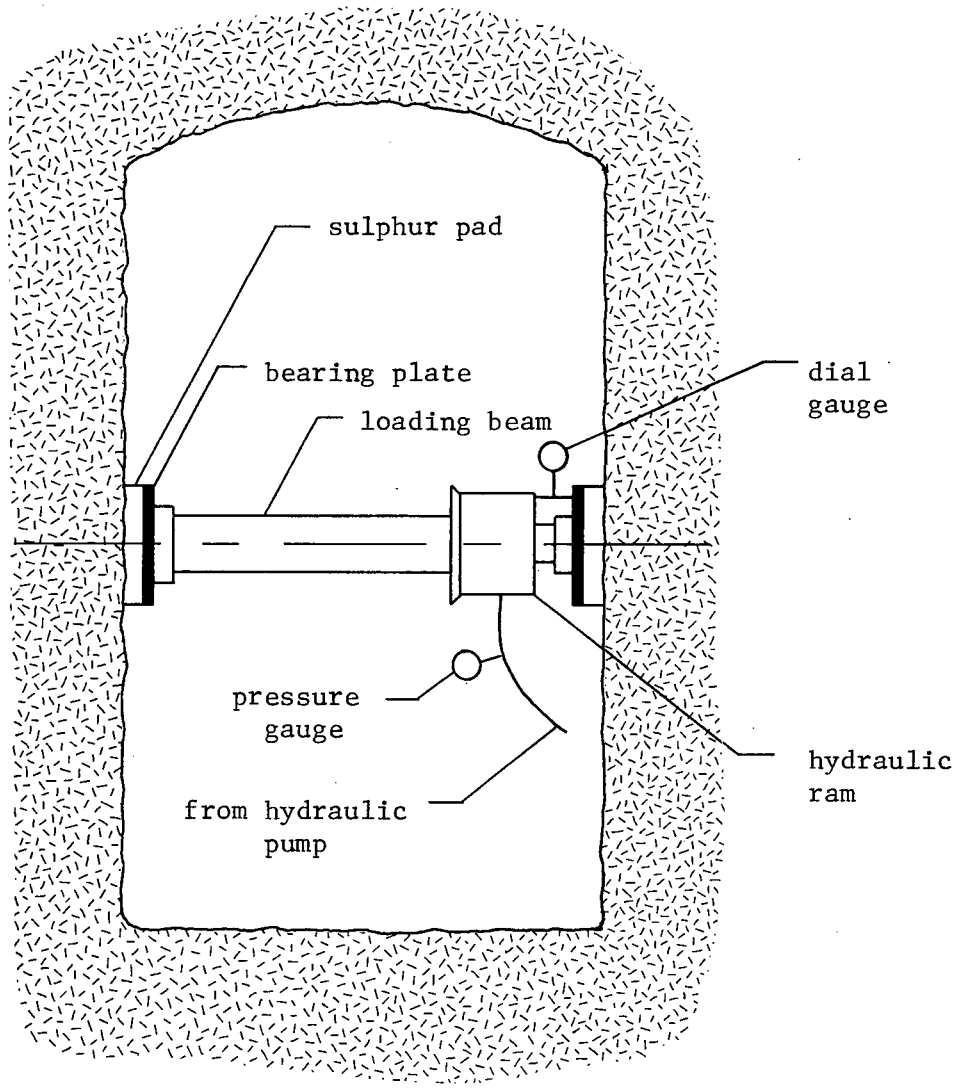

SCHEMATIC ILLUSTRATION OF A PLATE LOADING TEST

As previously mentioned the plate loading tests were not performed by this writer. The following information was supplied by the company sponsoring this research work and it refers to work carried out during 1967.

Plate loading tests at this project were carried out at six separate locations in the exploratory drift giving twelve complete tests, since measurements were made at both ends of the loading assembly. Loads were applied by a 200 ton ram acting on 12 inch diameter circular or ten inch square bearing plates. Loads were carried to the pads by test beams made from 8 inch diameter double-extra heavy wall pipe. Sections of the pipe in different lengths could be bolted together so that the required distance across the tunnel could be spanned. Deflections were sensed with dial gauges, accurate to 0.0001 inch, mounted against the bearing plates.

2. Procedure

The plate loading tests were carried out in two orientations, vertically or horizontally across the tunnel. Each test consisted of four cycles of loading and unloading the bearing surfaces with progressively higher loads and recording the rock deflections. Ten readings were made during each cycle of loading and unloading with the load held constant for 30 minutes at the maximum and minimum load to allow the rock to adjust.

The cycles of one test consisted of: 50 tons maximum load in increments of 5 tons; 100 tons maximum load in increments of 10 tons;

150 tons maximum load in increments of 15 tons; and 200 tons maximum load in increments of 20 tons. One complete test, then, involved eighty steps and required six to eight hours.

CHAPTER V

INTERPRETATION OF TEST DATA

A. Laboratory Testing Programme

Since laboratory test samples have a consistent geometric shape and are subject to a uniform stress field, no theoretical considerations are required to determine the deformation modulus. In other words, the deformation modulus follows directly from its definition.

Many writers have reported factors which can affect the modulus value determined for a particular sample. See Hardy [5], Obert and Duvall [10], Hawkes and Mellor [11] or Stagg and Zienkiewicz [2]. Some of these factors include loading rate, moisture content and sample end conditions. Time considerations prevented a thorough study of these factors although the work of other investigators suggests that they are of comparatively minor significance. Hence, for this thesis, their effect is considered to be insignificant.

B. Goodman Jack Testing

The force applied by the Goodman Jack to the bore hole walls is unidirectional. Thus at all points along the bore hole wall, except the line of symmetry, the force is directed at an inclination to the normal to the bore hole wall. This means that pressure on the wall is not uniform and the theoretical solution for the deformation

modulus involves a constant displacement problem rather than constant pressure. [Goodman, et al. 12]

Tran [7] stated the following assumptions for the analytical solution for the bore hole jack problem:

"1. The material studied is homogeneous, isotropic and linearly elastic and the bore hole is perfectly smooth.
2. The applied pressure is uniaxial and uniform across the width of the plate, and along the axis of the bore hole. It acts at the wall of the bore hole.
3. External shear load does not exist, i.e., the jack is frictionless.
4. The jack is infinitely long in the third dimension."

Using the complex variable method the following solution was presented for the deformation modulus:

$$E = K(\nu, \beta) \frac{Qd}{\bar{U}_d} \qquad \ldots . (1)$$

where
- E deformation modulus
- K constant which is a function of Poisson's ratio, ν, and the plate width, β
- Q pressure applied to the rock
- d diameter of the bore hole
- $\bar{U}_d$ average diametral displacement.

Equation (1), although mathematically correct, is subject to the assumptions stated above and hence is not strictly applicable to the field conditions. Goodman et al. [12] investigated the effects

of the assumptions and other factors on the mathematical solution and refined equation (1) for the interpretation of field test data. Their findings will briefly be summarized:

1. The constant, $K(\nu, \beta)$, is a maximum at $\beta = 45$ degrees, the plate width of the Goodman Jack.
2. Since the analytical solution assumes linear elastic behaviour, rock exhibiting non-linearity can be interpreted qualitatively but not quantitatively.
3. Finite element analysis showed that the coupling effect of the steel plate and rock surface is minimal and that the bore hole jack is closely approximated by the constant displacement boundary condition.
4. The effect of loading a finite length was investigated with a three dimensional finite element programme. The findings indicated that the deformation modulus values should be decreased by 14% to take into account the third dimension. The revised equation for the interpretation of field data was presented by Tran [7]:

$$E = K_f \frac{Q_h}{U_d} \qquad \ldots .(2)$$

where E deformation modulus

K_f a constant which is a function of Poisson's ratio

Q_h hydraulic pressure

U_d diametral displacement.

5. As Figure 10 shows $K_f(\nu)$ is relatively insensitive to variation in Poisson's ratio. Assumptions for ν thus introduce minimal

RELATIONSHIP BETWEEN CONSTANT K_f IN EQUATION (2)
AND POISSON'S RATIO

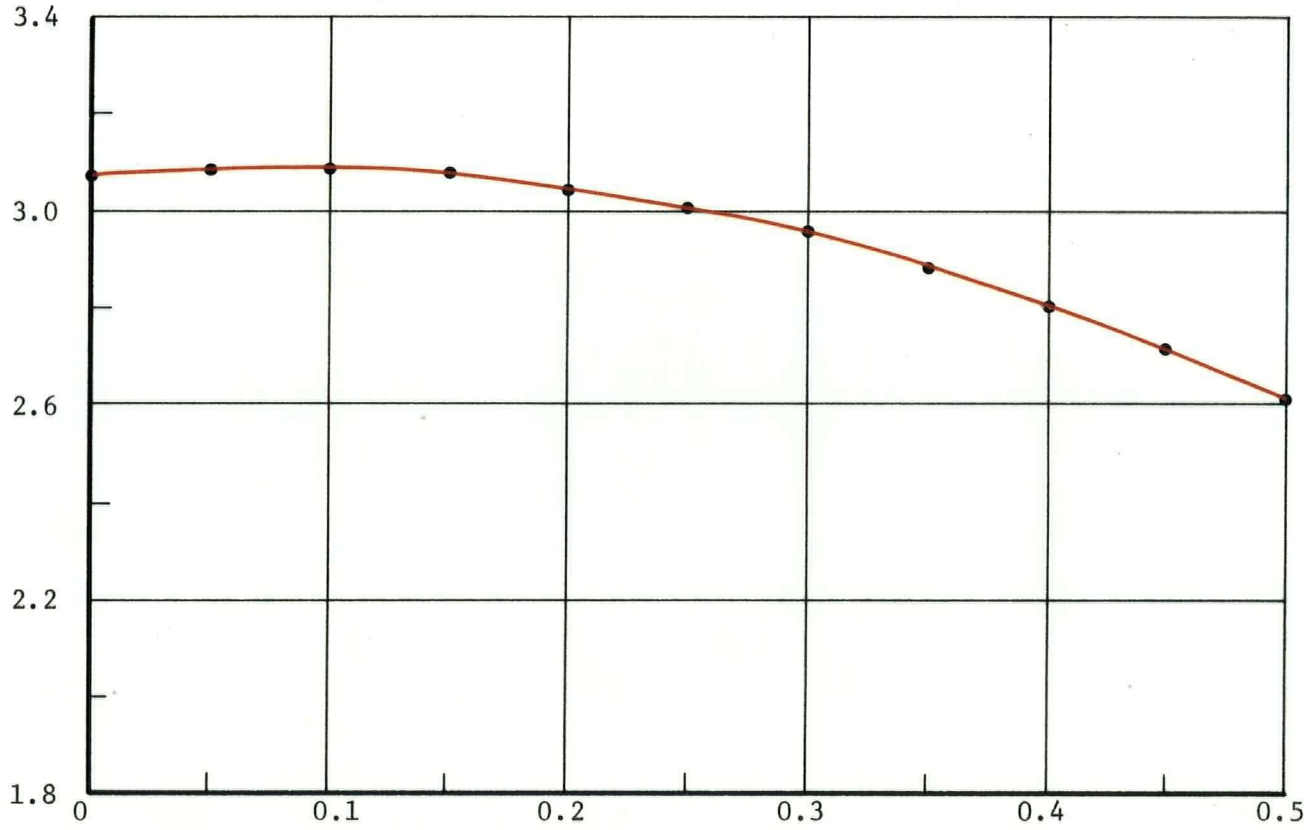

Figure 10

errors to the calculated value of deformation modulus.

6. The possibility of crack formation in the plane perpendicular to the jack loading was also investigated with a finite element model. This study showed that the probable maximum depth of crack would be one-half to one radius beyond the hole. This would result in an apparent modulus 15% less than the true value. Should the jacking take place across a pre-existing crack such as a joint the correction to the deformation modulus could reach 30%.
7. The effect of bore hole roughness is negligible after the first load increments providing complete unloading does not occur.
8. Study of the displacement and pressure decay with depth from the bore hole indicated the volume of rock affected by the Goodman Jack is approximately one cubic foot.

It is apparent from the foregoing discussion that a significant amount of theoretical formulation has gone into the development of the Goodman Jack. Verification of the jack's behaviour by comparison of field results with other testing techniques is therefore valuable.

C. Plate Load Tests

In order to interpret the results of plate loading tests, assumptions must be made about the stress distribution beneath the bearing pads. The usual method assumes that the rock behaves as a semi-infinite elastic solid under the action of a point normal load.

The standard Boussinesq solution is then applied to the plate deflections to obtain equations for the deformation modulus. These equations, as presented by Roark [13], are as follows:

for the circular plate: $$E = \frac{P(1-\nu^2)}{2\,r\,w} \quad \ldots .(3)$$

for the square plate: $$E = \frac{1.9\,pb(1-\nu^2)}{w} \quad \ldots .(4)$$

where
- E deformation modulus
- P concentrated normal load
- ν Poisson's ratio
- r distance between point of load application and point of deflection measurement
- w deflection
- p pressure (psi)
- b distance from center of bearing plate to edge.

The assumptions in the formulation of equations for modulus lead to inaccuracies in the interpretation of plate loading test results. The solution assumes an elastic and isotropic medium, conditions rarely found in rock.

When the equations are applied to plate loading tests carried out in drifts the departure from ideal is even greater. This is caused by the fact that due to the excavation process a zone of blast damaged and destressed rock surrounds the drift. The micro-fracturing of the rock is most intense at the drift walls and decreases rapidly with depth. This means that the assumptions of an elastic and isotropic material are in considerable error. Benson et al. [14] have

stated that "the greatest sources of error with the assumption of isotropy are that elasticity prevails and that the modulus remains constant with depth."

A further problem with plate loading tests is caused by the fact that although the applied loads are high the induced stresses are low. For example, the 200 ton loads of the tests in this report corresponded to stresses of only 4000 psi. This means that for very rigid rock the accuracy of the dial gauges can be a significant fraction of the deflection caused by the jacking. This can result in considerable error in the determined deformation modulus values.

In light of the foregoing discussion it is obvious that plate loading tests must be interpreted with a great deal of caution.

D. Definition of Modulus Types

Although the term deformation modulus refers to a specific rock property, further definition is required in order to compare the results of various testing techniques. The reason for this is that several types of deformation modulus exist depending on their location on the stress-strain curve.

For the purpose of this thesis, three types of deformation modulus will be defined. The definitions correspond to those defined by the company performing the plate load testing in order that valid comparisons may be made between testing methods. A further consideration in the modulus definitions was the desire to have computations automated in order to utilize the computer.

The company performing the plate load testing defined the following three deformation moduli:

1. Working modulus, E_w: "A tangent modulus taken at a point on the stress-strain curve which best represents the behaviour of the material."
2. Secant modulus, E_s: "The secant modulus is computed using maximum stress and strain values. A secant modulus greatly lower than the working modulus usually indicates open fractures in the material permitting high initial strain or a plastic material that creeps under load."
3. Recovery modulus, E_r: "The recovery modulus is a secant modulus taken on the recovery curve. Its value increases as the elastic response of the material decreases."

These definitions are illustrated in Figure 11, which is a typical load-deformation curve for the plate loading tests.

In spite of the fact that the plate loading tests utilized increasing cyclic loads whereas the laboratory tests and Goodman Jack tests cycled to a constant maximum load, three similar moduli can be defined for the latter two tests. The definitions are illustrated in Figure 12. Note that the percentage elastic recovery for the entire test loading is equivalent to the ratio of the secant to recovery modulus.

It should also be noted that the working modulus for these tests is a chord modulus rather than a tangent modulus. There were two main reasons for this. Firstly, it is very difficult to programme the

Figure 11

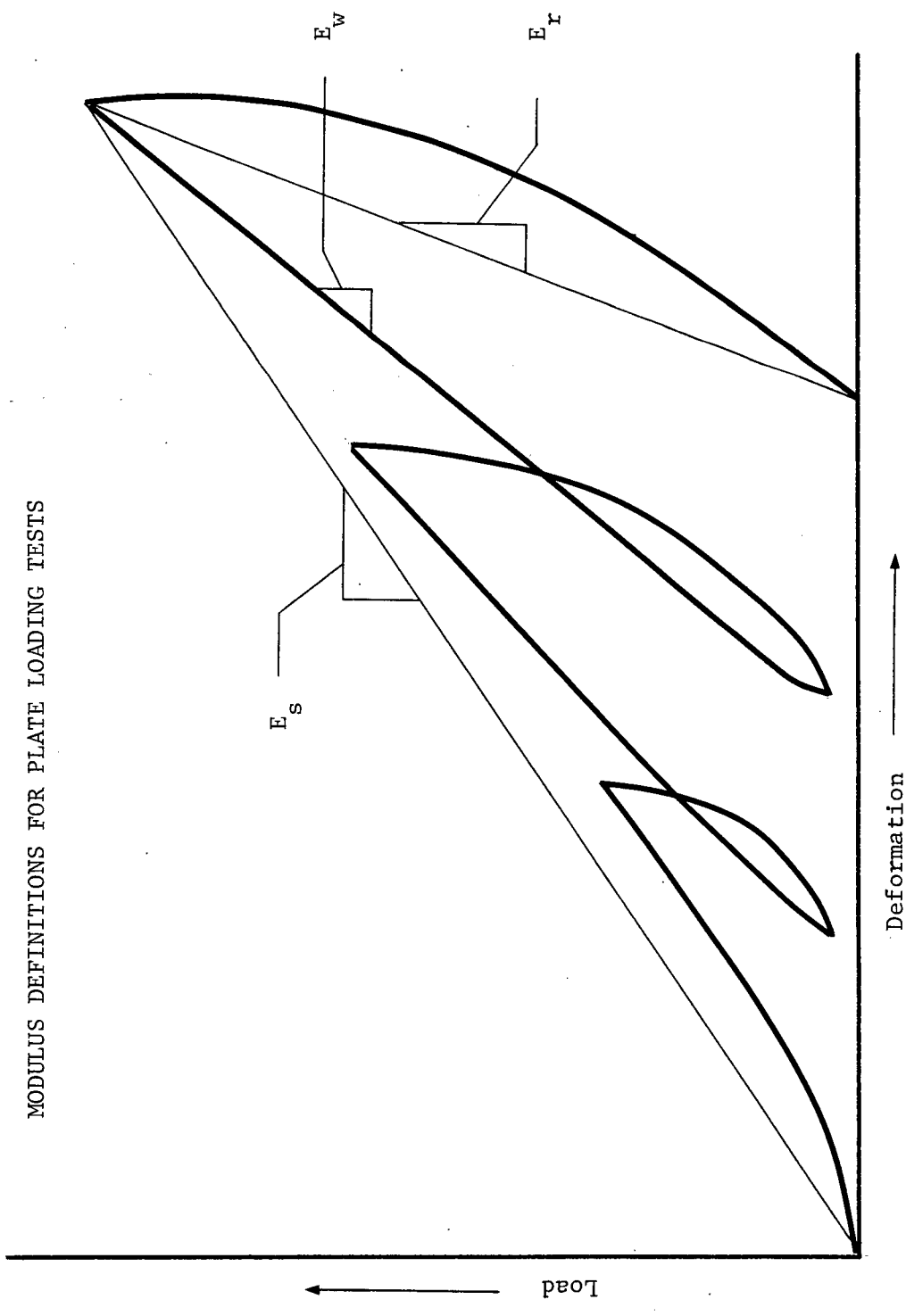

MODULUS DEFINITIONS FOR PLATE LOADING TESTS

MODULUS DEFINITIONS FOR LABORATORY AND GOODMAN JACK TESTS

E_w = chord modulus between points 1 and 2

Goodman Jack Tests: point 1 = 1/3 maximum stress

Laboratory Tests: point 1 = 1/2 maximum stress

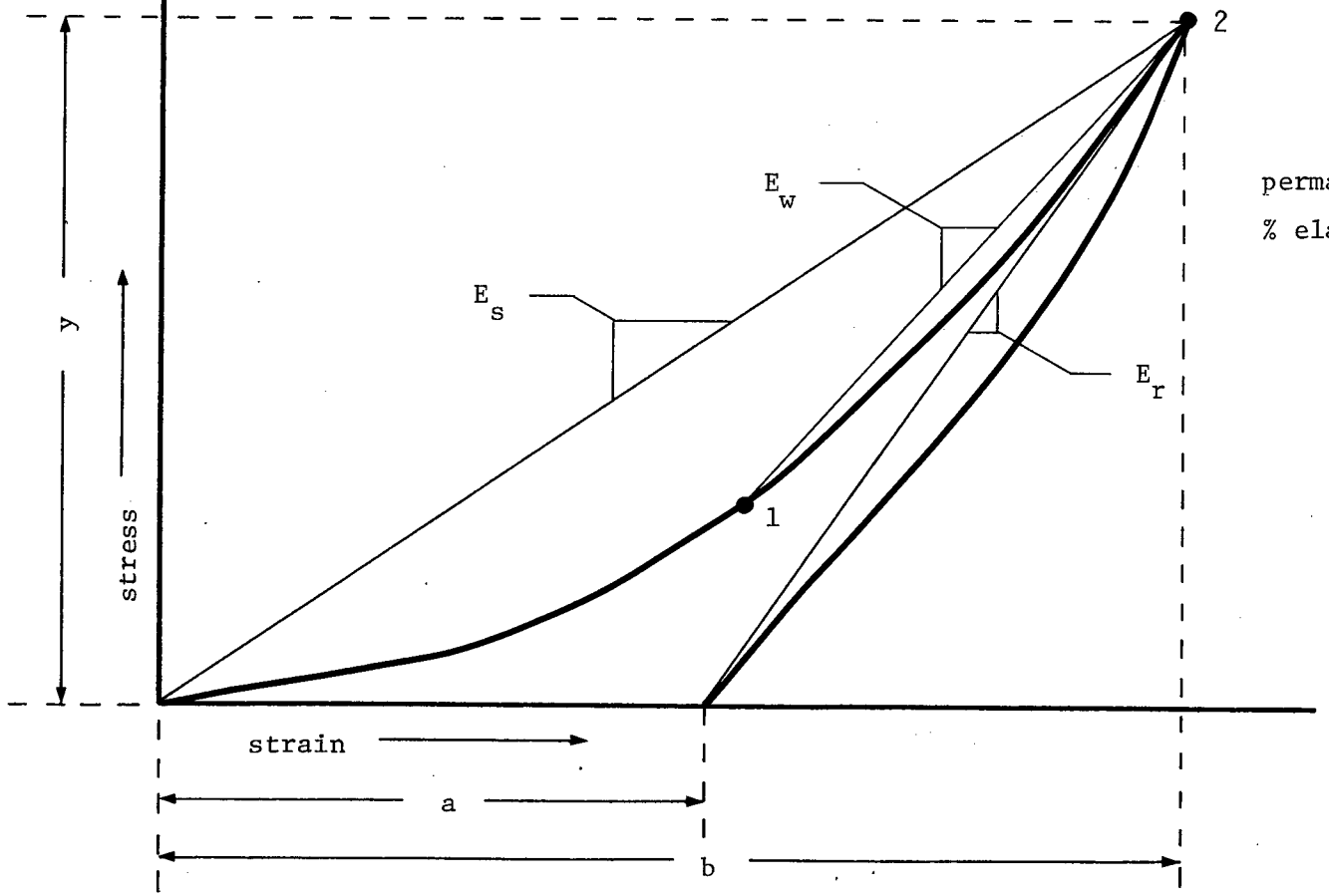

permanent deformation = $a\left(\frac{b-a}{b}\right)$

% elastic recovery = $100\left(\frac{b-a}{b}\right)$

$= 100\,\frac{E_s}{E_r}$

Figure 12

computer to calculate a tangent modulus from a set of stress-strain readings. On the other hand, a chord modulus calculation is very easily programmed. Secondly, it was felt that comparisons of working modulus between rock types would be more valid if this modulus was related to the shape of the stress-strain curve. In other words, the working modulus was determined over the most linear portion of the stress-strain curve regardless of stress level. In the author's opinion this comparison is more meaningful than the usual practice of comparing tangent moduli of various rock types at coincident stress levels. This latter practice introduces the variation of linearity of the stress-strain curves into the comparison; an effect which can be quite significant for rock types of differing competency.

CHAPTER VI

RESULTS OF TESTING PROGRAMMES

The detailed results of each testing programme are presented in the appendices. In this section the results of the various testing techniques are compared and analyzed in accord with definitions outlined in chapter V.D.

A. Laboratory Testing Programme

Seventy-one samples were tested in the laboratory testing programme although all samples did not yield usuable results. The three moduli previously defined were calculated for each cycle of loading. The working modulus, because it best represents the rock behaviour, was used as the basis for comparison. The secant and recovery moduli were used to interpret the type of deformations taking place. During preliminary studies the working modulus was taken over the upper two-thirds of the stress-strain curve. Analysis of the stress-strain curves showed that this value included significant non-linear deformation. The working modulus was then revised to include only the upper one-half of the stress-strain curve.

Prior to initiating rock testing an aluminum sample was tested to check the instrumentation. Figure 13 shows the stress-strain curve for the aluminum sample. As can be seen the curve indicates a perfect

LABORATORY TESTING

AXIAL STRESS vs. AXIAL STRAIN

Sample No. Aluminum

Rock Type _____

First cycle ——— Second cycle - - - - - -

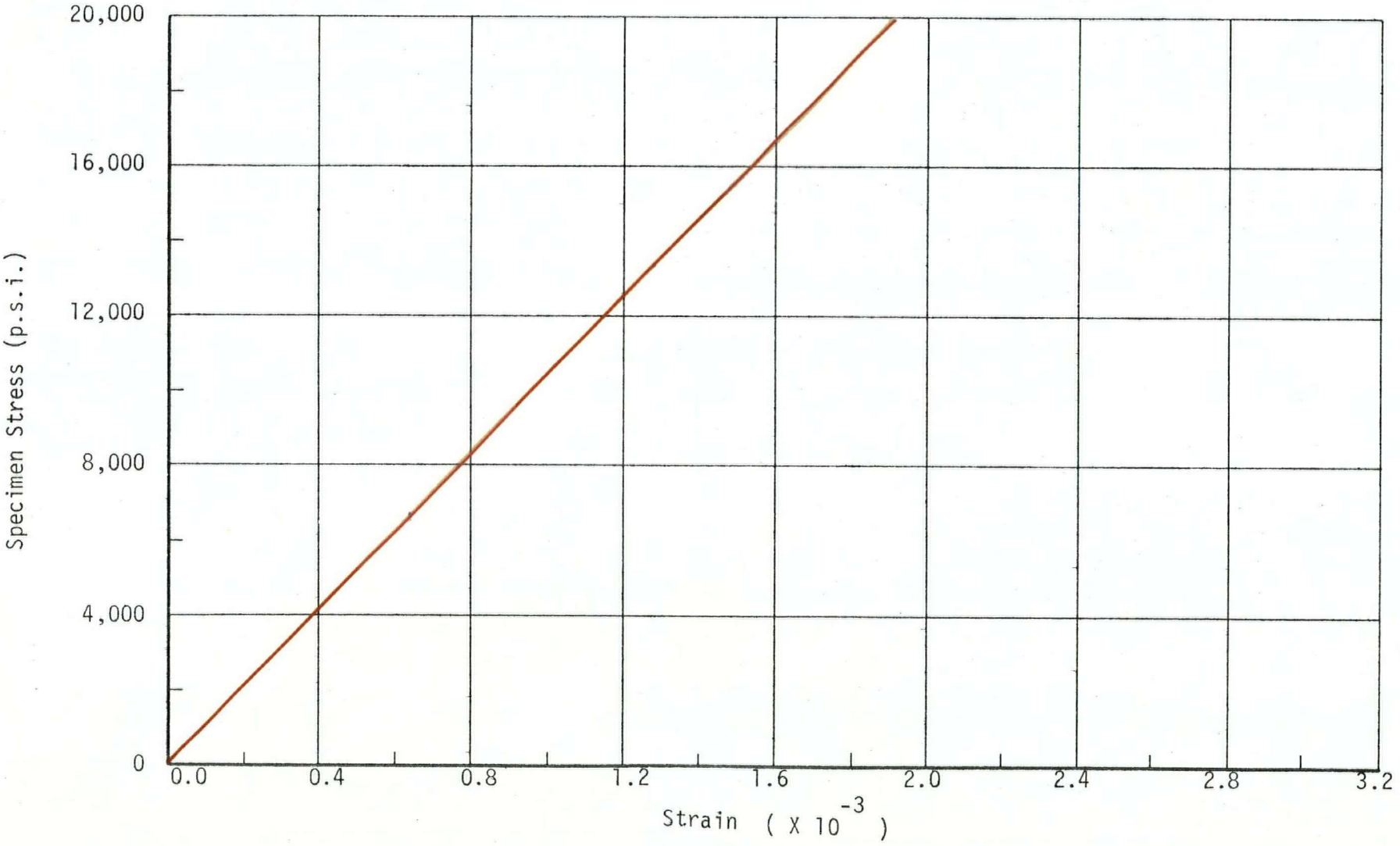

Figure 13

linearly elastic material. This confirms that the load cell and readout unit were calibrated correctly. The secant, working and recovery moduli all have values of 10.4×10^6 psi for both loading cycles. Poisson's ratio for this sample is 0.35. The published values for modulus of elasticity and Poisson's ratio for pure aluminum and alloys are $9.9 - 11.4 \times 10^6$ psi and 0.32 - 0.34 respectively. [Smithells, 15] These results indicated that the strain gauge system and load sensing system operated correctly and provided a means of checking the state of the testing system in the course of the experimental work.

1. Quartzite Gneiss

Forty-two quartzite gneiss samples were tested of which 39 yielded usable results. As stated earlier this rock type tends to be uniform, homogeneous and lacking foliation. A small number of samples did exhibit non-uniformity as either faint foliation, chloritization bands or healed fractures.

The gneiss samples were fitted with two axial and two circumferential strain gauges. This allowed calculation of Poisson's ratio as well as the various deformation moduli. The Poisson's ratio values were determined only to check those values assumed for the Goodman Jack testing and thus the values will be reported with little discussion. For the gneisses, Poisson's ratio generally increased from 0.05 to 0.35 (approximately) as the load increased. Although quite variable, the average value was about 0.20. Some values greater than the theoretical 0.5 maximum were recorded, reinforcing Hawkes' [16] claim that for rock Poisson's ratio is meaningless. Several reasons for

inconsistent Poisson's ratio values for rock have been reported. At low stress levels pore and micro fracture closure accounts for most of the axial strain. This inelastic deformation produces little lateral strain hence the low Poisson's ratio values. [Hawkes, 16] Another factor that can influence Poisson's ratio is the positioning of the strain gauges relative to geologic features such as foliation or relative to local stress concentrations within the sample.

Figures 14, 15, and 16 illustrate stress versus strain curves for laboratory tests on the quartzite gneiss samples. These curves are typical of those for this rock type and are representative of the gneiss behaviour. These figures illustrate several deformation characteristics of the gneiss. The most striking feature is the small amount of inelastic deformation. For the graphs shown the residual inelastic deformation amounted to an average of only 9% of the total deformation. Since the unloading curves for both cycles are very nearly coincident, negligible inelastic deformation occurs after the first cycle. Secondly, the narrow width of the load-unload loops indicates small hysteresis effects. A third feature of these curves is that after the initial curvilinear portion the curves become linear. This is a desirable rock property because it allows accurate prediction of rock behaviour under load. This linearity also means that the working modulus calculated for the upper 50% of the loading curve very nearly approaches a tangent modulus for this curve.

In order to reduce the data to a form more easily analyzed, distribution diagrams were prepared for first and second cycle

LABORATORY TESTING

AXIAL STRESS vs. AXIAL STRAIN

Sample No. N6

Rock Type quartzite gneiss

First cycle ——— Second cycle - - - - - -

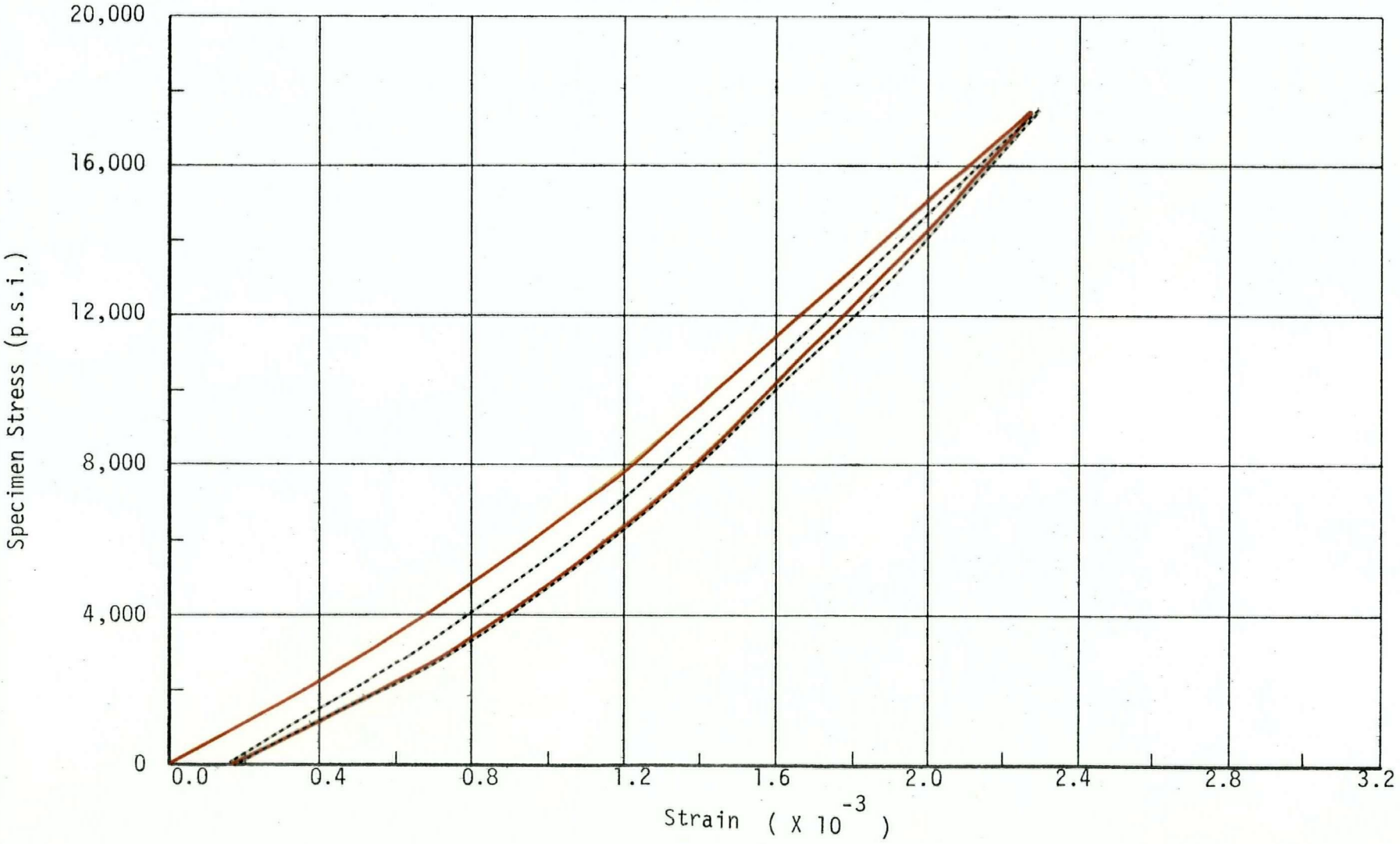

Figure 14

LABORATORY TESTING

AXIAL STRESS vs. AXIAL STRAIN

Sample No. N23

Rock Type quartzite gneiss

First cycle ——— Second cycle - - - - - -

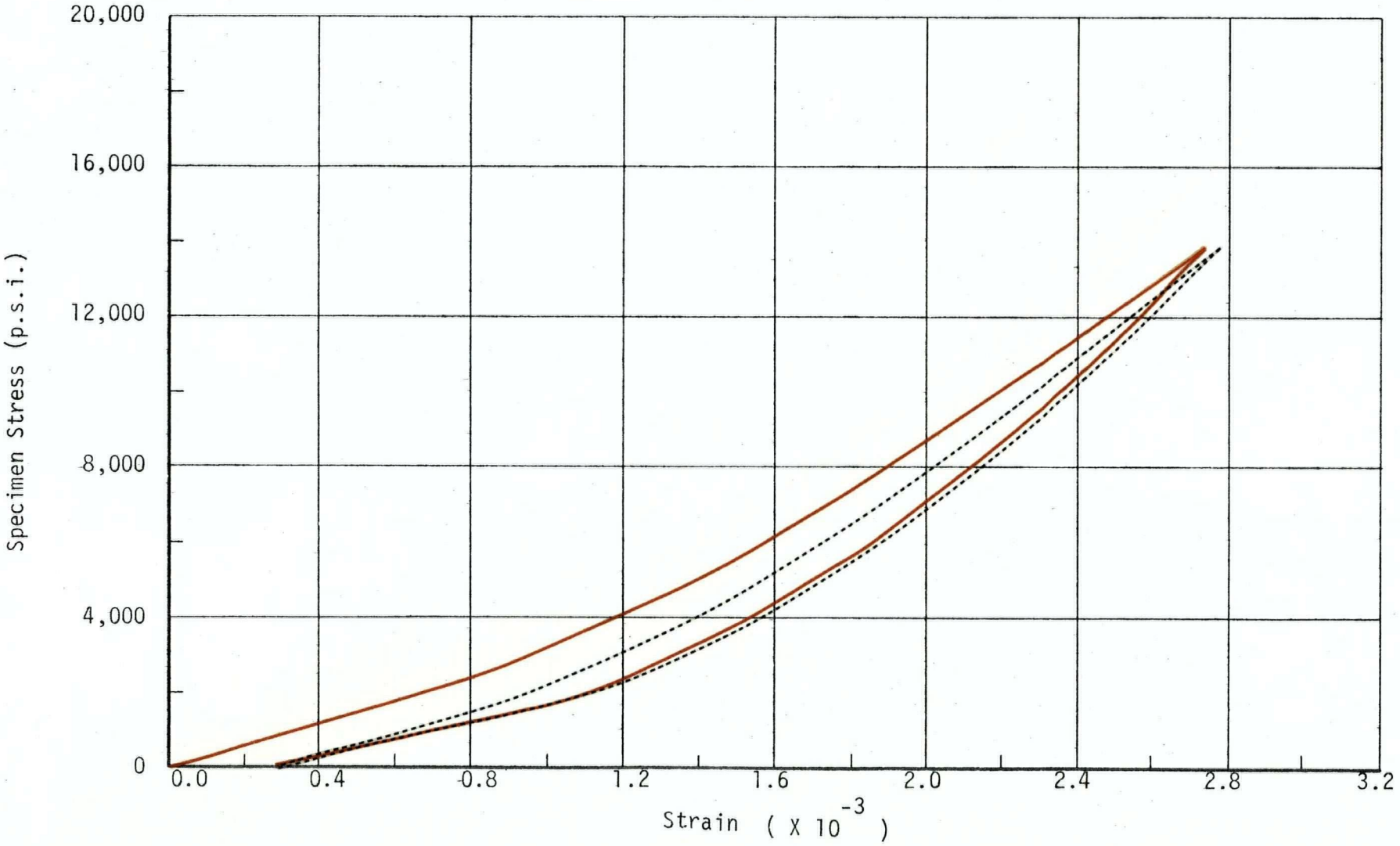

Figure 15

LABORATORY TESTING

AXIAL STRESS vs. AXIAL STRAIN

Sample No. N93

Rock Type guartzite

gneiss

First cycle ——————

Second cycle - - - - - - - - - - - - - - - - - - -

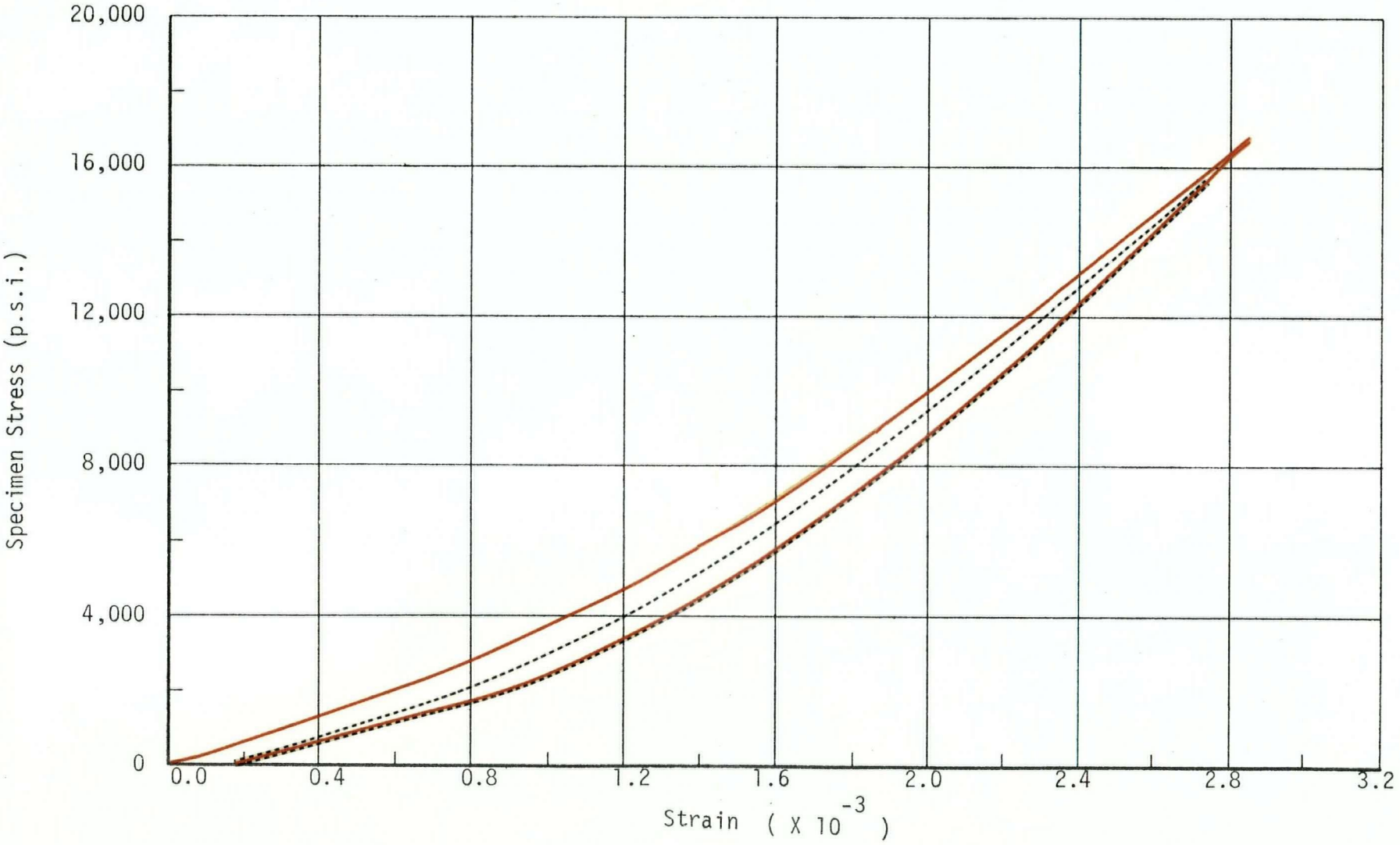

Figure 16

deformation moduli. Figure 17 shows distribution diagrams for first and second cycle working modulus for those gneiss samples where both loading cycles were completed. The significant features of these distribution diagrams are as follow:

1. The mean and standard deviation of the first cycle working modulus are 7.86×10^6 psi and 1.04×10^6 psi respectively. The standard deviation expressed as a percent of the mean, known as the coefficient of variation, is 13%.
2. The mean and standard deviation of the second cycle working modulus are 8.41×10^6 psi and 0.94×10^6 psi respectively. The coefficient of variation is 11%.
3. Although the distributions are slightly skewed, there is suggestion that both first and second cycle distributions are approaching the normal distribution. This is a questionable statement due to the small number of test results.

The fact that the second cycle mean working modulus is 7% greater than that of the first cycle must be related to the fact that very little inelastic deformation is occurring on the second cycle. That is, the closure of microfractures and porosity takes place during the first loading cycle resulting in a lower modulus. By listing the second cycle working moduli along with the corresponding sample descriptions no relationship is obvious between modulus and any of the following: grain size, foliation, or chloritization. This fact supports the hypothesis that the modulus values should be normally distributed.

Figure 17

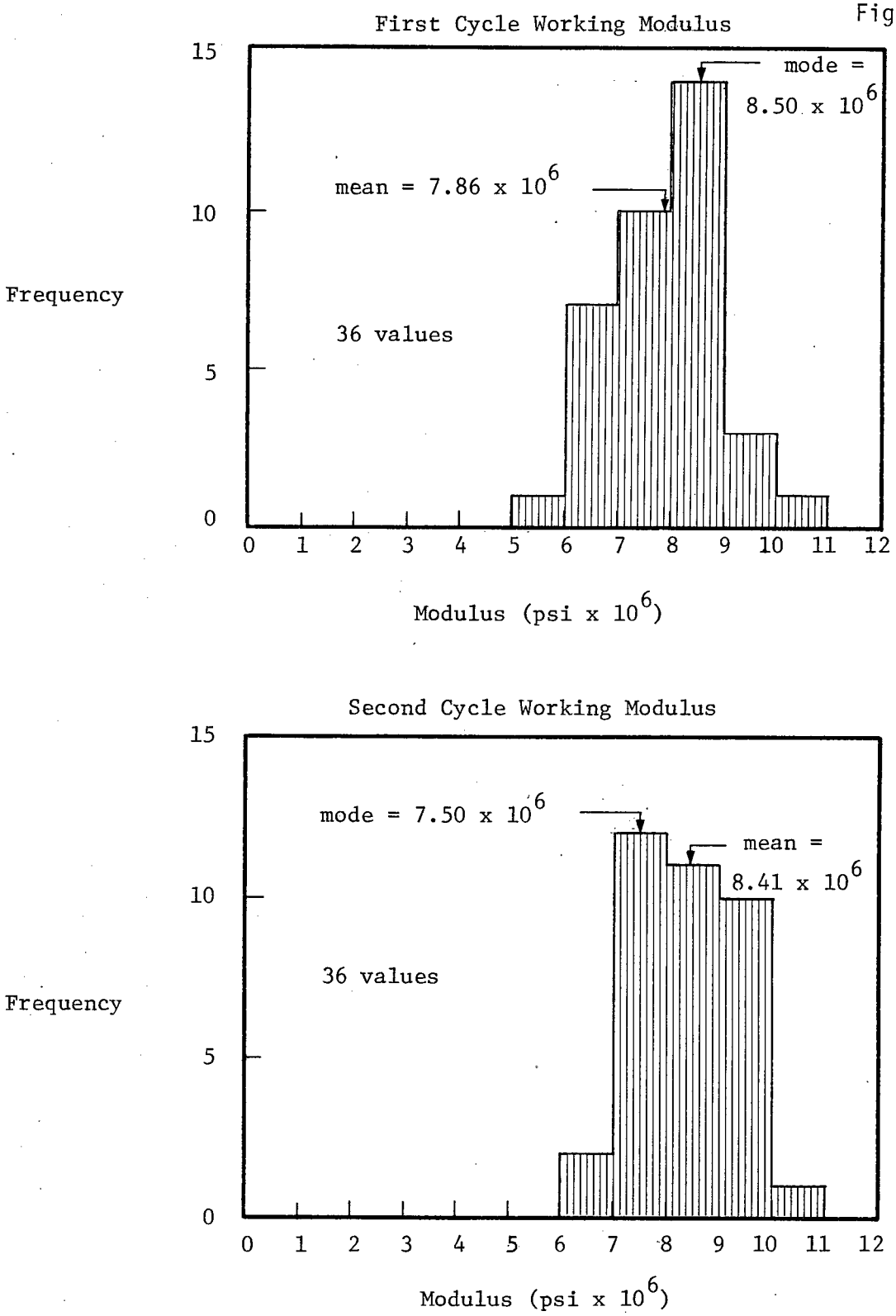

FREQUENCY HISTOGRAMS FOR LABORATORY TESTS OF QUARTZITE GNEISS

Although very few gneiss samples exhibited foliation, the anisotropy of this rock type can be investigated by plotting modulus versus foliation angle. The foliation angle for this report is defined as the acute angle between the axis of the sample (i.e. loading direction) and the plane of the foliation. Figure 18 shows the plots of first and second cycle working modulus versus foliation angle. From the limited data available the relationship between working modulus and orientation of mica particles is uncertain.

An important property of rock, from a design viewpoint, is its ability to undergo permanent deformation upon loading. This inelastic behaviour becomes important in rock structures subject to cyclic loading. The inelasticity of the rock samples tested in the laboratory was quantitatively studied using two parameters:

1. The percentage elastic recovery for the complete test loading and for the second cycle of loading.
2. The ratio of the working modulus to the secant modulus.

The quartzite gneiss samples had an average 93% elastic recovery for the entire test loading. This value ranged from 84% to 96% indicating that the gneiss samples undergo small amounts of permanent deformation. The elastic recovery for the second cycle of loading ranged from 98% to 99.8% with an average of 99.3%. This conclusively shows that the gneiss is almost perfectly elastic after the first loading cycle.

ANISOTROPY DIAGRAMS FOR QUARTZITE GNEISS

(Laboratory Testing)

Figure 18

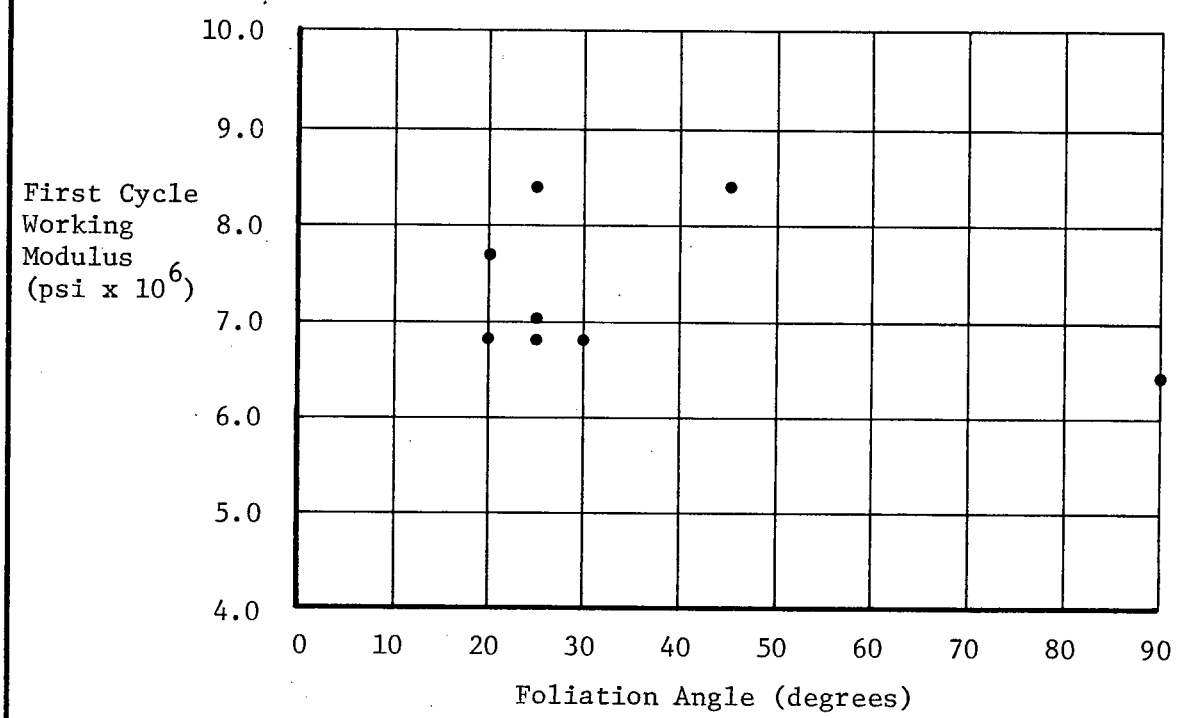

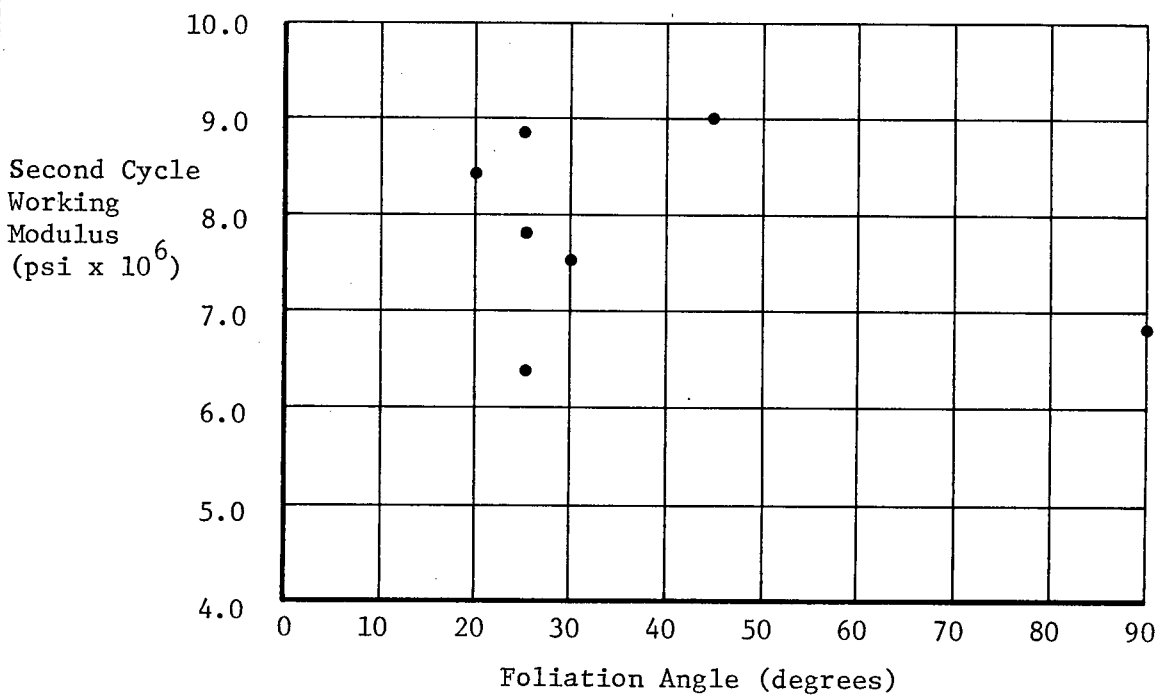

As previously stated a working modulus significantly greater than the secant modulus is an indication of open fractures in a rock sample. A ratio of E_w to E_s significantly greater than 1.0 would indicate likewise. For the gneiss samples, the ratio, E_w/E_s ranged from 1.09 to 1.47 and averaged 1.22. This indicates the laboratory samples are relatively free of open fractures thereby reinforcing the above conclusion that the gneiss samples have elastic deformation characteristics.

2. Quartz Feldspar Schist

Twenty-three quartz feldspar schist samples were tested all of which yielded usable results. This rock type exhibits distinct foliation so that all modulus values must be related to this feature.

The schist samples were fitted with four axial strain gauges. These gauges were located with respect to the foliation (Figure 5) so that one set was located parallel to the strike direction while the second set was located parallel to the dip direction. By monitoring these sets of gauges on individual strain boxes, results were obtained which would illustrate the deformation characteristics in these two directions.

Figures 19 through 24 illustrate stress-strain curves for the strike and dip direction of three samples. These figures show the range of deformation behaviour exhibited by the schist samples. Figures 19 and 20 show the behaviour of samples with a high foliation angle (70 to 90 degrees). These samples are characterized by large deformations,

Sample No. N40 strike

Foliation Angle 70°

LABORATORY TESTING

AXIAL STRESS vs. AXIAL STRAIN

Rock Type quartz-feldspar-schist

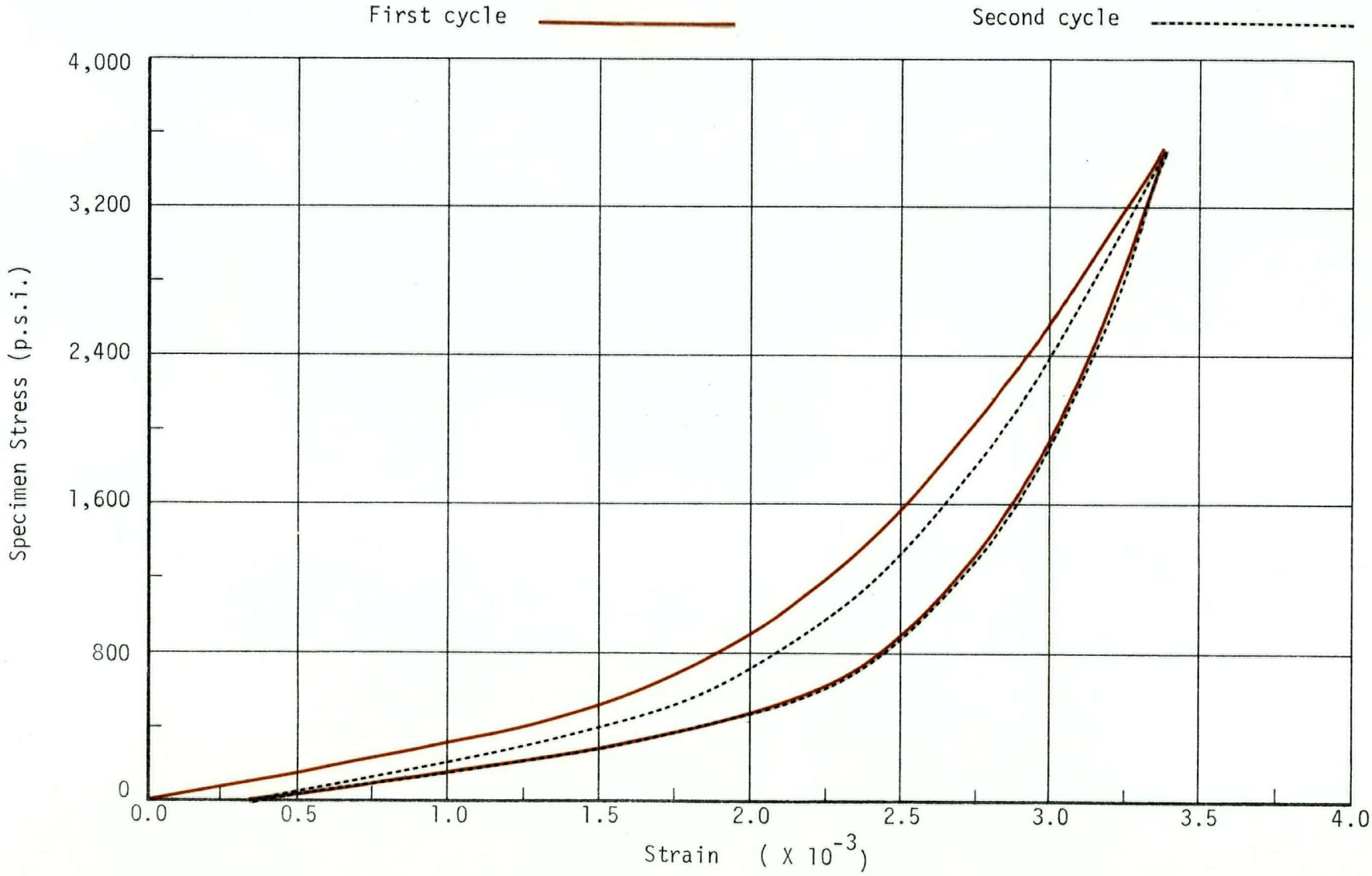

Figure 19

Sample No. N40 dip

Foliation Angle 70°

LABORATORY TESTING

AXIAL STRESS vs. AXIAL STRAIN

Rock Type quartz-feldspar-schist

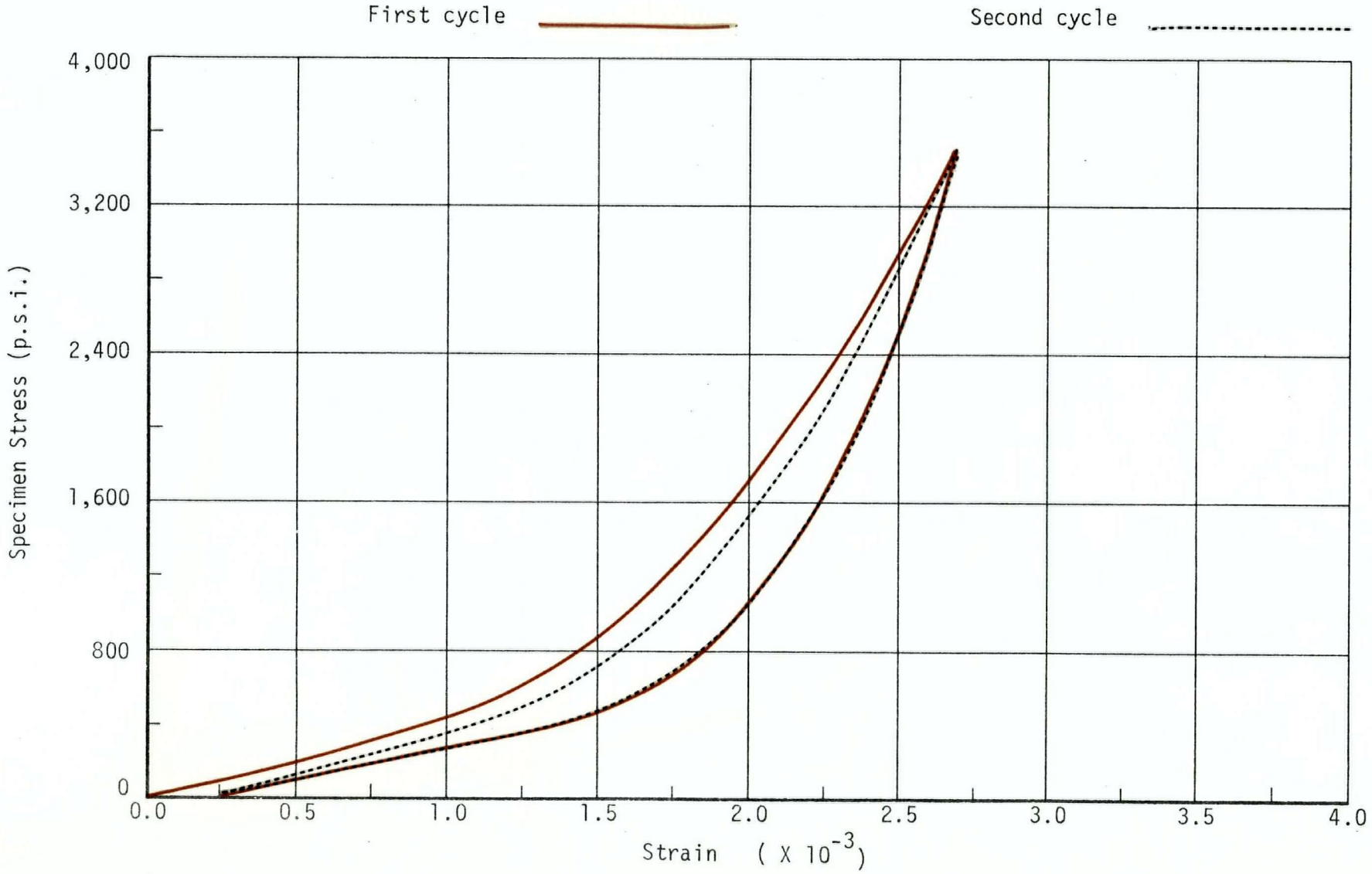

Figure 20

Sample No. N70 strike

Foliation Angle 0°

LABORATORY TESTING

AXIAL STRESS vs. AXIAL STRAIN

Rock Type quartz-feldspar-schist

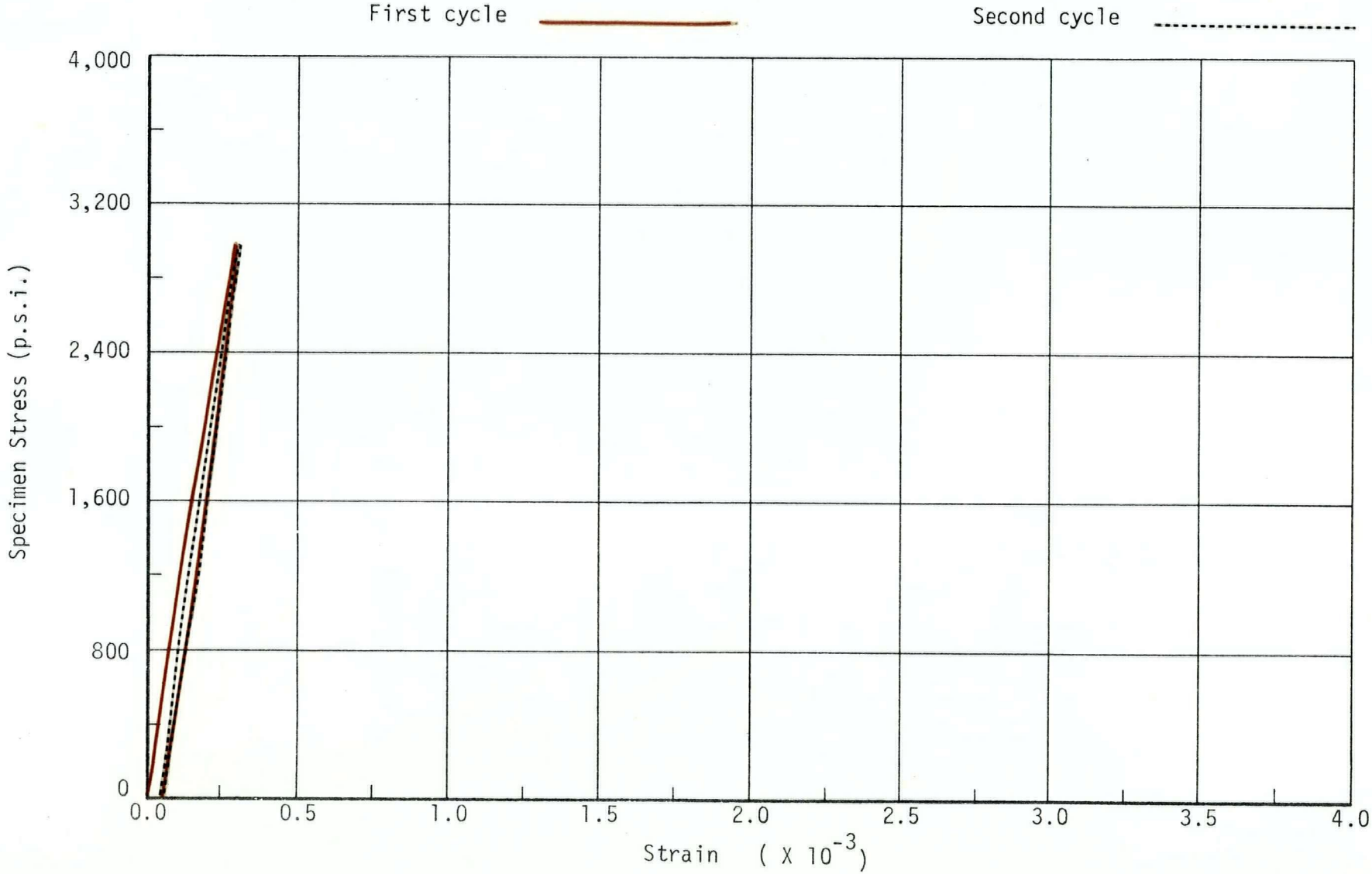

Figure 21

Sample No. N70 dip

Foliation Angle 0°

LABORATORY TESTING

AXIAL STRESS vs. AXIAL STRAIN

Rock Type quartz-feldspar-schist

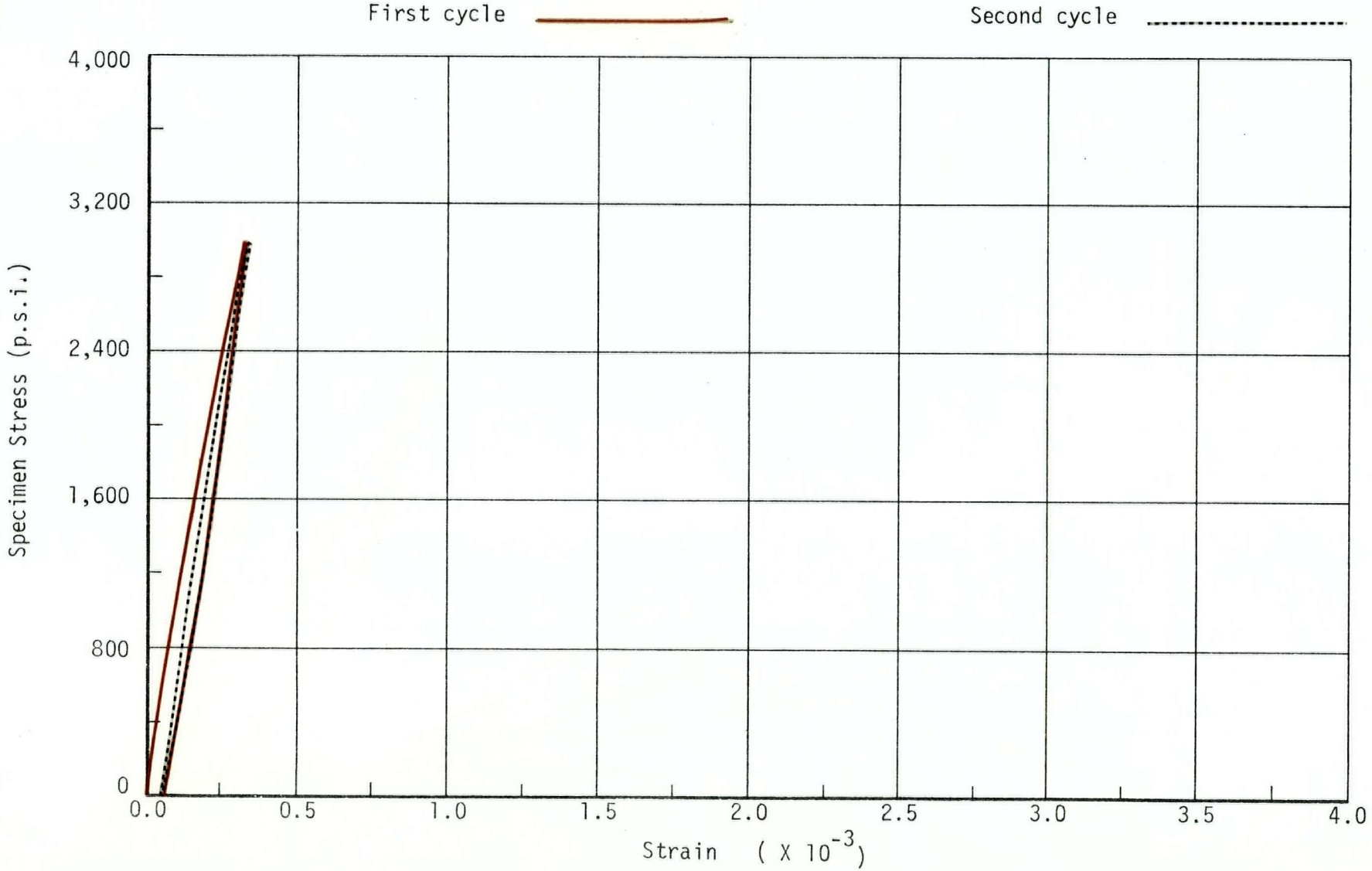

Figure 22

Sample No. N202 strike

Foliation Angle 35°

LABORATORY TESTING

AXIAL STRESS vs. AXIAL STRAIN

Rock Type quartz-feldspar-schist

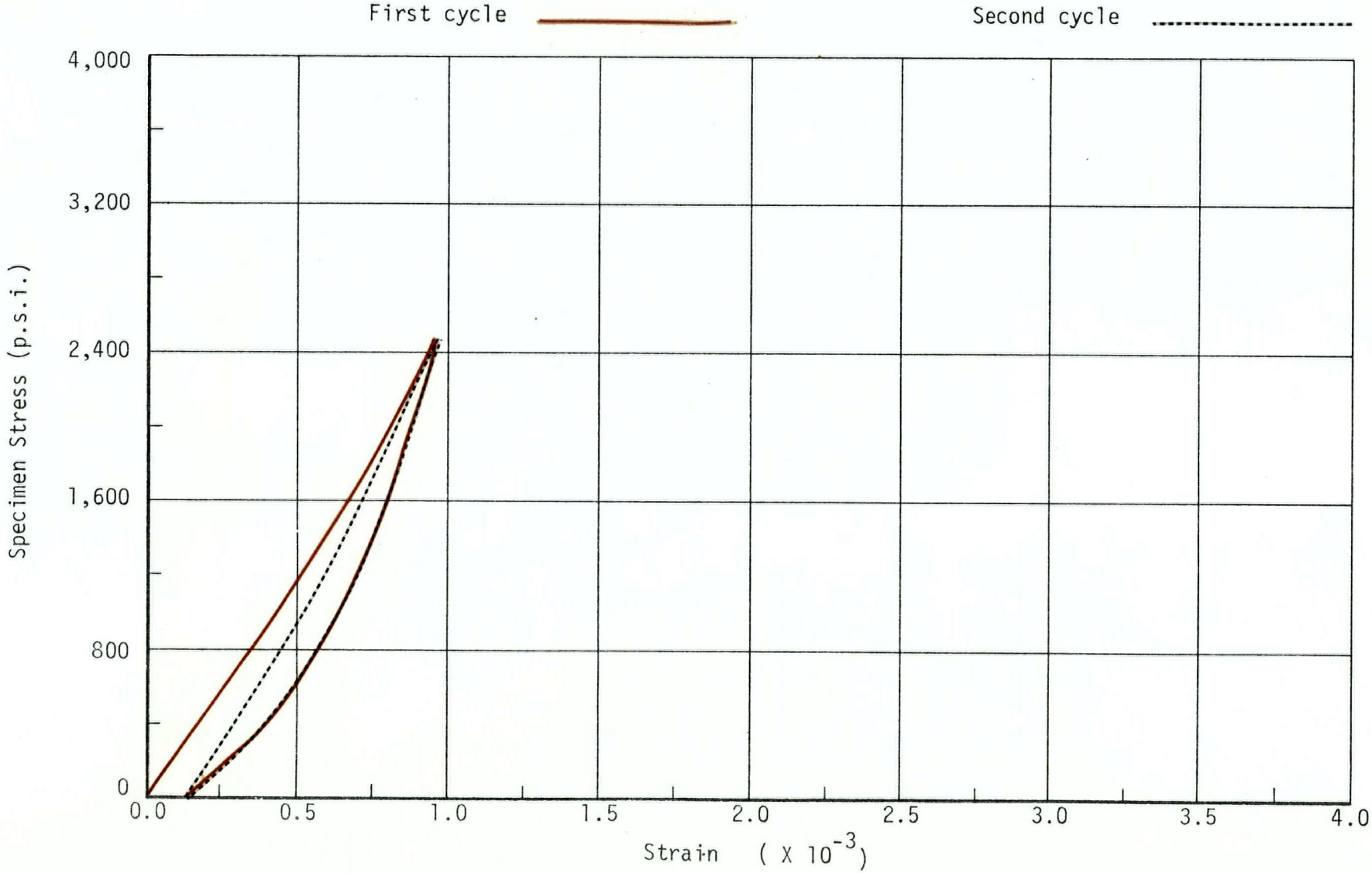

Figure 23

Sample No. N202 dip

Foliation Angle 35°

LABORATORY TESTING

AXIAL STRESS vs. AXIAL STRAIN

Rock Type quartz-feldspar-schist

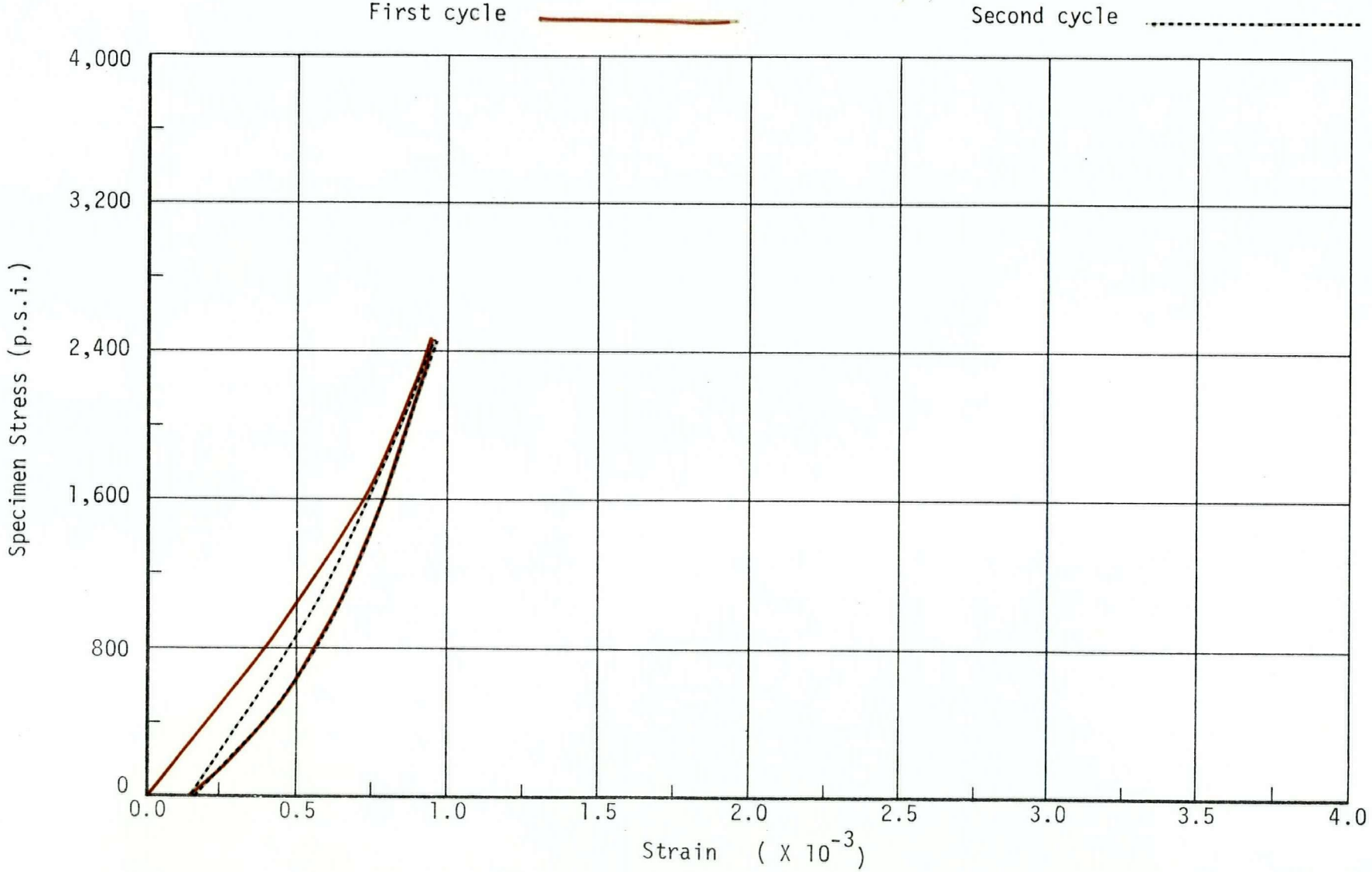

Figure 24

non-linear stress-strain curves, notable permanent deformations and significant hysteresis losses.

Figures 21 and 22 are representative of samples with low foliation angles (0 to 20 degrees). The most striking features of these samples are the small deformations and the almost linear stress-strain curves. These samples also exhibit small permanent deformations and insignificant hysteresis effects.

Figures 23 and 24 illustrate the deformation behaviour of samples with intermediate foliation angles. (30 to 60 degrees). Although these samples tend to have the lowest modulus values, their behaviour is intermediate to the samples with high and low foliation angles. A quantitative analysis of the properties exhibited by the stress-strain curves will follow.

Since the schist samples were fitted with two sets of strain gauges, the modulus values for a particular sample were taken as the average of the values for the strike and dip directions. Distribution diagrams for the first and second cycle working modulus are shown in Figure 25. The significant features of these distribution diagrams are as follows:

1. First cycle working modulus:

   mean = 3.64×10^6 psi

   standard deviation = 2.12×10^6 psi

   coefficient of variation = 58%

2. Second cycle working modulus

   mean = 4.32×10^6 psi

Figure 25

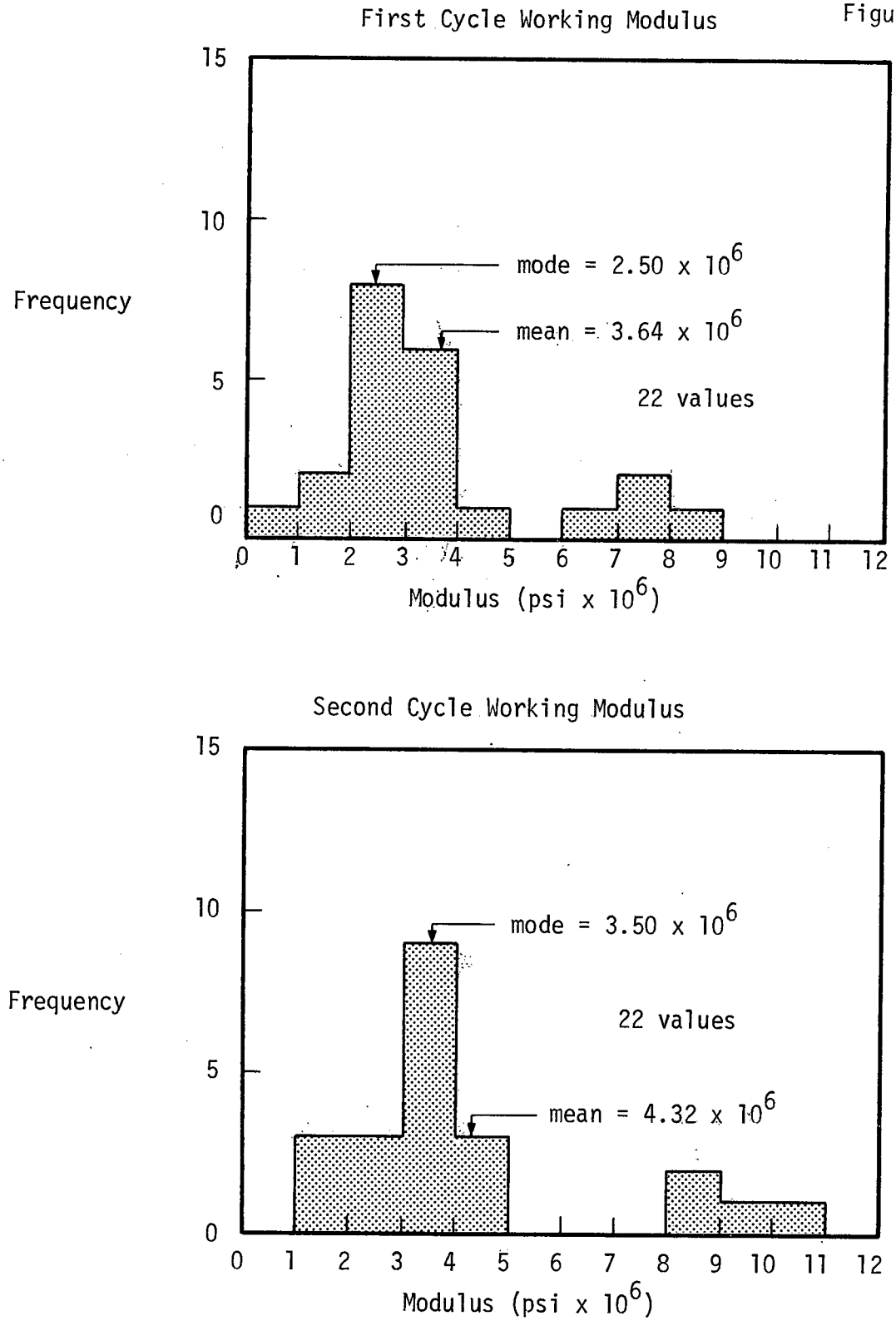

FREQUENCY HISTOGRAMS FOR LABORATORY TESTS OF QUARTZ FELDSPAR SCHIST

standard deviation = 2.58×10^6 psi

coefficient of variation = 60%

3. The modulus values have a wide range.

The large standard deviations and wide range of modulus values reflect the dependence of the modulus upon the foliation angle.

The anisotropy of the quartz feldspar schist samples is clearly illustrated in Figure 26. Note that this diagram assumes that the schist is transversly isotropic, in other words, the modulus is constant within the plane of the foliation. The very high values of modulus for low foliation angles can be explained as follows. If the quartz and feldspar layers within the schist are assumed to be continuous, loading parallel to these layers would result in a disproportionately high percentage of the load being carried by these layers. Thus the quartz and feldspar layers are acting as high modulus inclusions causing low deformations and high modulus values. The low modulus values of intermediate foliation angles are most easily explained by the fact that at these angles the foliation is favourably oriented for inter-layer slippage. This would result in high strains and low modulus values. The slight increase in modulus values for high foliation angles is probably due to the fact that little inter-layer movement occurs and deformation is due mainly to the compression of micaceous layers.

The deformation characteristics of the schist samples as monitored in the strike and dip directions are illustrated by Figure 27.

ANISOTROPY DIAGRAM FOR QUARTZ FELDSPAR SCHIST

Laboratory Testing

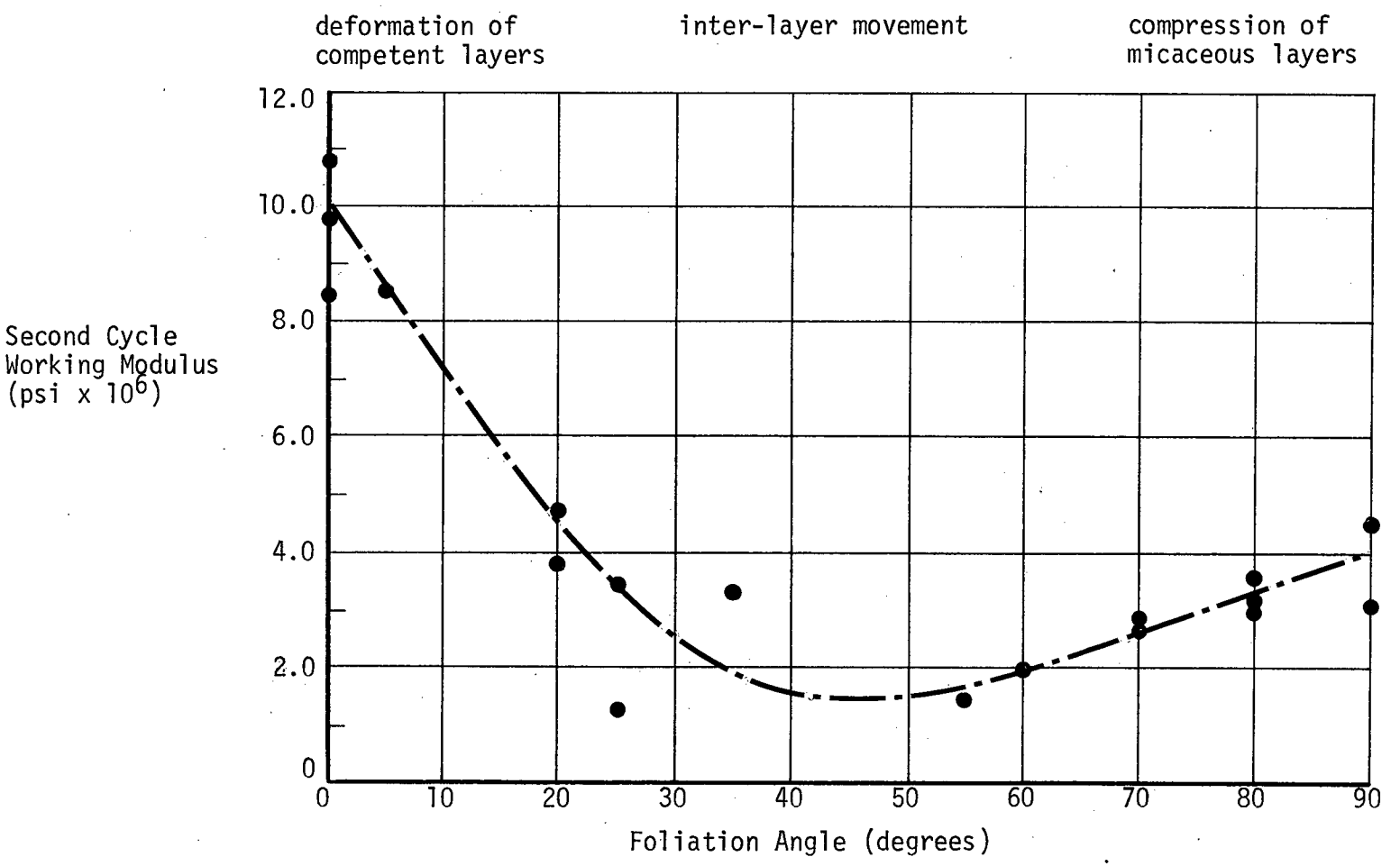

Figure 26

RATIO OF $E_{w\ strike}/E_{w\ dip}$ vs. FOLIATION ANGLE

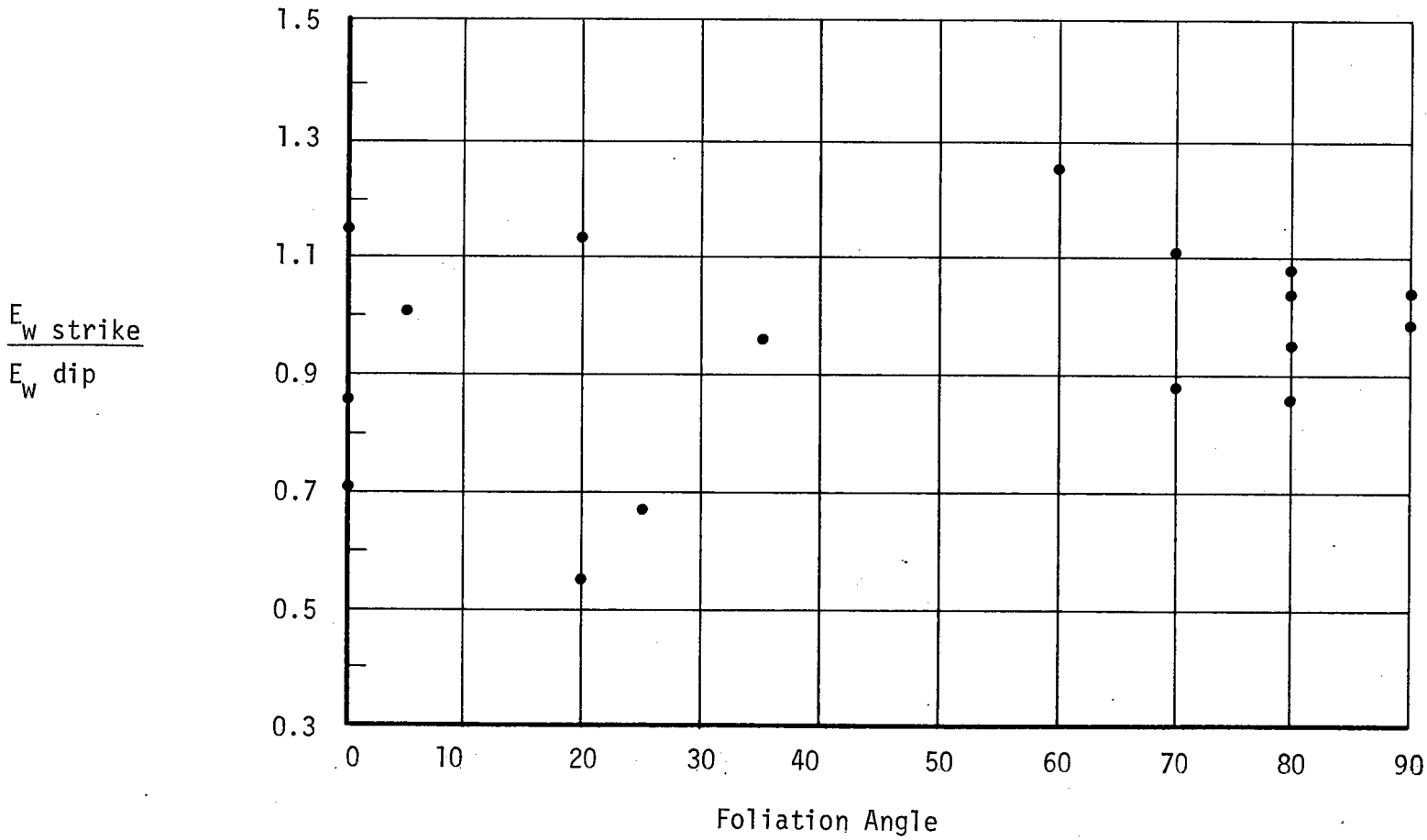

Figure 27

This figure shows a plot of the ratio $E_{w\ strike}/E_{w\ dip}$ versus foliation angle. The graph shows that at high foliation angles the ratio approaches unity with little scatter. This is to be expected since, at a foliation angle of 90 degrees strike and dip directions are indistinguishable and the ratio should thus be unity. For low foliation angles the ratio, $E_{w\ strike}/E_{\ dip}$, shows much variation. This is probably due to the fact that inter-layer movements account for most of the deformation. These inter-layer movements probably localize along one or more foliation planes and thus the movements may be detected by only one set of gauges. This would cause variation of the working modulus ratio. Note that if all four strain gauges were mounted across the same inclined foliation plane the working modulus ratio would be unity assuming the inter-layer movement was uniform on this plane. This means that axial strain gauges mounted in the strike and dip directions cannot be used to detect inter-layer movement. They are useful to determine an average modulus for the rock sample.

The elastic recovery of the quartz feldspar schist samples for the entire loading averaged 84%. This value ranged from 78% to 92% indicating that significant permanent deformation occurs in this rock type. The elastic recovery for the second cycle averaged 99% and shows that the schist samples deform elastically after the first loading cycle. Figure 28 shows the variation of the elastic recovery with foliation angle. The scatter of the plot indicates that each of the deformation mechanisms has variable elastic recoveries. This places some doubt on the mechanisms shown in Figure 26 but does not rule them out.

VARIATION OF ELASTIC RECOVERY WITH FOLIATION ANGLE

Laboratory Testing of Quartz Feldspar Schist

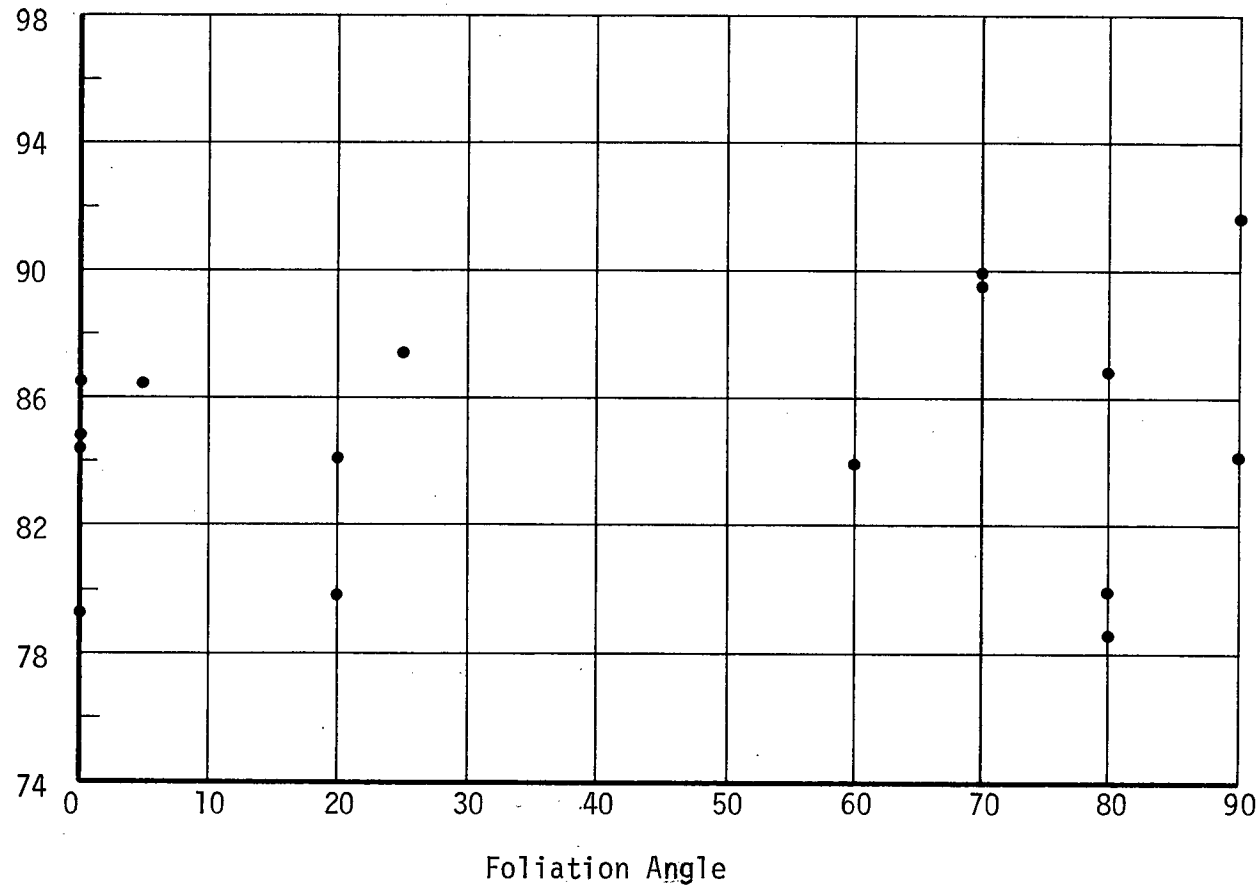

Figure 28

Figure 29 illustrates the variation of the ratio, E_w/E_s, with the foliation angle. This ratio is an indication of open fractures in the sample or of a plastic material. The graph indicates that at low foliation angles few open fractures are suitably oriented to deform. Thus the sample deforms by longitudinal compression of the layering. At high foliation angles many open fractures are available to deform as indicated by the large ratio values. These results tend to confirm the deformation mechanisms of Figure 26.

C. Pegmatite

Only six pegmatite samples were tested in the laboratory programme. Of these, one sample failed at about 11,000 psi so that only five samples yielded results. Obviously statistical studies could not be carried out for this rock type. Figures 30 and 31 illustrate representative stress-strain curves for pegmatite samples. These figures indicate that the stress-strain curves are non-linear and that the deformations are highly elastic. The narrow width of the load-unload cycles means that hysteresis losses are very small.

The average working moduli for the first and second loading cycles were 5.40×10^6 psi and 6.27×10^6 psi. The fact that the second cycle working modulus is 16% greater than that of the first cycle again illustrates that very little inelastic deformation occurs after the first cycle. This is also emphasized by the fact that the elastic recovery for the entire loading averaged 89% while for the second cycle it averaged 99%.

VARIATION OF THE RATIO E_w/E_s WITH FOLIATION ANGLE

Laboratory Testing of Quartz Feldspar Schist

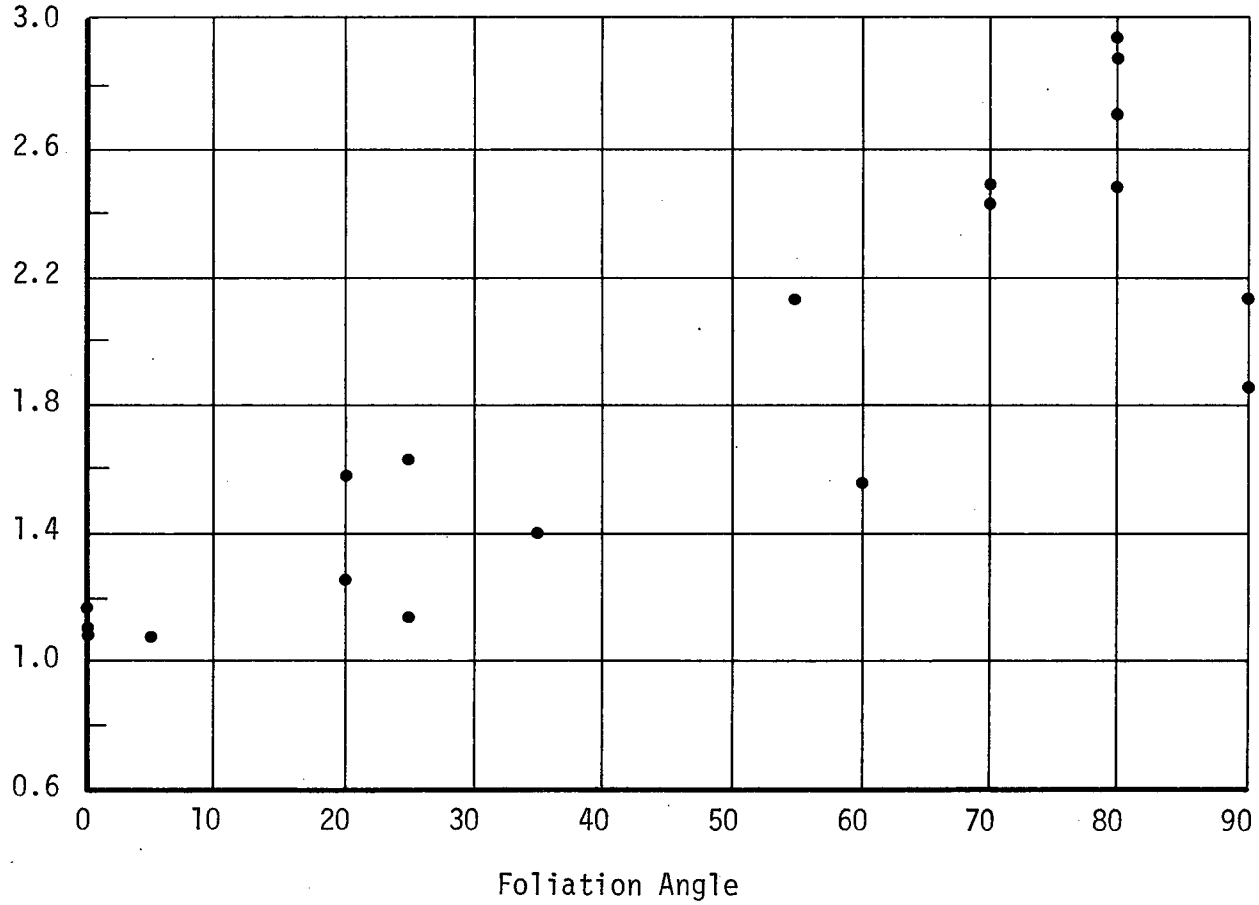

Figure 29

LABORATORY TESTING

AXIAL STRESS vs. AXIAL STRAIN

Sample No. N31

Rock Type pegmatite

First cycle ——————

Second cycle -

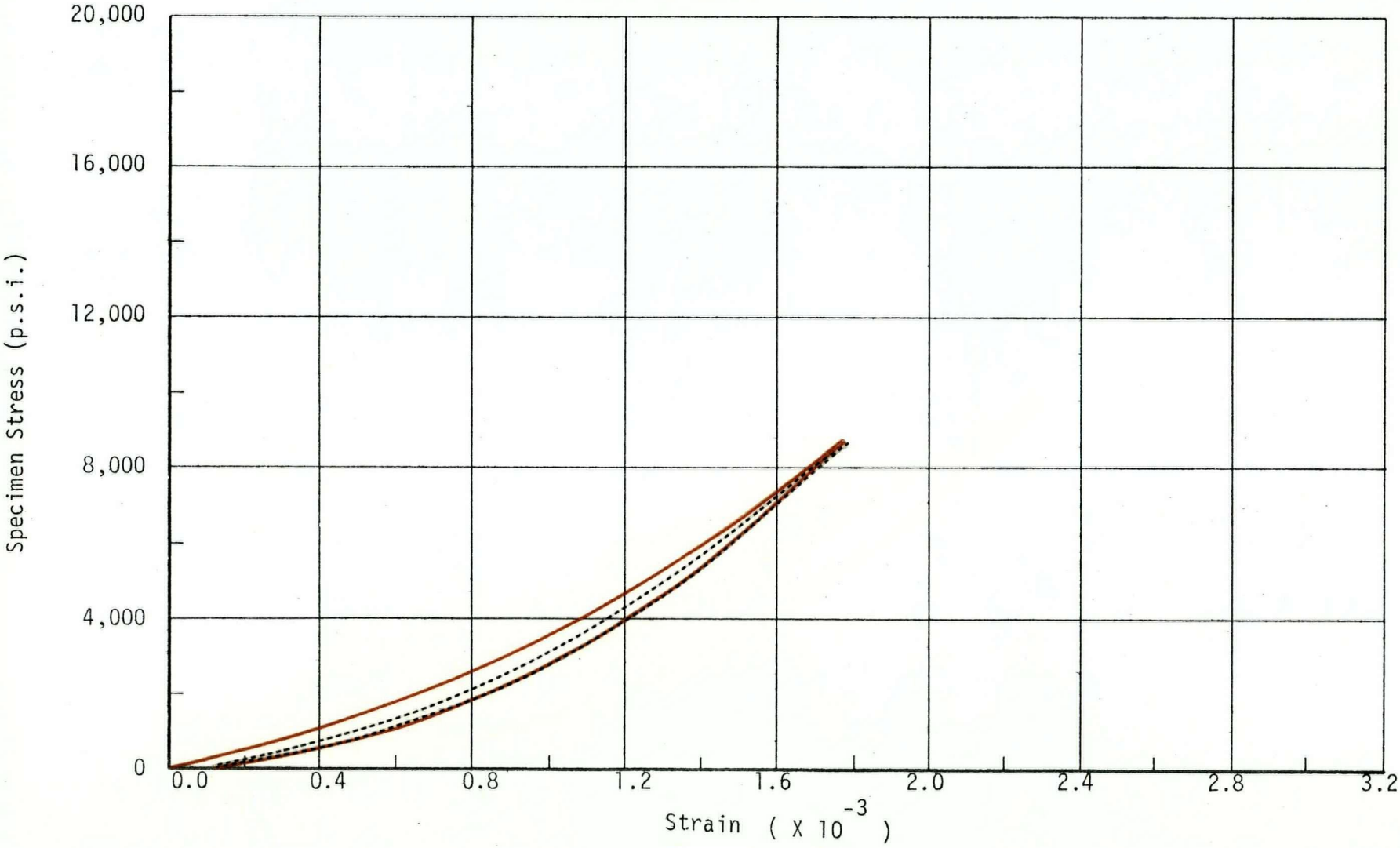

Figure 30

LABORATORY TESTING

AXIAL STRESS vs. AXIAL STRAIN

Sample No. N33

Rock Type pegmatite

First cycle ——————

Second cycle -

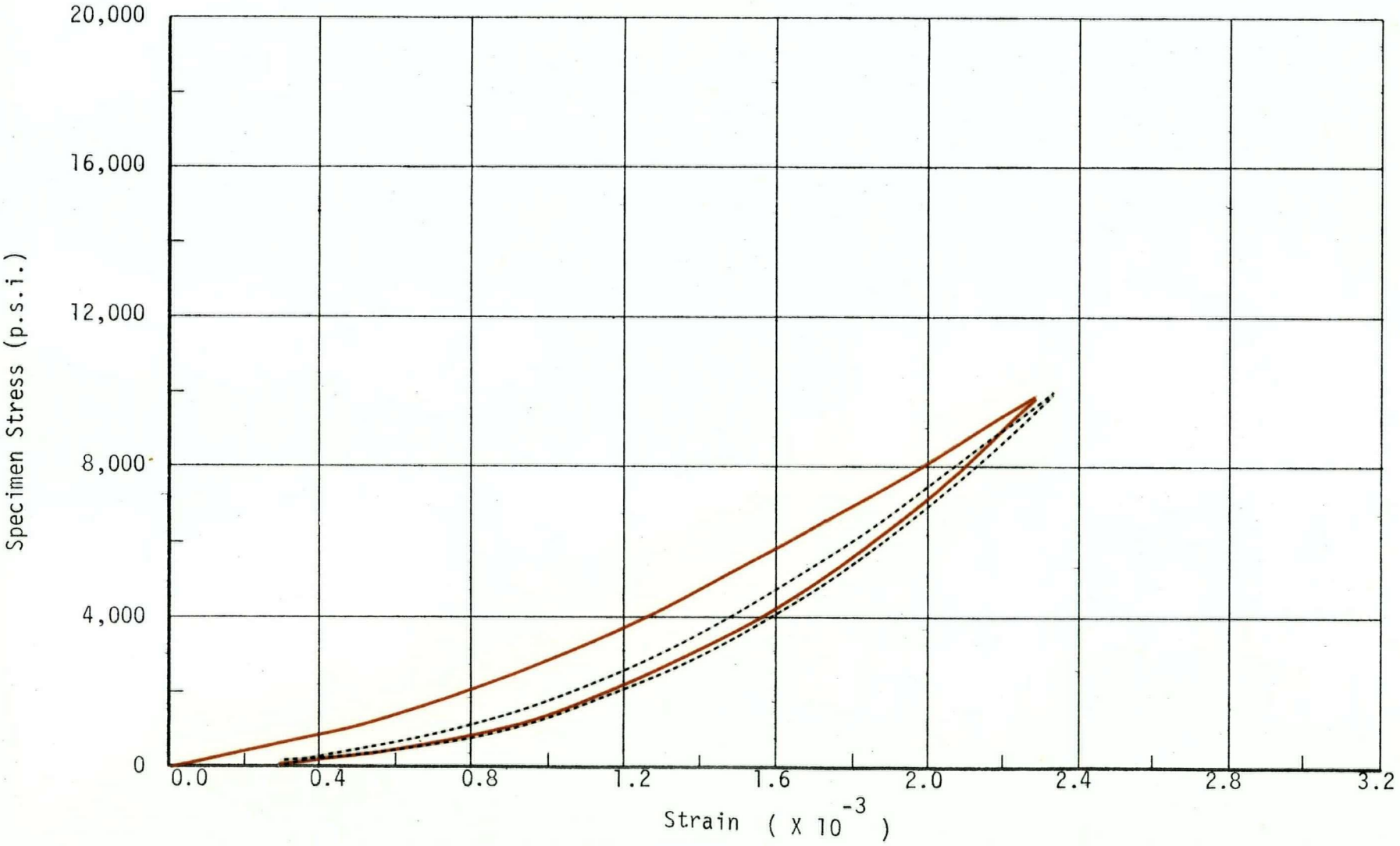

Figure 31

4. Summary and Comparison of Laboratory Results

The relationship between second cycle working modulus and unit weight for the laboratory samples is shown in Figure 32. Two conclusions can be drawn from this graph. Firstly, the three rock types are readily classified on the basis of modulus and unit weight. Secondly, the working modulus and unit weight have an approximate inverse relationship. This is due to the fact that the more deformable micaceous minerals are also the heaviest.

The results of the laboratory testing programme are summarized in Table 2 for easy comparison of rock types.

Referring to Table 2 it is noted that the average second cycle working modulus for the quartzite gneiss is 1.9 times that of the quartz feldspar schist and 1.3 times that of the pegmatite. As indicated by the standard deviation and range of working modulus values, the schist samples exhibited far greater variability. As previously shown, this variation is due to the foliation.

Comparison of the stress-strain curves for the three rock types shows that the gneiss and low foliation angle schist samples have linear stress-strain curves. The high foliation angle schist and pegmatite samples tend to have non-linear curves. All rock types except high angle schists exhibit negligible hysteresis effects. This condition in high angle schist probably reflects frictional losses in the compression of the micaceous layers.

The average elastic recovery for all rock types is suitably high for engineering purposes; 85% being considered satisfactory. However, the schist samples are quite variable, ranging from 75 to 90%

VARIATION OF MODULUS WITH UNIT WEIGHT FOR VARIOUS ROCK TYPES

(Laboratory Testing)

• = quartzite gneiss, + = quartz feldspar schist, * = pegmatite

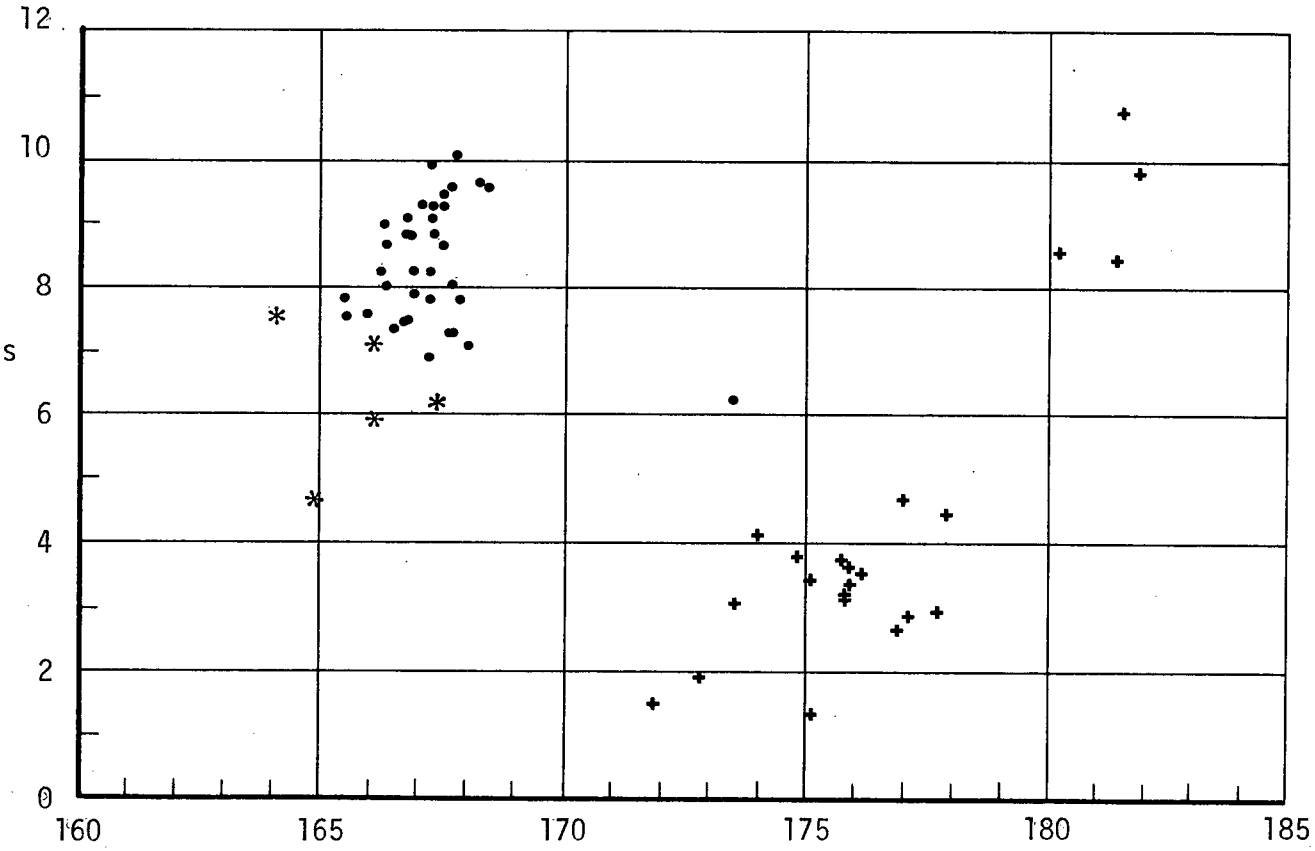

Figure 32

TABLE 2

SUMMARY OF LABORATORY RESULTS

Note: All modulus values in psi x 10^6

	Property	Quartzite Gneiss	Quartz Feldspar Schist	Pegmatite
a.	Number of samples	42	23	6
b.	Mean second cycle secant modulus	6.40	3.06	3.86
c.	Mean second cycle recovery modulus	6.88	3.68	4.32
d.	Mean first cycle working modulus	7.86	3.64	5.40
e.	Standard deviation of d	1.04	2.12	1.08
f.	Coefficient of variation	13%	58%	20%
g.	Mean second cycle working modulus	8.41	4.32	6.27
h.	Standard deviation of g	0.94	2.61	1.13
i.	Coefficient of variation	11%	60%	18%
j.	Range of second cycle working modulus	6.26 to 10.1	1.32 to 10.7	4.64 to 7.55
k.	% E_w second cycle greater E_w first cycle	7%	19%	16%
l.	Average % elastic recovery for total test	93%	84%	89%
m.	Average % elastic recovery for second cycle	99%	99%	99%
n.	Average ratio, E_w/E_s	1.22	1.78	1.66

The gneiss samples are the most elastic followed by the pegmatite and the schist samples. This indicates that the inelastic deformations may be related to mica content.

Comparison of properties numbered k and n in Table 2 shows a correlation between the percentage increase of the second cycle working modulus over the first cycle and the average ratio, E_w/E_s. These results indicate that the gneiss samples are relatively free of micro-fracturing compared to the schist and pegmatite samples. This is reasonable for the well foliated schist samples but is hard to explain for the pegmatite. A possible explanation is that the large grains of the pegmatite are not well connected thereby allowing inter-granular movement under load.

B. Goodman Jack Testing

During the course of the jack testing 129 test were performed. Many of these individual tests consisted of 3 or 4 loading cycles. Great care was taken to divide these tests by rock type. This was done by comparing the test depth with the bore hole logs. Any test that was carried out within one foot of a rock type boundary was rejected and not included in the results of this thesis. As for the laboratory testing, the rock types considered were quartzite gneiss, quartz feldspar schist and pegmatite.

In the case of the jacking tests the working modulus was determined over the upper 2/3 of the stress-deformation curve. Generally, this portion of the curve was linear and expressed the behaviour of the rock.

It is again pointed out that the Goodman Jack tests yielded stress-deformation curves rather than stress-strain curves. The reason for this is that no deformation readings could be taken for the first load increment. As a result the percent elastic recovery is an approximation calculated from the residual deformation at 1000 psi hydraulic pressure. Also, the ratio of working modulus to secant modulus, an indication of open fractures within the rock or bore hole wall roughness, is less valuable. The reason being that a large portion of the inelastic deformation will occur in the first load increment and will not be reflected by the secant modulus.

As stated in the section dealing with the interpretation of the test data, a constant dependent upon Poisson's ratio is necessary to calculate modulus values. The following values for Poisson's ratio were thus assumed:

quartzite gneiss: 0.20

quartz feldspar schist: 0.35

pegmatite: 0.20

In order to investigate the anisotropy of the rock mass it is necessary to know the orientation of the jack loading with respect to the foliation planes, which, as previously defined, is the foliation angle. In other words, it is necessary to know the orientation of the bore hole and the attitude of the rock foliation at the exact positions where the tests are performed. Ideally,oriented core or a bore hole camera technique would provide this information. Since neither of these techniques were available an alternative method was utilized.

The necessary data for the method consisted of:

1. Orientation of the bore hole (assumed constant along length).
2. Angle between axis of core and foliation plane at the test location (obtained from drill log).
3. An assumed strike for the foliation planes which was appropriate for the particular bore hole (extrapolated from mapping of the exploratory drift).
4. Orientation of the Goodman Jack in the bore hole.

Points 1 and 2 could be determined quite accurately. In spite of the overall consistent strike direction at the test site, local irregularities did occur. Thus point 3 introduced most of the error into the analysis. The Goodman Jack was oriented in the bore hole by rotating the insertion rods in such a way that an orientation convention was maintained with the exploratory drift (see Figure 8). Thus an error of about 5 degrees could be introduced by point 4 but in the majority of cases would be much less than point 3.

These four points of data were analyzed by sterographic projection to determine the spatial arrangement of loading directions and foliation planes. This method is illustrated by example in Appendix 4.

The complete results of the jack testing are presented in Appendix 5. These results are now analyzed in terms of specific rock type.

1. Quartzite Gneiss

Thirty Goodman Jack tests were carried out in the quartzite gneiss. Figures 33, 34 and 35 are stress-deformation curves that illustrate the range of the quartzite gneiss behavior.

Figures 33 and 34 illustrate the average deformation characteristics of the gneiss. The curves exhibit linearity after the first load increments, particularly on second and subsequent loading cycles. Permanent deformations are significant, approaching 40% for the total test loading. The coincidence of second and subsequent loading loops indicates the deformation is elastic after the first cycle. Actual hysteresis effects are generally insignificant when the effect of transducer backlash is eliminated.

Figure 35 illustrates quartzite gneiss behaviour which deviates from the normal. The noteworthy features of this graph are that significant inelastic deformation occurs on both loading cycles and that the hysteresis losses are greater than normal.

Distribution diagrams for the first and second cycle working modulus are shown in Figure 36. The significant features of these diagrams are as follows:

1. First cycle working modulus:

   mean = 1.95×10^6

   standard deviation = 0.38×10^6

   coefficient of variation = 19%

Hole No. NX - 2

Depth 85.0 ft.

Goodman Jack Testing

APPLIED LOAD vs. DIAMETRAL BORE HOLE DEFORMATION

Orientation 90°

Rock Type quartzite gneiss

First cycle ——— Second cycle ..... Third cycle – – ———

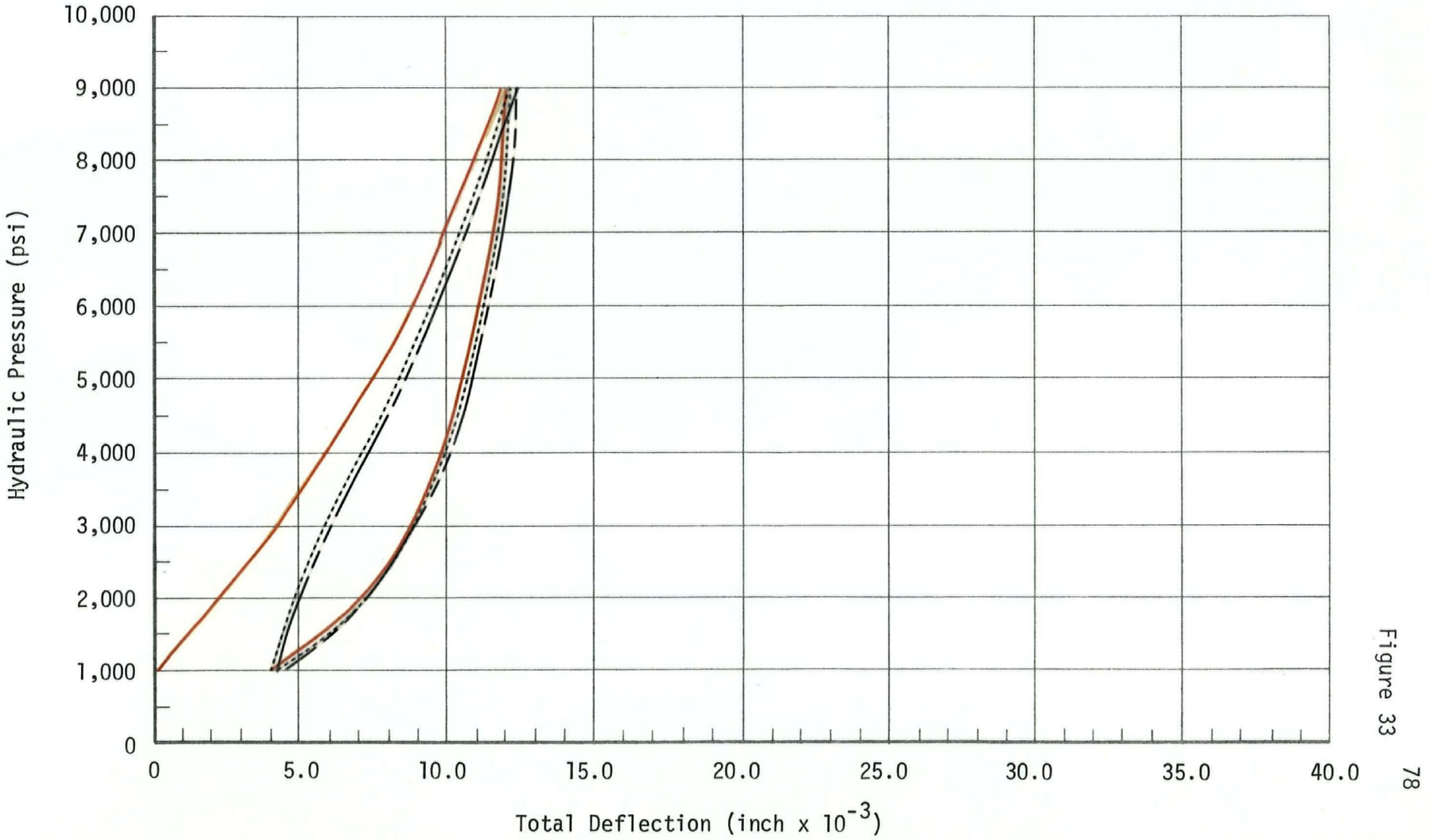

Figure 33

Hole No. NX - 7

Depth 50.0 ft.

Goodman Jack Testing

APPLIED LOAD vs. DIAMETRAL BORE HOLE DEFORMATION

Orientation 90°

Rock Type quartzite gneiss

First cycle ——— Second cycle - - - - - - - - - - Third cycle ——— — —

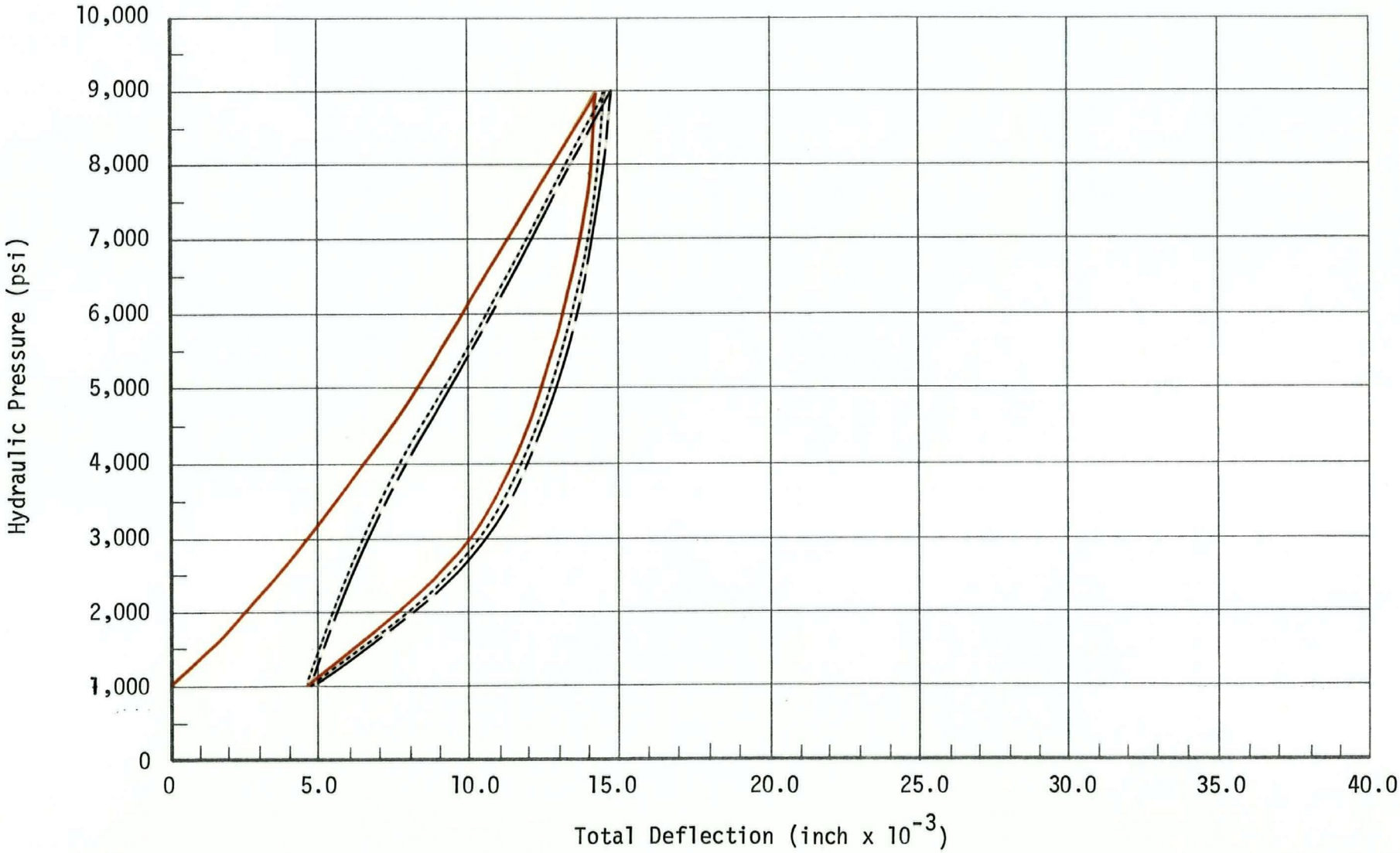

Figure 34

Hole No. NX - 3

Depth 90.0 ft.

Goodman Jack Testing

APPLIED LOAD vs. DIAMETRAL BORE HOLE DEFORMATION

Orientation 0°

Rock Type quartzite gneiss

First cycle ——— Second cycle ---------- Third cycle — — ———

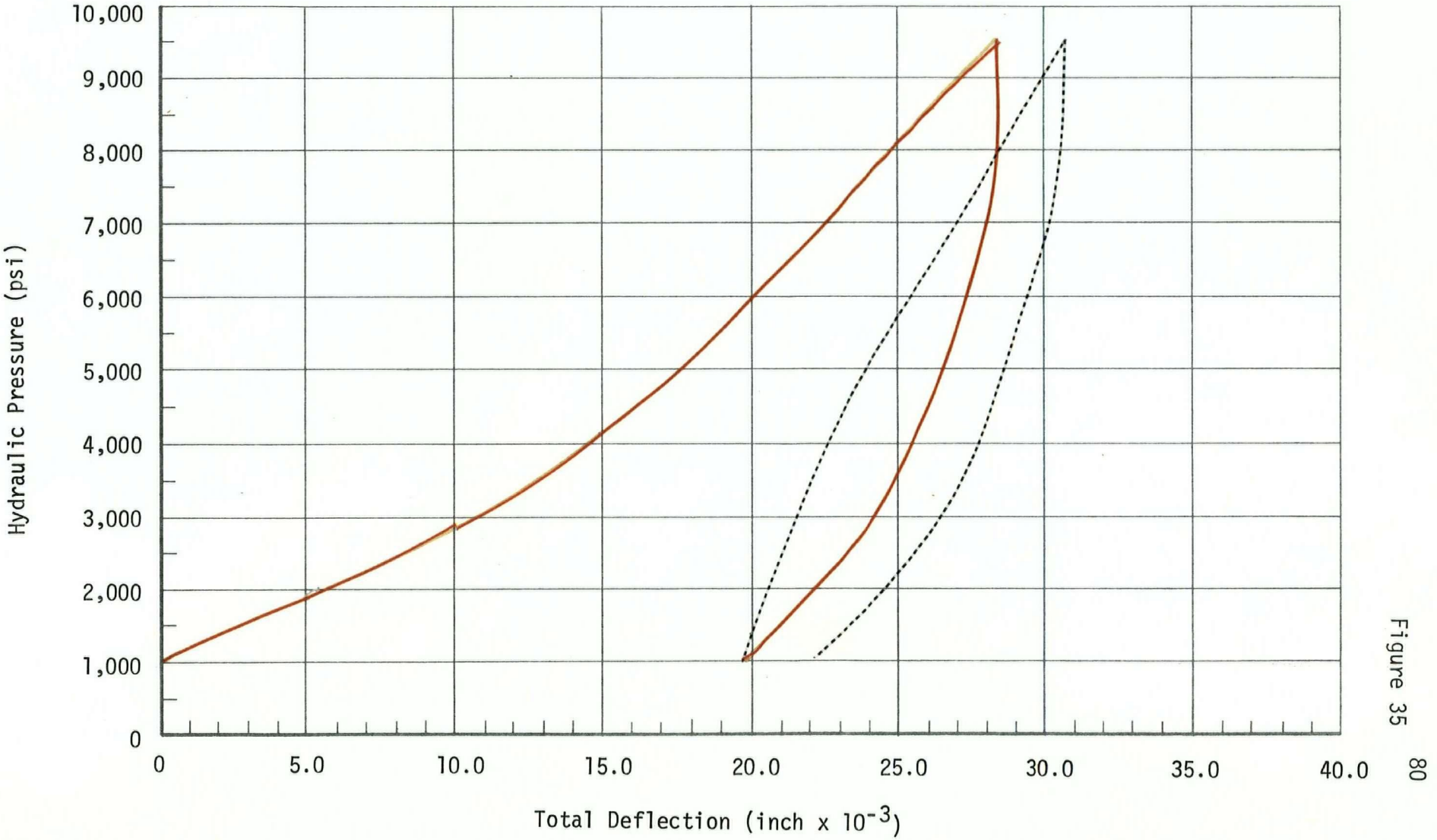

Figure 35

Figure 36

First Cycle Working Modulus

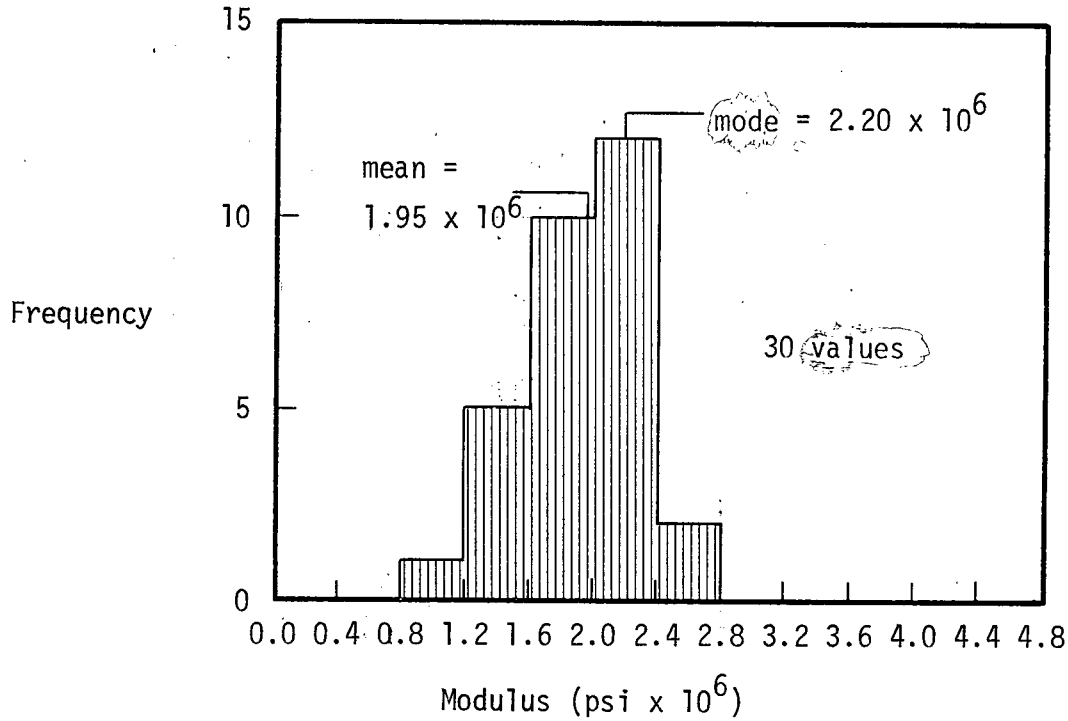

Second Cycle Working Modulus

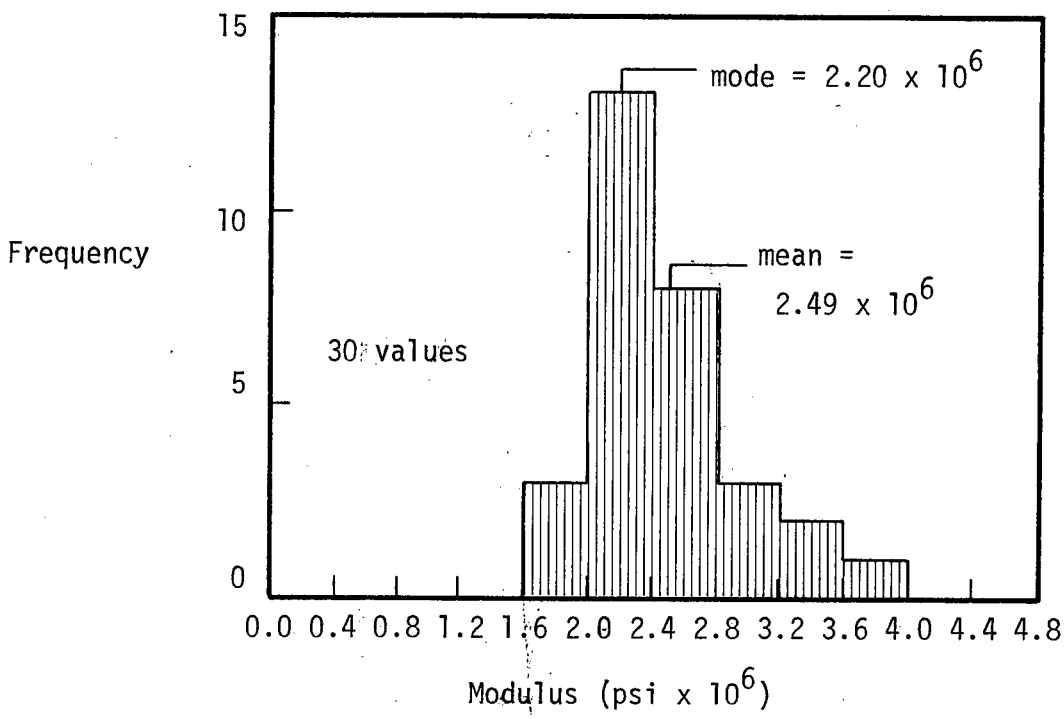

FREQUENCY HISTOGRAMS FOR GOODMAN JACK TESTS
IN QUARTZITE GNEISS

2. Second cycle working modulus:

   mean = 2.49×10^6

   standard deviation = 0.47×10^6

   coefficient of variation = 19%

3. The distributions are definitely skewed in opposite directions.

The lower first cycle modulus is to be expected since it probably reflects inelastic deformation such as the closing of cracks or seating of the jack. The difference in shape of the distribution diagrams is probably a reflection of the fact that most of the inelastic deformation occurs during the first loading cycle. Thus a greater proportion of low modulus values occur during the first cycle than occur for the second cycle. This accounts for the positive skewness of the first cycle modulus values and the negative skewness of the second cycle values.

The anisotropy diagram for the tests conducted in quartzite gneiss is shown in Figure 37. As previously described, hand samples of this rock type exhibited little foliation. However, in the field, small discontinuous schist layers often occurred within the gneiss. The foliation angle thus refers to the layering of the rock complex and not specifically to foliation within the gneiss. The fitted regression line in Figure 37 has a low correlation coefficient. The lack of correlation of the anisotropy diagram has two possible explanations. Firstly, the quartzite gneiss may not contain representative layering in the volume of rock affected by the Goodman Jack. Thus, there is no clearly defined anisotropy. A second possible reason is that the determination of the foliation angle is too imprecise. The *in situ* anisotropy is

ANISOTROPY OF THE QUARTZITE GNEISS AS REFLECTED BY
THE GOODMAN JACK

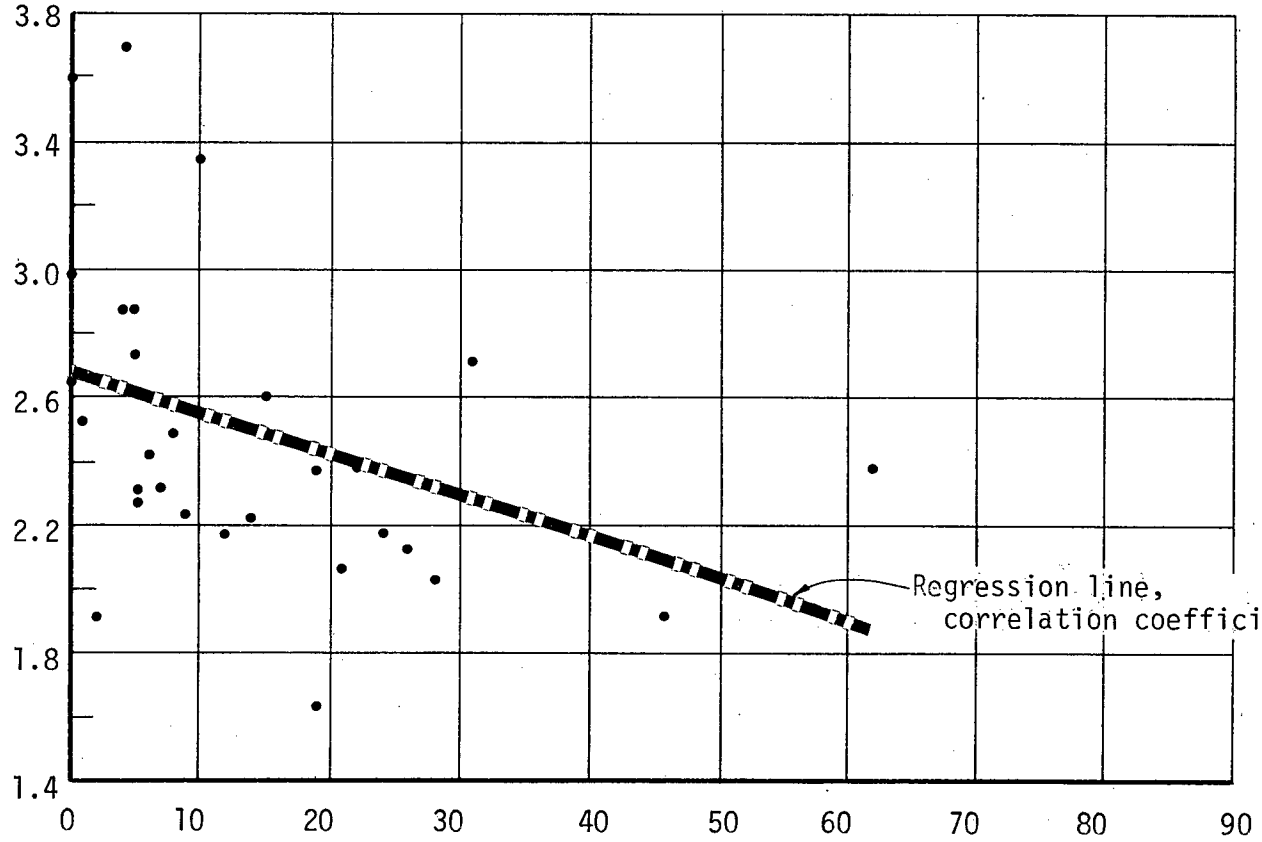

Figure 37

analyzed more thoroughly for the quartz feldspar schist to follow.

The *in situ* elastic recovery of the quartzite gneiss averaged 60% for the first two loading cycles. The elastic recovery on the second cycle averaged 96%. In spite of the approximate calculation of the elastic recovery, these results are significant. The permanent deformation for the *in situ* quartzite gneiss is quite large. However, loading cycles after the first have near elastic deformation.

The ratio of the working modulus to secant modulus averages 1.48 to 2.54 so that the presence of discontinuities within the gneiss is quite variable. These results have more significance when compared to other rock types.

2. Quartz Feldspar Schist

Figures 38 and 39 show deformation curves representative of the behaviour of the 61 tests carried out in quartz feldspar schist. The notable characteristics of these curves are the linearity and small permanent deformations after the first loading cycle. The hysteresis exhibited by Figure 38 is the normal while that of Figure 39 is a deviation. This latter figure illustrates the effect of the free play in the transducers when the direction of loading is changed. The free play results in a trapezoidal-shaped loop indicating greater hysteresis losses than actually occur. This feature is noticed in most of the Goodman Jack deformation curves to an extent dependent on the deformation characteristics of the rock.

An extreme in the behaviour of the quartz feldspar schist is shown in Figure 40. The rock at this location exhibits a fairly

Hole No. NX - 12 Goodman Jack Testing Orientation 90°

Depth 70.0 ft. APPLIED LOAD vs. DIAMETRAL BORE HOLE DEFORMATION Rock Type ~~quartz feldspar~~ schist

First cycle ——— Second cycle ---------- Third cycle — — ———

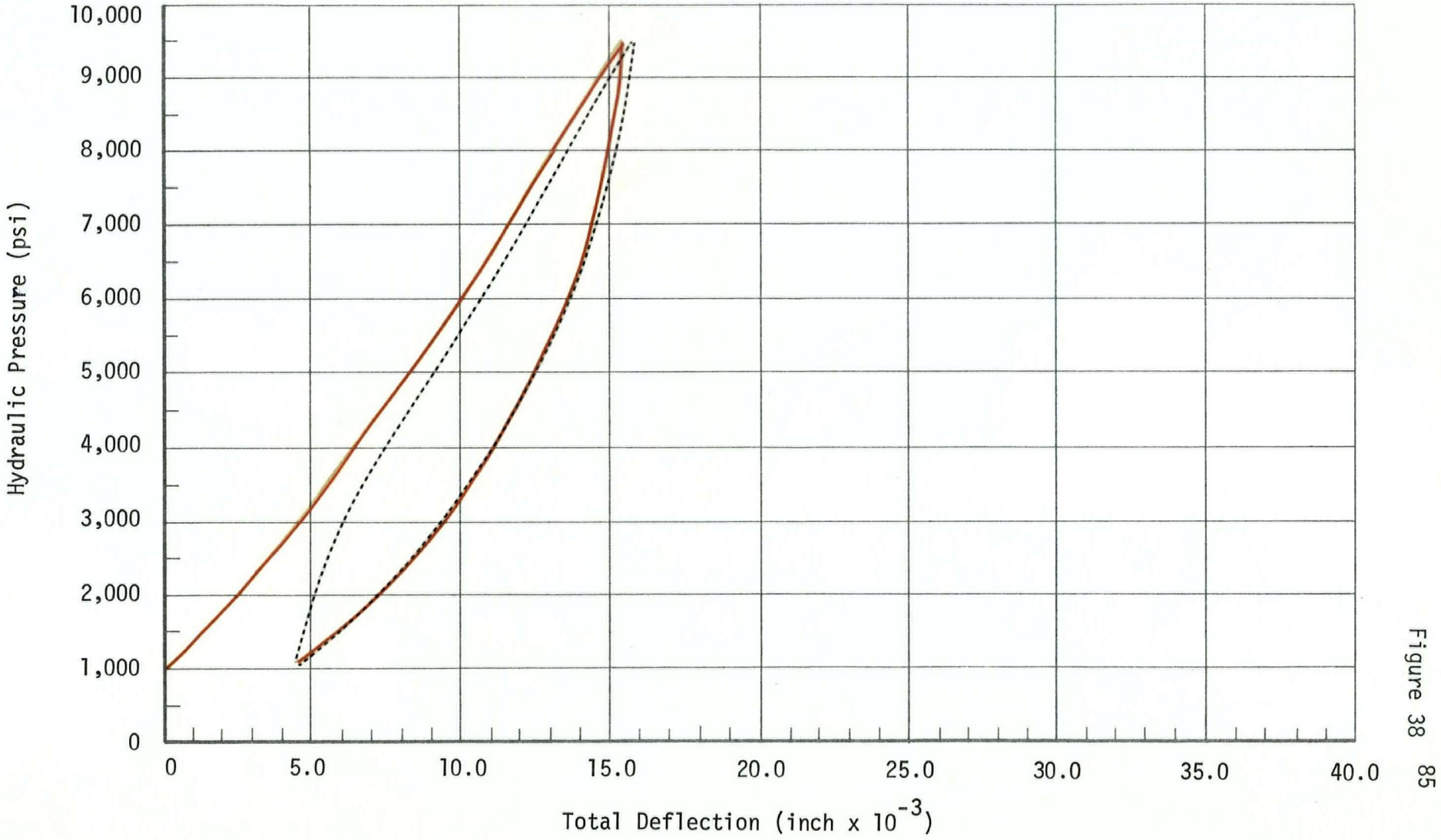

Figure 38

Hole No. NX - 12

Depth 75.0 ft.

Goodman Jack Testing

APPLIED LOAD vs. DIAMETRAL BORE HOLE DEFORMATION

Orientation 0°

Rock Type quartz feldspar schist

First cycle ——— Second cycle ---------- Third cycle — — ———

Figure 39

Hole No. NX - 20

Depth 70.0 ft.

Goodman Jack Testing

APPLIED LOAD vs. DIAMETRAL BORE HOLE DEFORMATION

Orientation 0°

Rock Type quartz feldspar schist

First cycle ——— Second cycle ---------- Third cycle — — ———

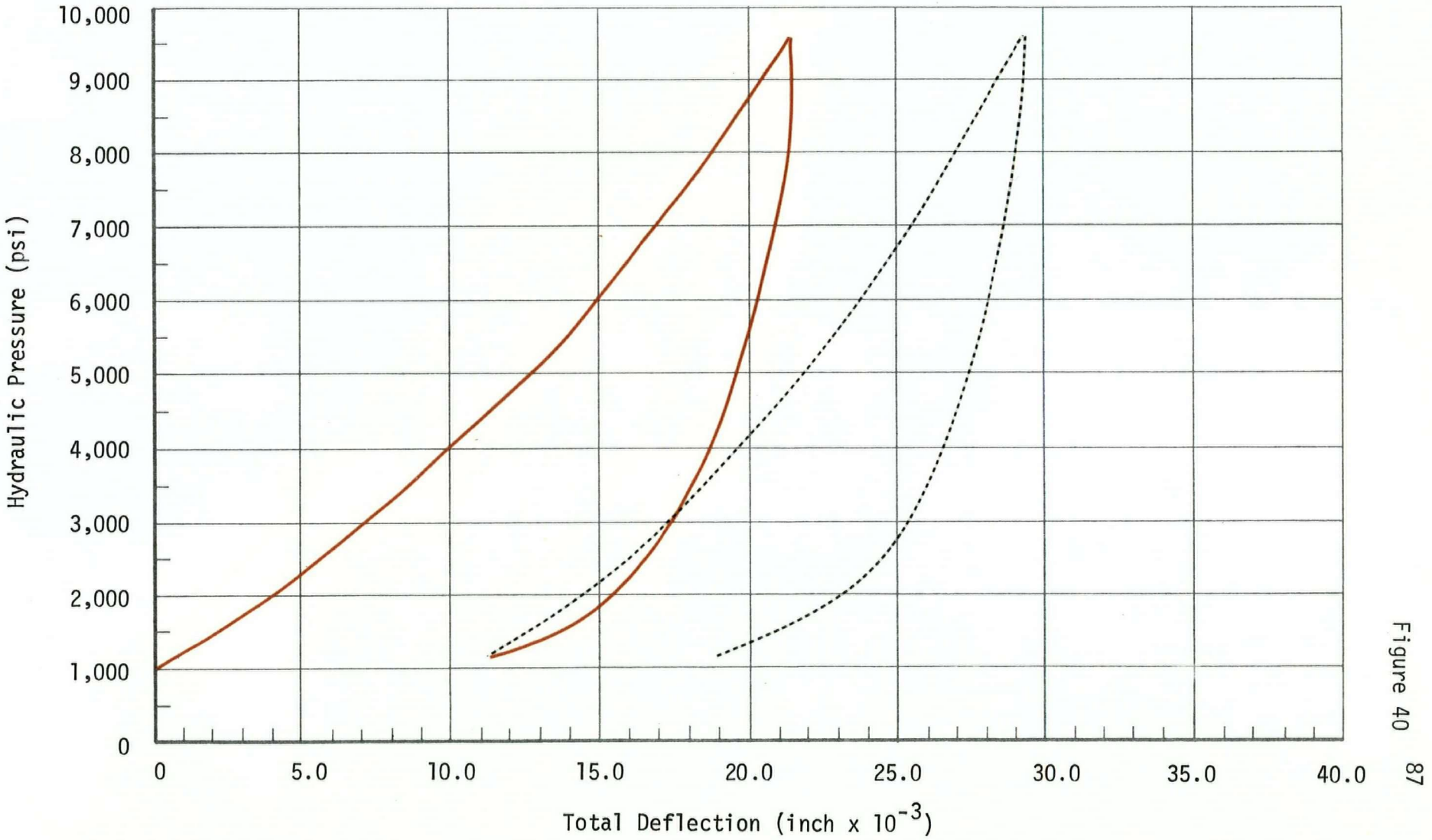

Figure 40

linear stress-deformation curve yet undergoes very large permanent deformations. A possible explanation is that the jack loading is causing rock movement along a pre-existing fracture plane. Rock behaviour of this type was found for the three orientations of only one test location.

Distribution diagrams for the working modulus of the first, second and third cycles are shown in Figures 41 and 42. The following points are illustrated by these diagrams:

1. First cycle working modulus:
   mean = 1.46×10^6
   standard deviation = 0.32×10^6
   coefficient of variation = 22%
2. Second cycle working modulus:
   mean = 1.92×10^6
   standard deviation = 0.43×10^6
   coefficient of variation = 22%
3. Third cycle working modulus:
   mean = 2.00×10^6
   standard deviation = 0.45×10^6
   coefficient of variation = 23%
4. All three distributions, but particularly that for the second cycle, approach the normal distribution. This is graphically shown by the plot on normal probability paper, Figure 43. On this paper a normal distribution plots as a straight line.

As for the tests in quartzite gneiss, the average working modulus for the second cycle is significantly larger than that of the first cycle. How-

Figure 41

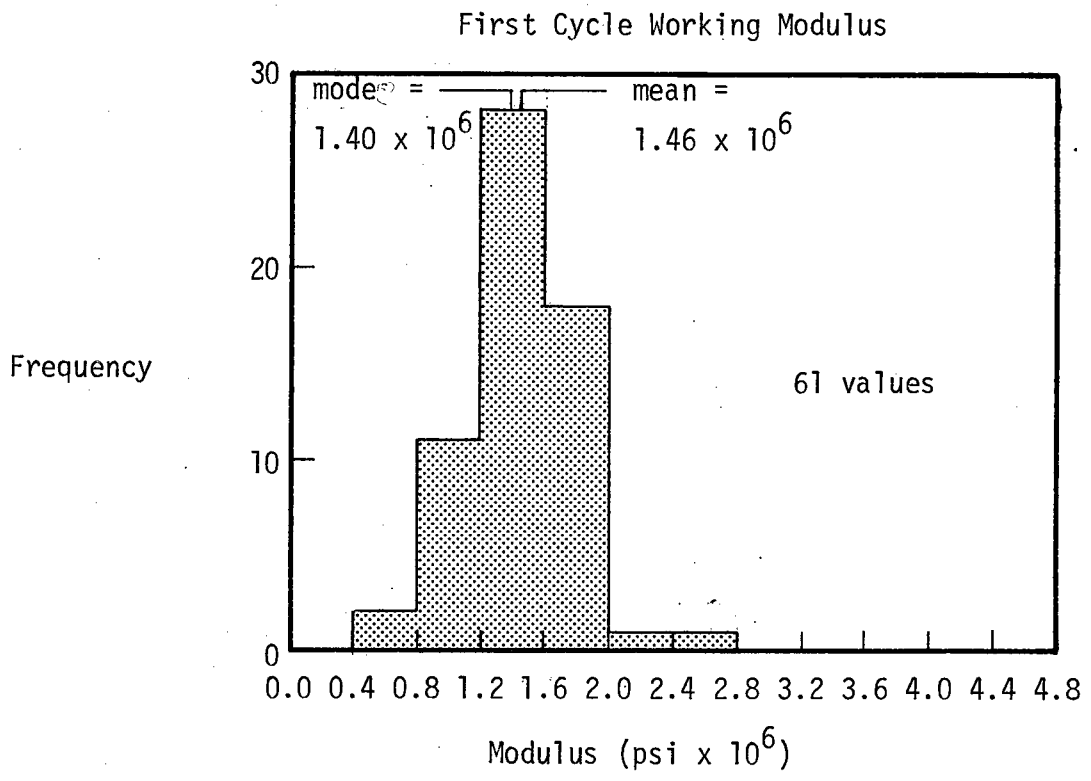

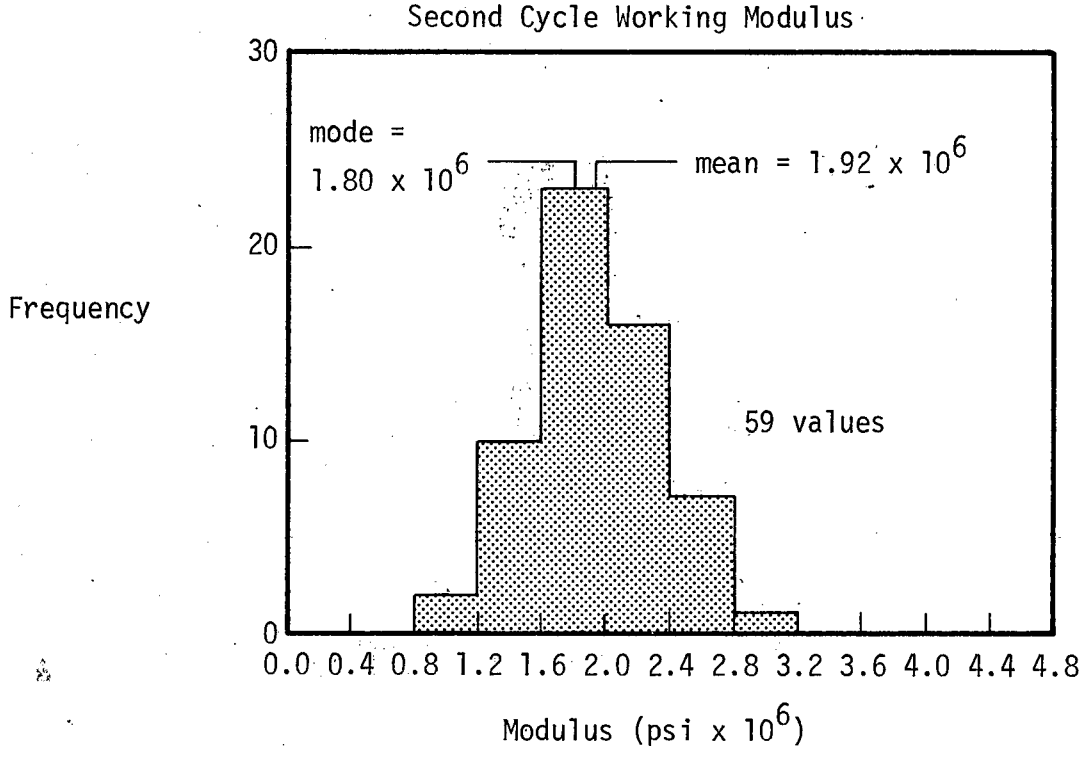

FREQUENCY HISTOGRAMS FOR GOODMAN JACK TESTS IN QUARTZ FELDSPAR SCHIST

Figure 42

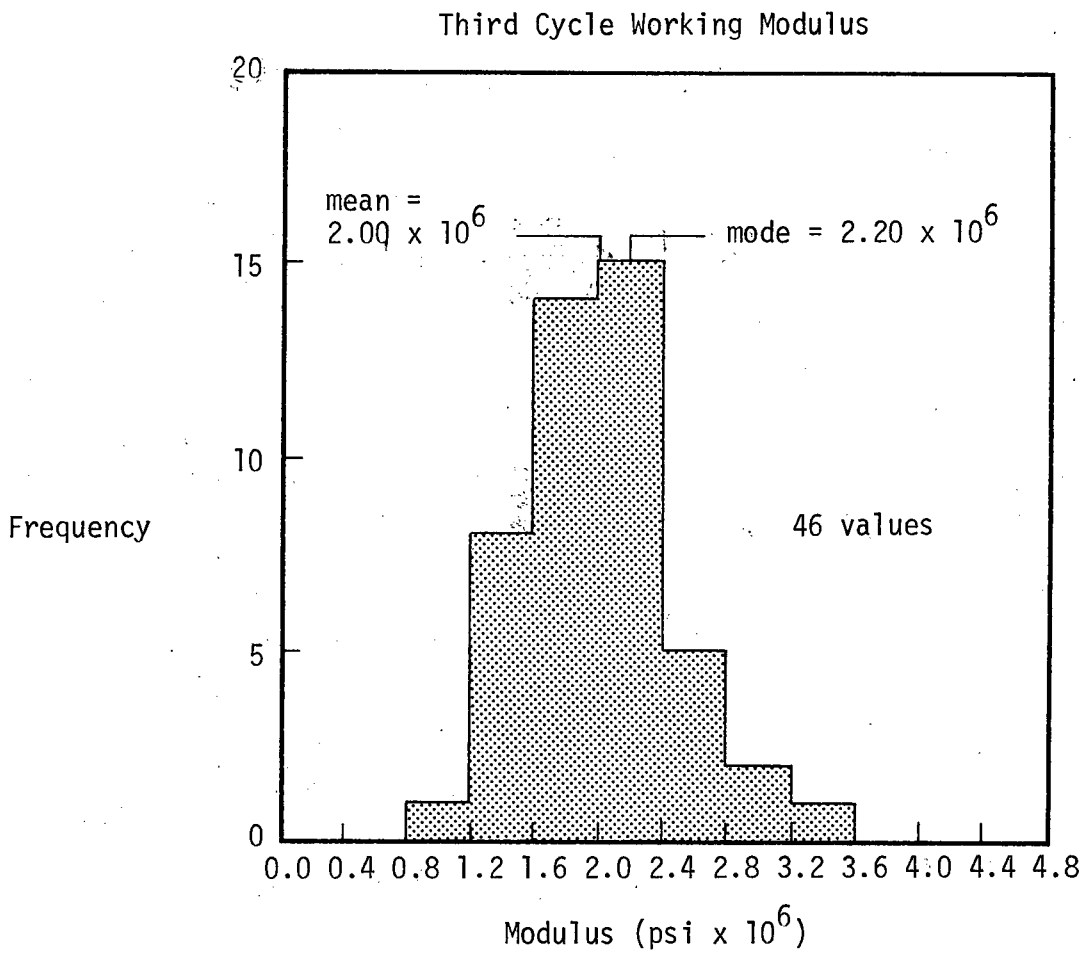

FREQUENCY HISTOGRAM FOR GOODMAN JACK TESTS IN QUARTZ FELDSPAR SCHIST

Figure 43

FREQUENCY DISTRIBUTION OF SECOND CYCLE WORKING MODULUS FOR QUARTZ FELDSPAR SCHIST

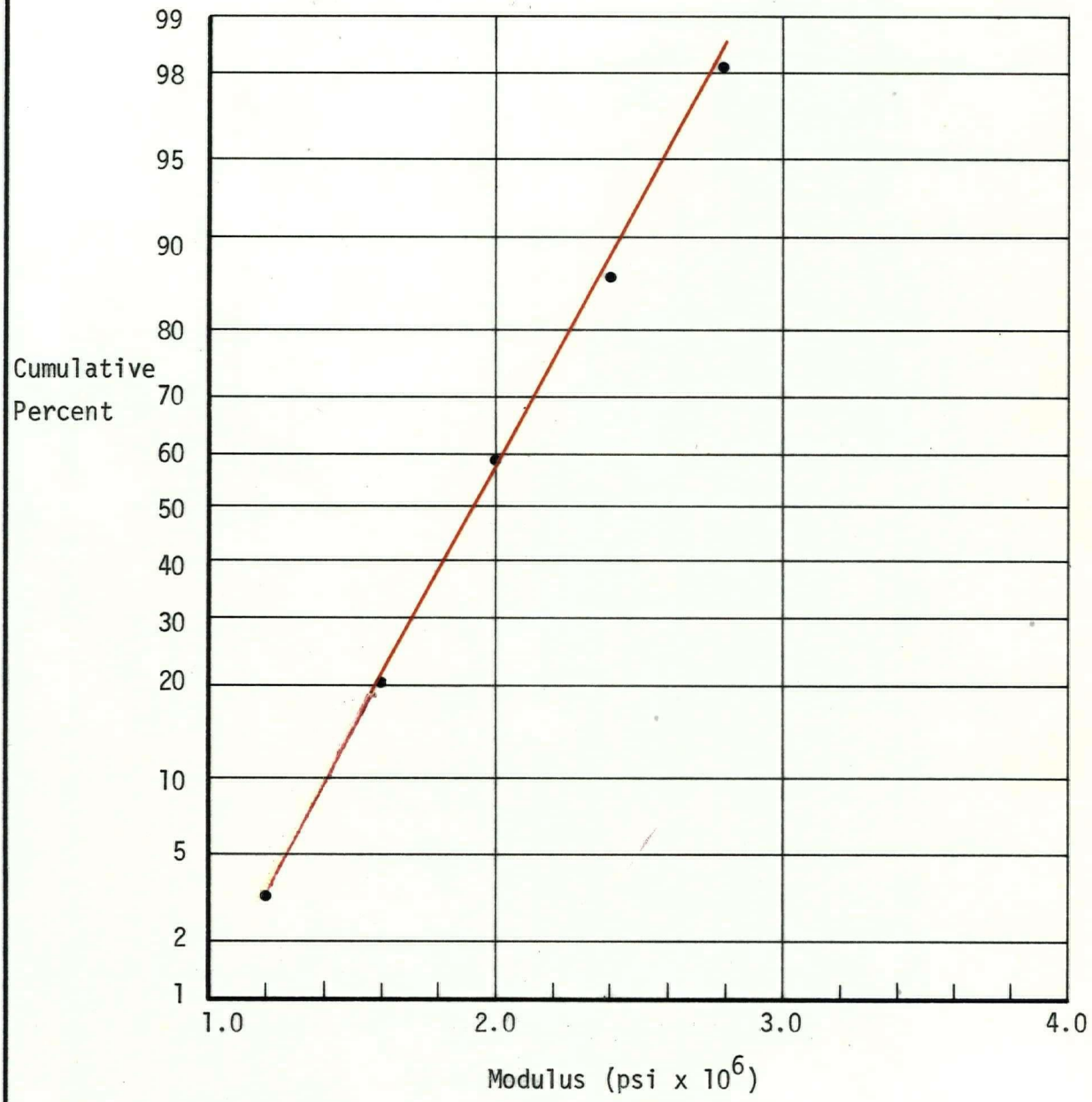

ever, the values for the second and third cycles are almost identical. This points out the necessity of only performing two loading cycles in this rock type. The fact that the distributions are very nearly normal must indicate that a representative sample of the schist was tested.

Figure 44 shows the anisotropy of the *in situ* quartz feldspar schist. As can be seen a great deal of scatter is present in this plot and the correlation coefficient for the fitted regression line is only 0.44. The only information that can be obtained from this diagram is the vague generalization that the highest modulus values tend to correspond to the low foliation angles. The scatter of anisotropy diagram could be due to the following:

1. As shown in Figure 45 different orientations of the jack can have the same loading direction-foliation plane relationship. For example, the loading can be parallel to the foliation while the jack itself is either parallel or perpendicular to the foliation. Thus the modulus determined by the jack could be dependent not only on the foliation angle but also on the jack orientation.
2. *In situ* features such as structural discontinuities or *in situ* stresses which cause inhomogeneity in the schist and thus distortion of the modulus-foliation angle relationship.
3. Inaccuracy in the determination of the foliation angle.

Point 1 was investigated by dividing the tests according to the angle between the long axis of the jack (i.e. the bore hole) and

ANISOTROPY OF THE QUARTZ FELDSPAR SCHIST AS REFLECTED BY THE GOODMAN JACK

Angle between bore hole and foliation: • = 0° to 30°, * = 30° to 60°, + = 60° to 90°

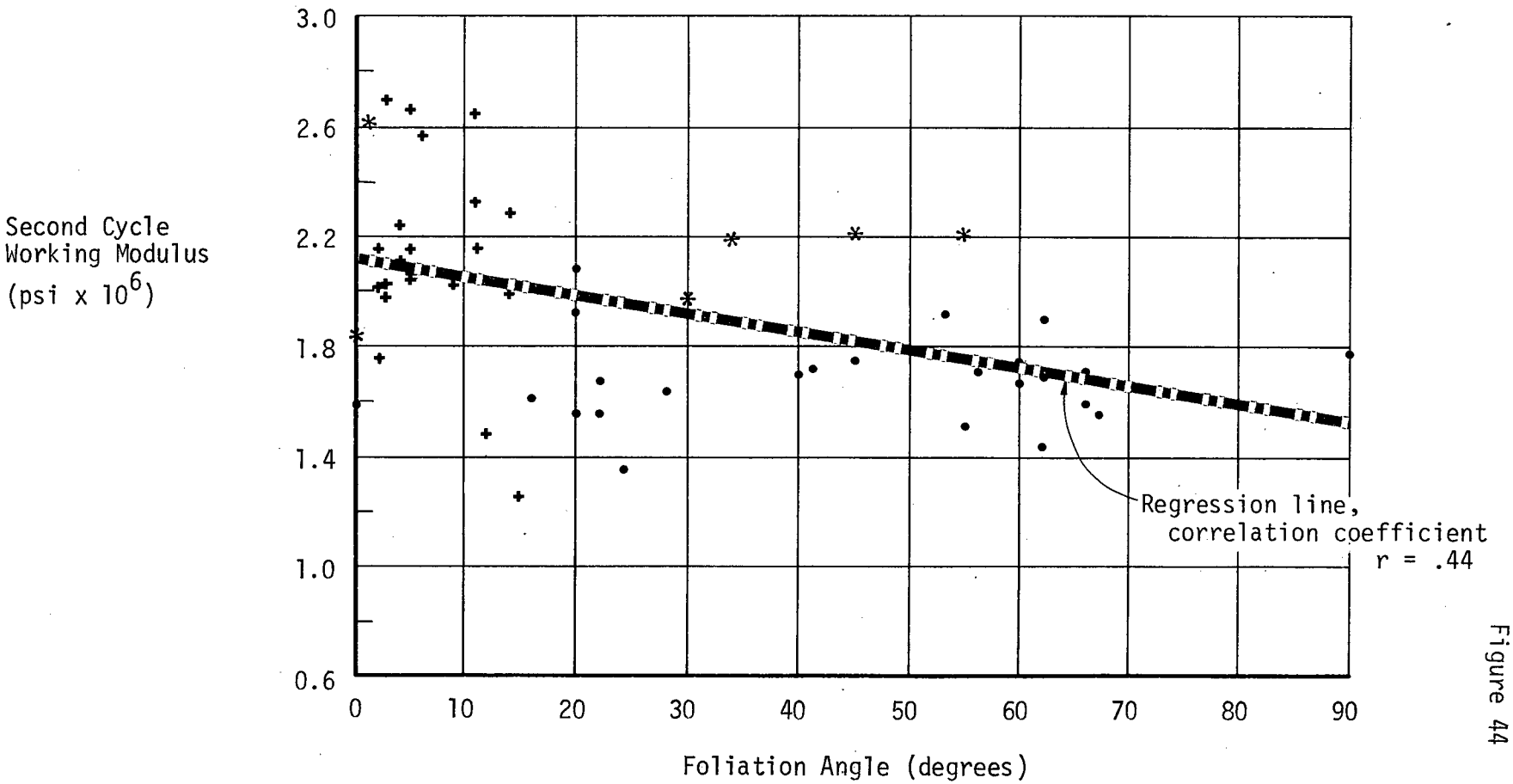

Figure 44

THREE POSSIBLE ORIENTATIONS OF THE GOODMAN JACK WITH REGARD TO THE DIRECTION OF LOADING AND FOLIATION PLANE

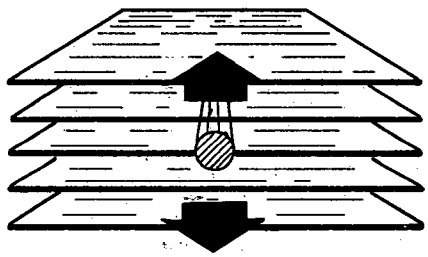

Jack parallel to foliation, loading perpendicular to foliation. (i.e. foliation angle = 90°)

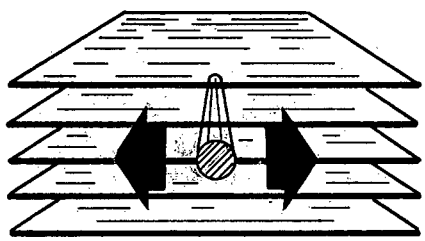

Jack parallel to foliation, loading parallel to foliation. (i.e. foliation angle = 0°)

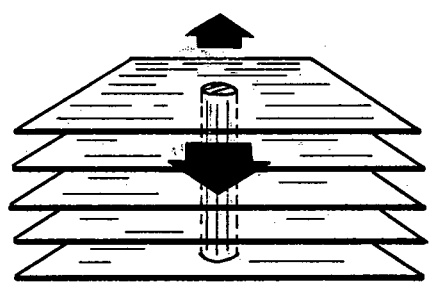

Jack perpendicular to foliation, loading parallel to foliation. (i.e. foliation angle = 0°)

the rock schistosity. Re-examination of Figure 44 shows that this angle has been divided into three groups. Although the symbols are fairly well grouped there is little overlap of tests with the same foliation angle and different jack orientations. The dependence of indicated rock anisotropy upon orientation of the jack thus remains obscure.

Point 2 was investigated by determining the variation of deformation modulus expressed as a percentage of the lowest determined value for each test location. This variation would more closely represent the effect of foliation angle while negating the effect of large scale inhomogeneity in the schist. It was found that the variation in the three modulus values for a particular test depth ranged from 6% to 40% and averaged 20%.

In summary, the Goodman Jack indicates that the schist is anisotropic. However, the exact relationship between modulus and foliation angle is obscure without more accurate geologic control at the test locations.

The elastic recovery of the quartz feldspar schist averaged 56% for the first two loading cycles. This means that significant permanent deformation occurs in this rock type. For the second cycle only, 91% of the deformation was recoverable. Thus inelastic behaviour is restricted to the first loading cycle.

The average ratio of the second cycle working modulus to secant modulus is 1.59. The significance of this result will be demonstrated in the comparison of rock types.

3. Pegmatite

Twelve Goodman Jack tests were carried out in pegmatite. As for the laboratory testing, frequency histograms could not be prepared for this rock type.

Figure 46 shows a representative deformation curve for the pegmatite. The material displays a linear deformation curve and an elastic response after the first loading cycle. Hysteresis effects are generally insignificant as exemplified by the narrow load-unload loops.

The average first cycle working modulus is 1.57×10^6 psi while that of the second cycle is 2.06×10^6 psi. The difference is 31%, indicating that large inelastic deformations are occurring in the first load cycle. The average percent elastic recovery for the first two loading cycles is 59%. For the second cycle only, this value is 96% reinforcing the indication above.

4. Summary and Comparison of Goodman Jack Results

The results of the Goodman Jack testing are summarized in Table 3.

Examination of the summarized results reveals that for a particular modulus type very little difference exists between rock types. For example, the mean second cycle working modulus for quartzite gneiss is only 1.3 times that of the quartz feldspar schist and 1.2 times that of pegmatite. Further, the standard deviation and range of second cycle working modulus are similar for all rock types.

Hole No. NX - 15 | Goodman Jack Testing | Orientation 90°

Depth 60.0 ft. | APPLIED LOAD vs. DIAMETRAL BORE HOLE DEFORMATION | Rock Type Pegmatite

First cycle ——— Second cycle - - - - - - - - - - - - - - - - Third cycle ——— — —

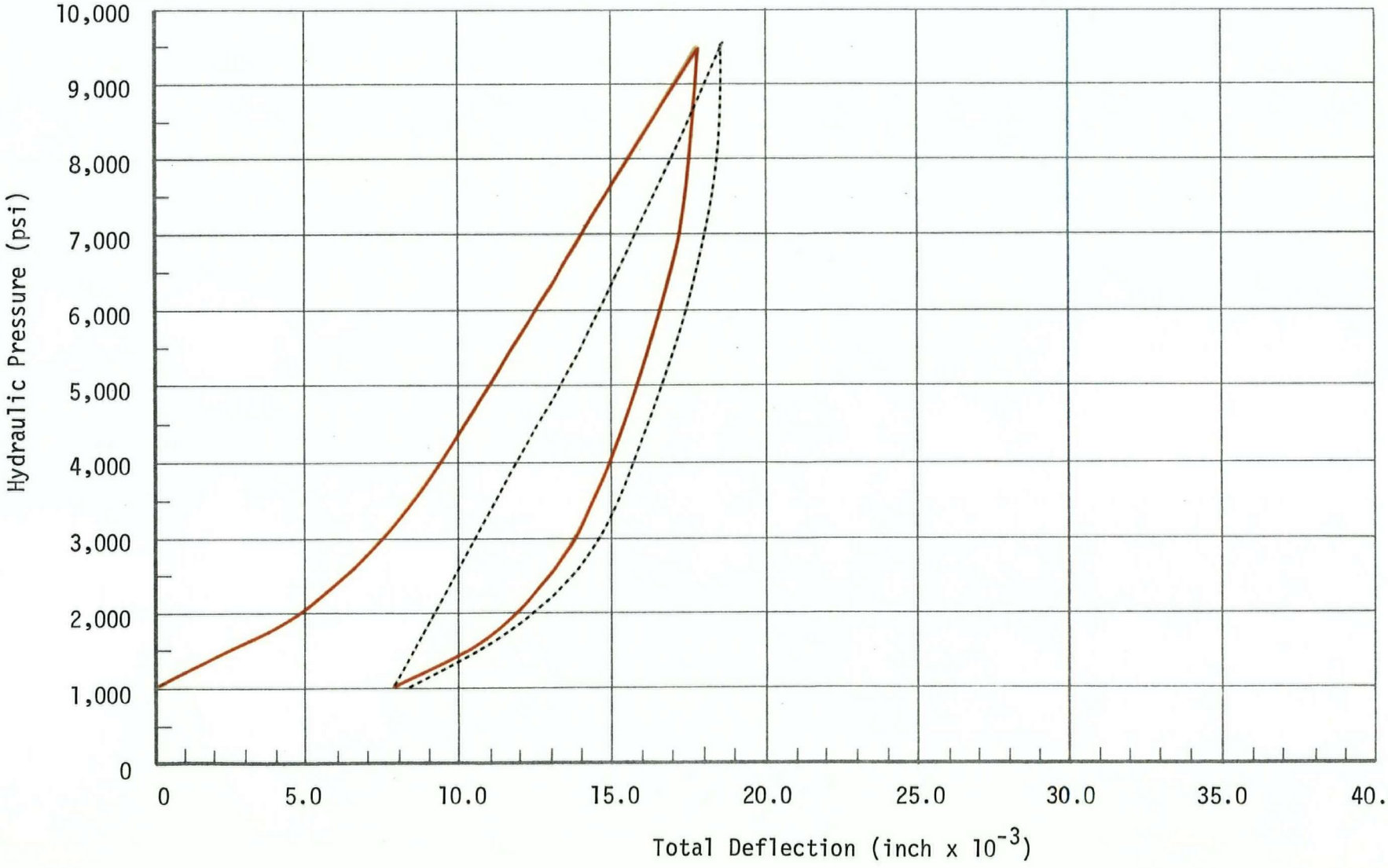

Figure 46

TABLE 3

SUMMARY OF GOODMAN JACK RESULTS

Note: All modulus values in psi x 10^6

Property	Quartzite Gneiss	Quartz Feldspar Schist	Pegmatite
a. Number of tests	30	61	12
b. Mean second cycle secant modulus	1.71	1.25	1.41
c. Mean second cycle recovery modulus	2.86	2.24	2.38
d. Mean first cycle working modulus	1.95	1.46	1.57
e. Standard deviation of d	0.38	0.32	0.33
f. Coefficient of variation	19%	22%	21%
g. Mean second cycle working modulus	2.49	1.92	2.06
h. Standard deviation of g	0.47	0.43	0.42
i. Coefficient of variation	19%	22%	20%
j. Range of second cycle working modulus	1.64 to 3.70	0.87 to 3.16	1.32 to 2.80
k. "x"*	2.77	2.11	2.37
l. "y"**	2.23	1.76	1.81
m. Anisotropy Index, A.I.	22%	19%	27%
n. % E_w (second cycle) greater E_w (first cycle)	28%	31%	31%
o. Average % elastic recovery for two cycles	60%	56%	59%
p. Average % elastic recovery for second cycle	96%	91%	96%
q. Average ratio, E_w/E_s	1.48	1.59	1.48

*x mean of the maximum second cycle working modulus values at each test location regardless of orientation

**y mean of the minimum second cycle working modulus values at each test location regardless of orientation

To reduce the effect of rock anisotropy in the comparison of mean modulus values, properties k and l of Table 3 were computed. These values represent the mean of the maximum (k) or minimum (l) second cycle working modulus values at each test location regardless of orientation. Note that the ratio of quartzite gneiss to quartz feldspar schist is 1.3 for both properties k and l. The ratios for quartzite gneiss to pegmatite are both 1.2. It is concluded that all rock types have modulus values that differ by less than 30%.

Discounting extreme examples, very little variation in deformation behaviour is exhibited by the stress-deformation curves. All rock types show fairly linear response after the first loading cycle. Permanent deformations are significant on the first loading but elastic behaviour follows during subsequent loading. Hysteresis losses are low but are noticeably larger for the schists than the other two rock types. This probably reflects the deformation of micaceous minerals.

As described in sections VI.B.1 and 2 the Goodman Jack did not reflect the modulus anisotropy for the schist or gneiss. A number of possible reasons were presented. However, to compare the relative anisotropy of the various rock types an anisotropy index, A.I., has been defined:

$$A.I. = \frac{x-y}{m} (100\%)$$

where x mean of the maximum second cycle working modulus values at each test location regardless of orientation

y mean of the minimum second cycle working modulus values at each test location regardless of orientation

m mean of all second cycle working moduli for a particular rock type

Referring to Table 3 the A.I. values are 22%, 19% and 27% for the quartzite gneiss, quartz feldspar schist and pegmatite respectively. These index values represent not only the anisotropy of the rock but also preferential roughness of the bore hole and the *in situ* stress field. The index values represent an apparent anisotropy for each rock type. Hence it is concluded that the apparent anisotropies are significant, though not absolute, and are similar for the three rock types.

Comparison of properties n through q of Table 3 reveals little difference between rock types. The percentage that the mean second cycle working modulus is greater than that of the first cycle averages 30%. Elastic recovery for the first two loading cycles is fairly low, about 60%. For the second cycle only, the elastic recovery is greater than 90% for all rock types. In both cases, the recovery for the schist is slightly less, indicating more permanent deformation in this rock type. The ratio, E_w/E_s, is slightly larger for the schist while the gneiss and pegmatite are the same. As previously explained, the failure to record the deformation for the first load increment can reduce the observed ratio difference between rock types. However it is felt that the greater ratio, E_w/E_s, for the quartz feldspar schist is significant. This indicates the schists undergo a greater amount of inelastic deformation which could be caused by:

(a) The closure of fractures or foliation in the destressed zone immediately around the bore hole.

(b) The deformation of asperities on the bore hole walls assuming the holes in schist were rougher than those in the other rock types. Visual examination of rock cores confirm this assumption in that the core exhibited marked diameter fluctuations as well as a rough pitted nature depending on the foliation orientation.

In summary, the Goodman Jack has shown that the three rock types have similar *in situ* deformation properties.

C. Plate Loading Tests

The results of the plate loading tests, based on the conclusions reached by company performing them, will be presented in less detail than the previous programmes. Measurements were taken on opposite walls at each of the six test locations yielding twelve sets of results. However, the mortar cap failed at one location so that eleven sets of usable data were obtained.

The complete set of results are shown in Table 4. Note that the quartz feldspar schist is referred to as biotite schist which is not indicative of any compositional difference but rather represents mapping by different geologists. Similarly, the quartzite gneiss is referred to as granitic gneiss.

Figures 47 and 48 show load deformation curves for the gneiss and schist respectively. These curves are representative of the rock

TABLE 4

RESULTS OF PLATE LOADING TESTS

*VHV = very high value

**This value not used

All modulus values x 10^6 psi

Test Number	Orientation	Moduli of Elasticity			Percent Elastic Recovery		
		E_s	E_w	E_r	Complete Test	Last Cycle	E_w/E_s
For granitic gneiss:							
PL-3	Ram horizontal	2.20	3.85	12.40	17	58	1.75
PL-3	Butt horizontal	2.20	3.87	12.40	17	45	1.76
PL-4	Ram vertical	2.25	2.65	4.54	41	67	1.18
PL-5	Ram vertical	2.61	2.97	9.12	29	62	1.14
PL-5	Butt vertical	1.09	1.25	2.21	47	90	1.15
PL-6	Ram horizontal	5.62	6.95	VHV*	31	100	1.23
PL-6	Butt horizontal	12.18	7.08	VHV	-	-	-
Gneiss Averages:		4.02	4.09	8.13	30	70	1.37
For biotite schist:							
PL-1	Ram horizontal	0.90	1.29	2.53	35	93	1.43
PL-1	Butt horizontal	0.79	0.71	3.78	20	53	0.89**
PL-2	Ram vertical	0.23	0.30	0.62	36	66	1.30
PL-4	Butt vertical	0.46	0.60	2.21	23	49	1.30
Schist Averages:		0.60	0.73	2.28	29	65	1.34

Figure 47

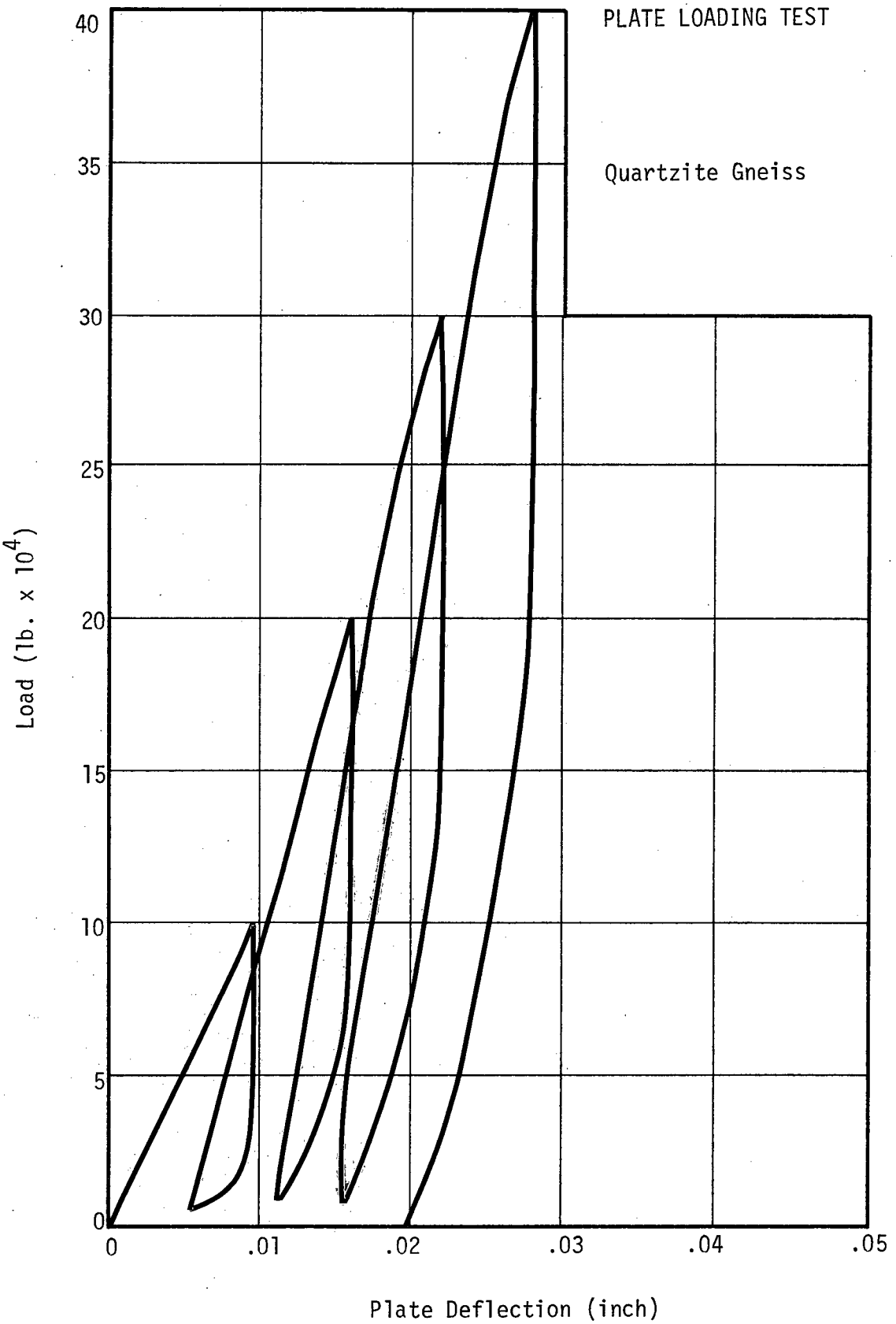
PLATE LOADING TEST
Quartzite Gneiss
Load (lb. x 10^4)
40
35
30
25
20
15
10
5
0
0
.01
.02
.03
.04
.05
Plate Deflection (inch)

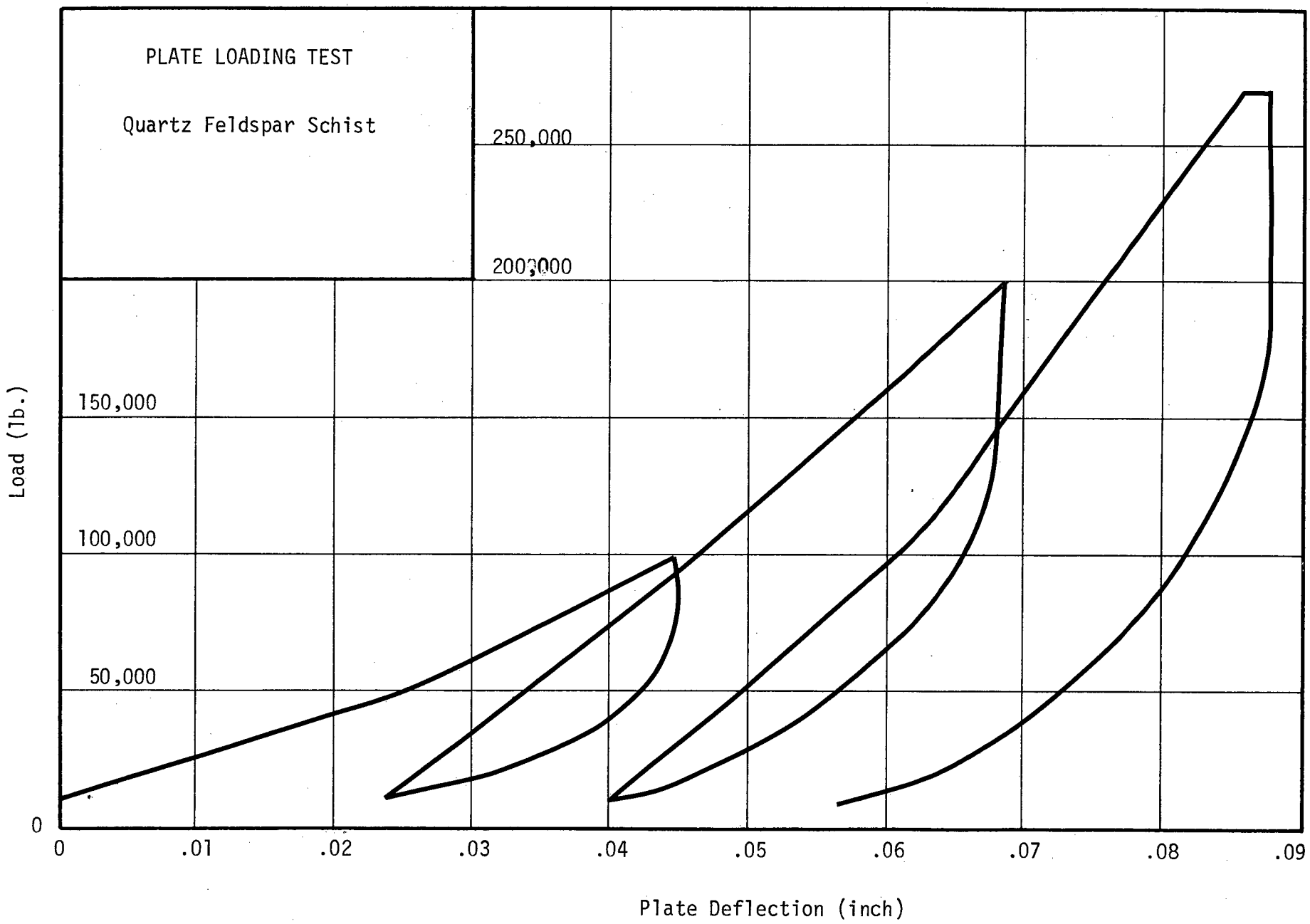
PLATE LOADING TEST
Quartz Feldspar Schist
250,000
200,000
150,000
100,000
50,000
0
Load (lb.)
0
.01
.02
.03
.04
.05
.06
.07
.08
.09
Plate Deflection (inch)

Figure 48

behaviour during the plate load testing. Several differences between the gneiss and schist rock types are to be noted. The most obvious difference is that the schists undergo much larger deformations, thus their lower modulus. The gneisses show significantly less hysteresis loss as expressed by tightness of the load-unload loops. Both rock types exhibit linear deformation curves on the loading portion of the cycles. Also, the permanent deformation for each rock type is quite high. On the basis of the load-deformation curves alone, the gneiss and schist behaviour have been well differentiated by the plate load tests.

Examining the averaged results of Table 4 reveals that all three modulus values for the gneiss are very much higher than those of the schist. The average working modulus for the gneiss is 5.6 times that of the schist. This indicates that the *in situ* rock types have very distinctive deformation properties. Both rock types exhibit a large range in working modulus; the schist from 0.30 to 1.29 x 10^6 psi and the gneiss from 1.25 to 7.08 x 10^6 psi. However, the overlap of these ranges is very small.

The distribution of the results of the plate loading tests can be investigated in an approximate manner. (see Guttman and Wilks, pp. 222-223) The distribution of plate loading results are shown in Figure 49 on normal probability paper. Distinct and approximately normal distributions are indicated for the two rock types.

Since the plate loading tests were carried out in horizontal and vertical directions within the exploratory tunnel, a rough check on the anistropy of the rock is possible. The horizontal tests loaded approximately parallel to the rock layering while the vertical tests loaded nearly perpendicular to it.

Figure 49

FREQUENCY DISTRIBUTIONS FOR THE PLATE LOADING TESTS

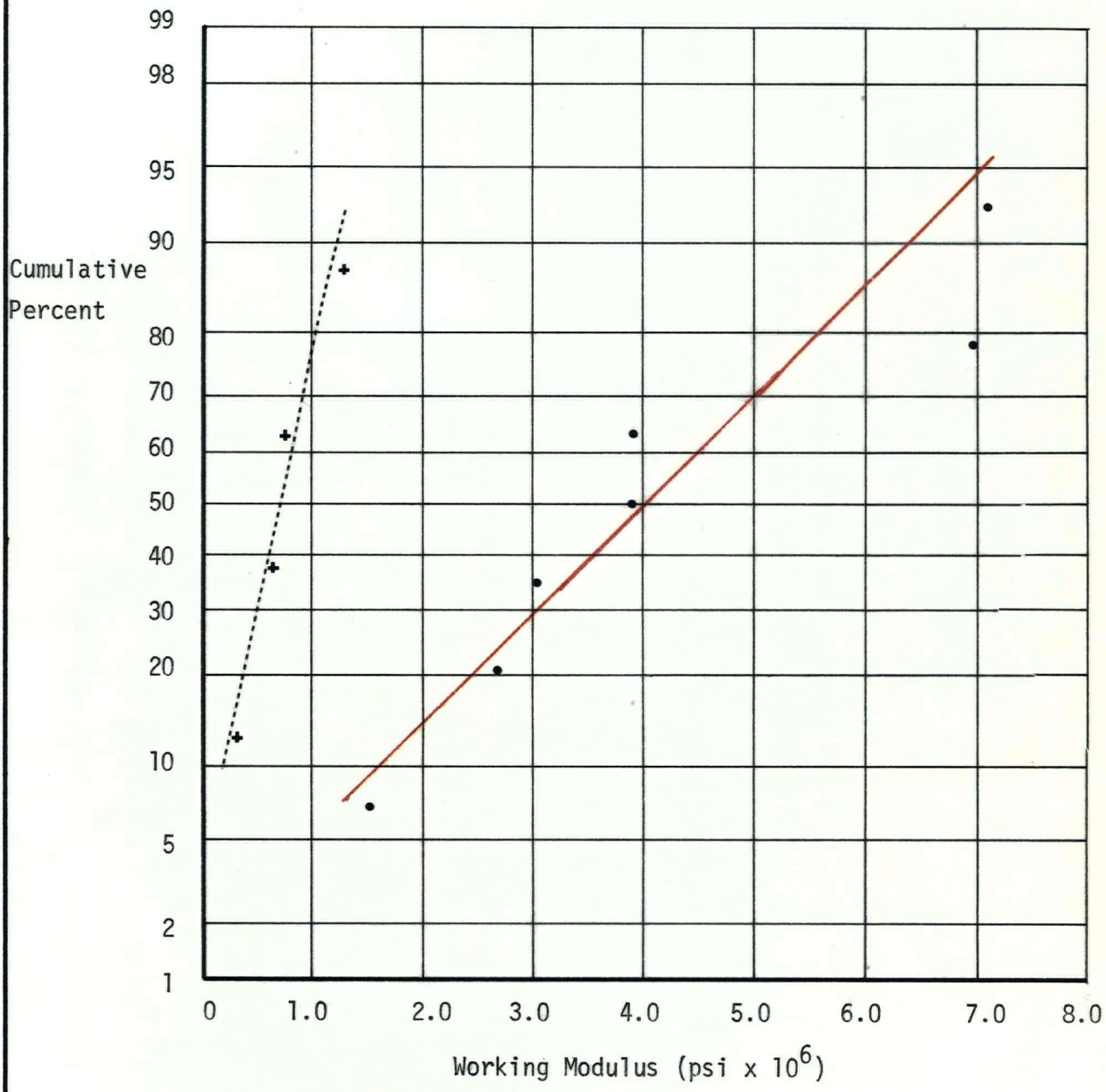

The average working modulus for the gneiss loaded parallel to the layering is 5.44 x 10^6 psi while that for loading perpendicular to the foliation is 2.27 x 10^6 psi. The gneiss is thus 2.4 times as rigid when loaded parallel to the rock layering. For the schist the values are 1.00 x 10^6 psi and 0.45 x 10^6 psi for loading parallel and perpendicular respectively. The schist is thus 2.2 times as rigid when loaded parallel to the rock layering.

The anisotropy indicated by the preceding results cannot be interpreted as a reflection of rock properties alone. Due to the excavation process a zone of rock variable in blast damage and stress concentration surrounds the drift. The relative importance of these factors on the anisotropy results is difficult to predict.

The rather small elastic recoveries shown in Table 4 are significant to the *in situ* behaviour of the two rock types. However, it is felt that the true *in situ* elastic response is significantly greater than that indicated by the plate loading tests. The reason being that the dial gauge system is reflecting not only the response of the rock fabric but also the deformation of the blast induced microfractures and the deformation of the sulphur pad. This is supported by the fact that the gneiss and schist have nearly identical elastic recoveries. Thus the large permanent deformations must be considered a function of both the testing method and the *in situ* rock behaviour.

To summarize the plate loading tests,it can be said that the two rock types have very distinctive *in situ* deformation moduli.

CHAPTER VII

COMPARISON OF TESTING TECHNIQUES

A. Magnitude of Moduli

1. Factors Relevent to Comparison

Figure 50 illustrates both the range and mean of the second cycle working modulus for the three testing programmes. Two points must be kept in mind when interpreting this figure, the rock quality and the size of the zone of influence of the test.

The rock quality and its variability will affect both the range and mean of the modulus values. The expected rock quality for each testing programme can be summarized as follows:

1. Laboratory tests: These tests are carried out on sound pieces of rock core which the processes of drilling, handling and preparation have not been able to destroy. The modulus values should tend to be higher and have a low range.
2. Goodman Jack tests: The random location of tests relative to geologic features should result in a wide range of modulus results.
3. Plate loading tests: These tests are performed in a zone of rock susceptible to destressing and blast damage. Modulus values should exhibit a wide range and could tend to be consistently lower than other testing methods.

Figure 50

MODULUS RANGE FOR VARIOUS TESTING METHODS

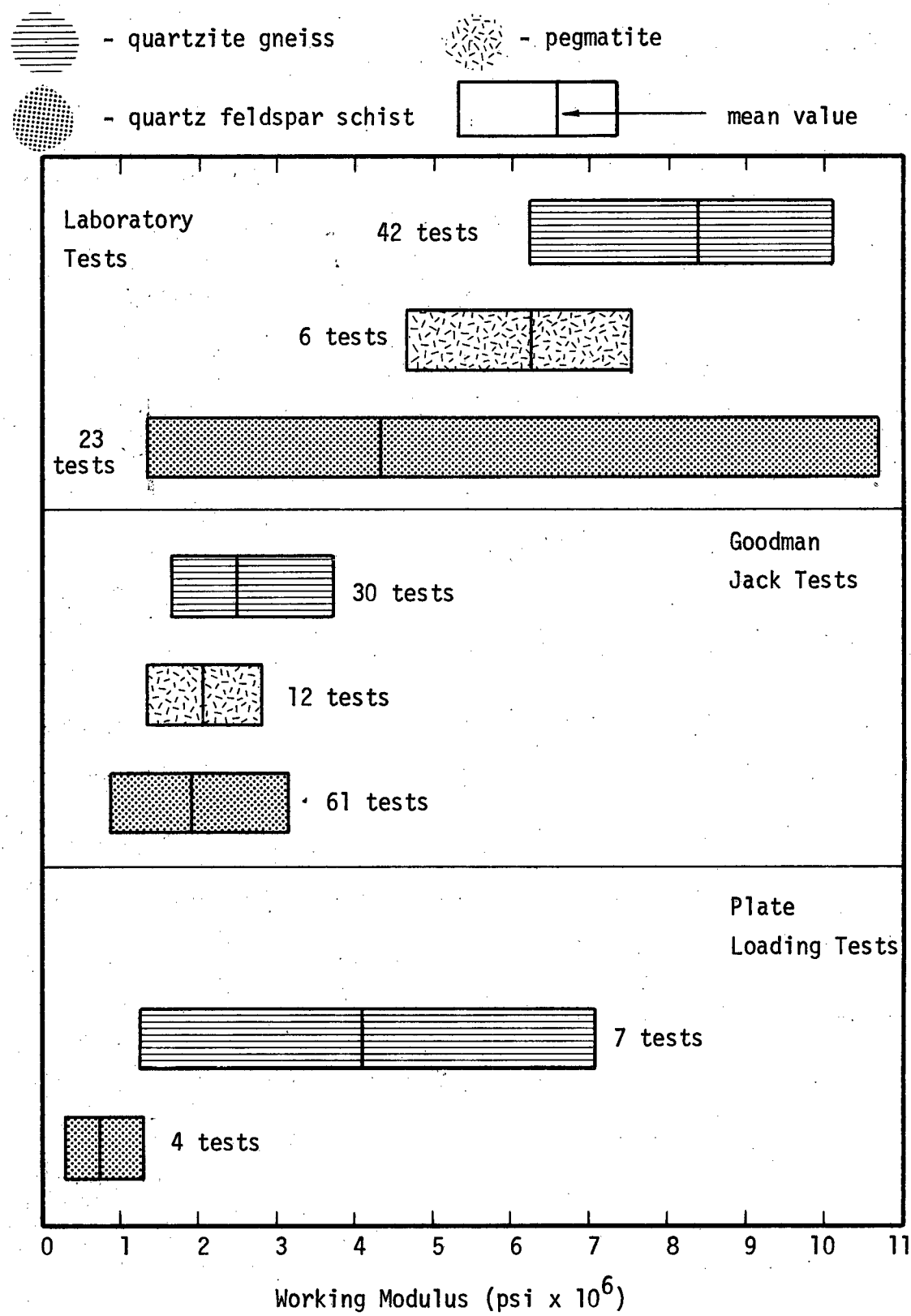

The second point to consider is the volume of rock influenced by a particular testing method. For the three testing methods the following rock volumes would be influenced:

1. Laboratory tests: fraction of a cubic foot.
2. Goodman Jack tests: approximately one cubic foot.
3. Plate loading tests: approximately two cubic feet.

The degree to which a representative volume of the rock is tested is known as the scale effect. Many writers including Bukovansky [3] have reported on the variation of deformation modulus with the technique used to determine it. The general conclusion is that the greater the volume of rock tested the lower and more representative the modulus tends to be.

2. Observations on the Three Groups of Modulus Results

The modulus results for the three testing methods illustrated in Figure 50 are interpreted bearing in mind the relevent factors outlined in the preceding section. On this basis several observations can be made:

1. As anticipated the laboratory results show the highest mean modulus values. Unexpectedly these results also show the greatest range of values.
2. The order of rock types from highest to lowest modulus is quartzite gneiss, pegmatite, quartz feldspar schist, and is consistent within each testing method. On the other hand the differentiation of rock type based on modulus is highly variable depending on the testing method.

3. The quartz feldspar schist modulus values decrease with increasing test volume and thus reflect the envisaged scale effect while the quartzite gneiss values do not.

On the basis of the observed results and the expected trends outlined in section VII.A.1. it is inferred that the three testing programmes have provided results which are only partially compatible. The following section discusses possible explanations for the observed discrepancies.

3. Discussion of the Modulus Results

The large range of modulus values reported by the laboratory testing is assumed to reflect the heterogeneous nature of the rock types at the scale of core specimens. This is pointedly demonstrated by the quartz feldspar schist in which the modulus is highly dependent on foliation orientation. Faulty instrumentation could contribute to a large range of values but is not considered significant in these results in view of the frequent calibration checks. Compared to the other testing techniques the mean values for the laboratory tests are significantly greater. These results thus establish the modulus of the intact rock material or in other words the upper limit for the modulus of a joint-rock mass system.

Compared to either of the other testing methods, the Goodman Jack results indicated three rock types of lower and more consistent modulus. Several possible explanations can be conjectured. On the assumption that the plate loading results for gneiss are anomolously high then the Goodman Jack results could be reflecting the true *in situ* modulus of the rock mass. This explanation also makes the assumption that structural features control equally the modulus of all rock types.

In view of the distinct difference in foliation between gneiss and schist this explanation is unlikely.

A second explanation is based on recent finite element modeling of the Goodman Jack carried out by Heuze and Dessenne [18]. In this work the effect of joint spacing and *in situ* stresses upon the measured deformation modulus was studied. Their method can be briefly described as follows. For each rock mass-joint system the true modulus could be determined from the assigned rock and joint properties. Several possible modes of jack-bore hole interaction were studied. The results were expressed in the forms of stress patterns around the bore hole, extent of rock breakage around and under the jack plates and the apparent modulus of deformation measured. This apparent modulus could be corrected to the true modulus of the rock-joint system by adjusting the K value. (see equation 1)

The results showed that for an unjointed, isotropic medium which exhibited elastic behaviour the K value is 1.25. This is the exact value predicted by elastic theory and incidentally is the value used for all computations in this thesis. The range of adjusted K values was from 0.75 to 3.13 depending on the presence of joints and *in situ* stresses. The investigators concluded that "there exist critical joint spacings which by allowing important rock breakage, introduce significant errors in test results unless the rock yielding is accounted for." They also advised that for a complete analysis of test results additional information consisting of the strength of the substance, the spacing of fractures and the *in situ* stresses is necessary. They also mentioned additional factors such as dilatancy of the joints and degree of rock anisotropy which may influence Goodman Jack tests but which to date have not been investigated.

In view of the recent work by Heuze and Dessenne the results of the Goodman Jack testing in Table 3 could be modified from -40% to + 165% depending on the applicable K factor at each test location. This large range of correction could easily account for the low range and low values of Goodman Jack modulus results.

The plate load results are surprising in view of the large modulus for the gneiss compared to that obtained from the Goodman Jack. This anomaly could result from discrepancies in the Goodman Jack (i.e. variation of the K factor) or from plate load tests in the following manner. The plate loading tests are interpretated using formulae developed from elasticity theory. This application is dubious in view of the rock quality surrounding the tunnel. It would thus be advisable to carry out a finite element study for the plate loading test similar to that carried out for the Goodman Jack by Heuze and Dessenne [18]. A second though less significant factor is the accuracy of the deformation sensing system. This is indicated by the lack of deformation response when changing from loading to unloading and is reflected by very steep unload curves. (see Figures 47 and 48) A lack of deformation sensitivity can increase the apparent rock modulus and is more pronounced for higher modulus rocks.

In summary, the results discussed above indicate that modulus values from different testing techniques cannot be realistically compared without detailed knowledge of each test environment and without valid interpretation formulae. In other words, the lack of correlation between the three testing programmes reflects the need to conveniently quantify important factors such as rock quality and *in situ* stresses and to

incorporate these factors into valid interpretive formulae. This topic will be expanded in Section VII.E. on the practical application of these results.

B. Anisotropy

Anisotropy results for the laboratory and plate loading tests are fairly consistent. The laboratory testing shows inconclusive anisotropy for the gneiss and excellent anisotropy for the schist. The indicated ratio of moduli for loading parallel and perpendicular to the foliation is about 2.5 for the schist. The plate loading tests indicate the gneiss is 2.4 times as rigid when loaded parallel to the layering than when loaded perpendicular. The result for the schist is 2.2 times. Anisotropy investigations on the Goodman Jack results are inconclusive. Although the jack indicates anisotropic behaviour for the schist, quantitative analysis is impossible without accurate geologic control at the test locations. Thus anisotropy can only be investigated with the jack under very uniform geologic conditions or where a supplementary programme of oriented core drilling or bore hole camera logging is employed.

C. Elastic Recovery

The elastic recoveries indicated by the three programmes show an interesting trend. For easy comparison the average elastic recoveries for complete tests are summarized:

Laboratory testing:
gneiss: 93%
pegmatite: 89%
schist: 84%

Goodman Jack testing:
gneiss: 60%
pegmatite: 56%
schist: 59%

Plate loading tests:
gneiss: 30%
schist: 29%

The obvious trend is that elastic recovery decreased with increasing volume of rock tested. This is to be expected since the larger volume tests incorporate a greater number of geologic discontinuities. For the laboratory and Goodman Jack tests the deformation is essentially elastic after the first loading cycle. The plate loading tests, on the other hand, showed an average of 30% permanent deformation on the final loading cycle. The discrepancy is probably due to the larger volume of rock affected by the plate loading test as well as the zone of micro-fractured and de-stressed rock around the drift.

D. Ease of Performance

A final comparison, based on the time required to obtain load-deformation data, can be made between testing techniques. The time required to reduce the data to modulus values is not included since it is equal for all methods. For the laboratory samples, including sample preparation and testing, the total time is 1 3/4 hours per two cycle

test. The time required for a two cycle test with the Goodman Jack is from 10 to 20 minutes depending on the time necessary to position the jack at the test location. This time assumes that bore holes are required for an earlier exploration phase of the project. The company performing the plate loading tests reports that a four cycle test required 6 to 8 hours exclusive of preparation time. Obviously this latter test is the most time consuming and hence most expensive to perform.

E. Evaluation of Testing Techniques

In view of the inconsistencies provided by the comparison of the three testing techniques some observations on the practical value of the results as well as possible improvements to the techniques would be relevent.

Before performing a test to determine a physical rock property such as deformation modulus, the required accuracy of the property should be evaluated. For example, to delineate zones of significantly different deformation modulus the required accuracy of the modulus may be ± 100%. On the other hand, the deformation modulus of the rock surrounding a pressure conduit may have to be known within 25%. Obviously the sophistication of the testing technique required in these two cases would be quite different. Following this reasoning it is convenient to distinguish tests as reporting either index values or design values. An index value is one which is proportional to the true value and thus will reflect trends. A design value very nearly reflects the true behaviour of the tested medium.

Consider the deformation behaviour of a joint-rock mass system as the property which must be determined. Each of the three

testing techniques in this thesis can be evaluated according to the design value versus index value criteria.

1. Laboratory Testing

Since the rock discontinuities are lost in the sampling process laboratory testing provides only an index to the deformation behaviour of a joint-rock mass system. The test is valuable in that it conveniently determines an upper bound to the deformation modulus of a rock mass as was shown in Figure 50. Attempts have been made to improve the value of laboratory testing as an index test by correlating the modulus of the rock sample with indices related to the quality of the rock mass. Several indices for rock quality have been proposed:

1. The fracture frequency.
2. The Rock Quality Designation or RQD. The RQD is defined as the percent of the coring interval represented in the core box by sound, unweathered cylinders at least four inches in length. [Stagg and Zienkiewicz, 2]
3. The ratio of the *in situ* compressional wave velocity to that obtained from laboratory specimens.

Investigations into the possibility of correlating deformation modulus with rock quality indices have been carried out by Deere, Hendron, et al. [19], Onodera [20], and Coon and Merritt [21]. Although approximate relationships have been defined it is unlikely that a reliable method will be found to reduce the modulus of a laboratory sample to that of a joint-rock mass system using rock quality indices. The reason being that

these indices reflect the population of the rock discontinuities but not their deformation behaviour.

Finite element modelling of a joint-rock mass system can incorporate the deformation properties of the rock substance and joints separately. It is therefore conceivable that laboratory testing could provide data for the determination of design modulus values for a joint-rock mass system. At present there are two obstacles to this procedure:

1. A convenient sampling technique for obtaining rock samples including joints is needed. [Bukovansky, 3]
2. A simple method of determining joint deformation properties is required. [Bukovansky, 3]

In summary, laboratory testing provides an index to the deformation properties of a joint-rock mass system. This index can be improved by correlation with rock quality indices. In the future, laboratory testing coupled with finite element analysis may provide design modulus values.

2. Goodman Jack Testing

The results in this thesis illustrate two main points of the Goodman Jack testing technique:

1. The jack provides an extremely efficient method for obtaining a large amount of load-deformation data for an extensive number of *in situ* test locations.

2. The lack of rock type differentiation based on modulus probably reflects the need to utilize appropriate K values in the interpretive formula.

The supplementary testing programmes necessary to determine the appropriate K value for each test location would offset the efficiency of the method. Two alternative Goodman Jack techniques to provide index modulus values follow from this. Firstly, the testing can be carried out as for this thesis with no supplementary programmes and the results interpreted using the K value for an elastic medium or alternatively, a value appropriate for an "average" rock mass. As such the test would provide a rough index to the modulus of a joint-rock mass system. In the author's opinion a second more desirable method could be devised as follows:

1. Further finite element modelling of the jack as recommended by Heuze and Dessenne [18] should be carried out to investigate all rock parameters which can affect the K value.
2. Knowing the relevent parameters the K value could be correlated with one or more simple rock quality indices. These indices should be obtained from the NX core corresponding to the Goodman Jack test location. Suitable rock quality indices for correlation would be RQD and Point Load Strength. For an extensive description of the Point Load Strength Test see Broch and Franklin [22].

3. The appropriate K value for each Goodman Jack test location would be derived from correlations between K and the various rock indices.

The proposed test procedure would require theoretical verification as well as extensive field evaluation and if successful should improve the index modulus values reported by the Goodman Jack.

Recent finite element investigations by Heuze and Dessenne [18] indicate that in closely jointed rock the jack could also provide design modulus values. This application of the jack would require further theoretical investigation as well as consideration to practical ways of determining the additional test data, including *in situ* stress, joint spacing, rock strength and perhaps additional factors.

In order to further validate the design values reported by the jack and in view of the less than adequate tests reported by Tran [7] and by Heuze, et al. [23], this author would recommend a thorough laboratory study to confirm the theoretical investigations. This programme would utilize a large homogeneous, non-composite block of rock. Tests carried out in NX bore holes in the block would be compared to uniaxial or triaxial deformation tests carried out on large volume core samples from the same rock block. By utilizing special drill bits the effects of bore hole roughness and eccentricity could be studied. With specialized equipment external loads could be applied to the rock block to investigate the dependence of modulus on the loading direction-stress relationship. Obviously not all the *in situ* parameters could be duplicated in the laboratory but the ability to vary selected parameters should provide valuable information.

In summary, the results of this thesis have indicated that the Goodman Jack provides an excellent method of determining an index to the *in situ* deformation behaviour of a joint-rock mass system. With further research the jack should provide improved index modulus values and possibly design modulus values under specific site conditions.

3. Plate Loading Tests

The plate loading tests as carried out for this thesis are considered an index test. This is based on the fact that a less than ideal deformation measuring system was utilized and because the application of elasticity theory to the zone of blast damaged, and destressed rock surrounding the drift is unreliable. In the author's opinion plate loading tests should be utilized to provide design values rather than index modulus values. The reason being that the utilization of expensive and cumbersome plate loading tests to provide index modulus values is not economically justified when compared to rapid, inexpensive methods such as the Goodman Jack.

In order to obtain design modulus values from the plate loading tests additional costs would be incurred, however the additional expense would be warranted when compared to the total cost of the method. The following additional requirements would have to be met:

1. The linear dimension of the loaded area should be large compared to the spacing of discontinuities in the rock. [Stagg and Zienkiewicz, 2]

2. The stress levels created by the test should be comparable to those generated by the prototype loading. The compliance of the plate load tests to points 1 and 2 obviously restricts the structural geologic environments in which plate loading tests can be utilized to provide design modulus values.
3. Bore holes should be drilled under the bearing pads at each test location for two reasons. Firstly, logging the core of the bore holes would provide detailed structural geology beneath the bearing pads. Secondly, the holes could be instrumented with multiple position bore hole extensometers in order to relate deformation to geologic structure. (For a description of such a system see Benson, et al., 14].
4. As a check on the total deformation the distance between the bearing pads should be monitored using a rod type extensometer.
5. A finite element model should be used to investigate the effects of joint spacing, *in situ* stresses and rock strength and thus provide a valid interpretive formula for plate loading tests.

In summary, the performing of plate load tests to provide index modulus values is considered unwarranted in view of the potential of design values at slight additional expense.

CHAPTER VIII

CONCLUSION

The results of the three testing programmes are subdivided into three groupings in order to reach conclusions; anisotropy, elastic behaviour and deformation modulus.

Quantitative anisotropy results were provided by the laboratory and plate loading tests. Although the scale of these tests is quite different the degree of anisotropy was comparable for both methods. The Goodman Jack provided only an indication of anisotropic rock behaviour. It is concluded that each of the testing methods have inherent limitations for investigating the dependence of modulus on loading direction. Laboratory tests provide excellent directional properties of the rock substance but have limited application to the anisotropy of a joint-rock mass system. Plate loading tests are restricted in that anisotropy results can be modified by the drift excavation process as well as by the bearing pad preparation. Goodman Jack tests suffer from the fact that very detailed bore hole data is required in order to obtain quantitative anisotropy results.

The elastic behaviour of the rock as reflected by the three testing methods illustrated the scale effect. The elastic recovery for a complete test loading was directly proportional to the rock volume influenced by the test method. Also, since an unjointed rock mass behave much more elastically than a joint-rock mass system the elastic recoveries also reflect the rock quality of the test environment.

From the comparison of modulus values reported by the three testing methods it was shown that the results deviated from and conformed to the expected results. In explanation, several possible external factors such as joint spacing, *in situ* stress and validity of the interpretive formula were presented. It is therefore concluded that without defining, quantifying and incorporating the important test variables, a comparison between testing techniques can only be made in generalized terms. The index value versus design value classification is an example of a generalized comparison.

In summary, the Goodman Jack tests provide excellent index modulus values for a joint-rock mass system, laboratory tests, though convenient to perform, yield index values of restricted application and plate loading tests are most economically utilized as design value tests.

B I B L I O G R A P H Y

BIBLIOGRAPHY

1. KRUSE, G.H., Deformability of Rock Structures, California State Water Project, Determination of the *In Situ* Modulus of Deformation of Rock, ASTM STP 477, Am. Soc. Testing Mats., 1970.

2. STAGG, K.G. and ZIENKIEWICZ, O.C., Rock Mechanics in Engineering Practice, John Wiley and Sons, New York, 1968.

3. BUKOVANSKY, M., Determination of Elastic Properties of Rocks Using Various On-Site and Laboratory Methods, Proceedings of the Second Congress of the International Society for Rock Mechanics 1, Belgrade, Yugoslavia, 1970.

4. DALLY, J.W. and RILEY, W.F., Experimental Stress Analysis,McGraw Hill Book Co., 1965.

5. HARDY, H.R., Standardized Procedures for the Determination of the Physical Properties of Mine Rock under Short-Period Uniaxial Compression, Department of Mines and Technical Surveys, Ottawa, Mines Branch Technical Bulletin TB 8, 1959.

6. CLARK, G.B., Deformation Modulus of Rocks, Testing Techniques for Rock Mechanics, ASTM STP 402, Am. Soc. Testing Mats., 1965.

7. TRAN, V.K., *In Situ* Determination of Rock Deformability by Borehole Jack Tests, unpublished M.Sc. Thesis, University of California, Berkeley, 1967.

8. ZIENKIEWICZ, O.C. and STAGG, K.G., Cable Method of *In Situ* Rock Testing, International Journal of Rock Mechanics and Mining Sciences 4, 1967.

9. WALLACE, G.B., SLEBIR, E.J. and ANDERSON, F.A., *In Situ* Methods for Determining Deformation Modulus Used by the Bureau of Reclamation, Determination of the *In Situ* Modulus of Deformation of Rock, ASTM STP 477, Am. Soc. Testing Mats., 1970.

10. OBERT, L. and DUVALL, W.I., Rock Mechanics and the Design of Structures in Rock, John Wiley and Sons, New York, 1967.

11. HAWKES, I. and MELLOR, M., Uniaxial Testing in Rock Mechanics Laboratories, Engineering Geology, Vol. 4, 1970.

12. GOODMAN, R.E., TRAN, V.K. and HEUZE, F.E., The Measurement of Rock Deformability in Bore Holes, Proceedings of the Tenth Symposium on Rock Mechanics, AIME, 1968.

13. ROARK, F.J., Formulas for Stress and Strain, McGraw-Hill Book Company, Inc., 1954.

14. BENSON, R.P., MURPHY, D.K. and McCREATH, D.R., Modulus Testing of Rock at the Churchill Falls Underground Powerhouse, Labrador, Determination of the *In Situ* Modulus of Deformation of Rock, ASTM STP 477, Am. Soc. Testing Mats., 1970.

15. SMITHELLS, C.J., Metals Reference Book, Interscience Publishers, Inc., New York, 1955.

16. HAWKES, I., Moduli Measurements on Rock Cores, Proceedings of the First Congress of the International Society for Rock Mechanics, Lisbon, 1966.

17. GUTTMAN, I. and WILKS, S.S., Introductory Engineering Statistics, John Wiley and Sons, Inc., 1965.

18. HEUZE, F.E. and DESSENNE, D., The Influence of Joint Spacing, and the Effect of Rock Breakage, on Borehole Deformability Test Results, Report to U.S. Army Corps of Engineers, Omaha, Nebraska, 1972.

19. DEERE, D.U., HENDRON, A.J., Jr., PATTON, F.D., and CORDING, E.J., Design of Surface and Near-surface Construction in Rock, Proc. 8th Symposium on Rock Mech., AIME, 1966.

20. ONODERA, T.F., Dynamic Investigation of Foundation Rocks *In Situ*, Proceedings of the Fifth Symposium on Rock Mechanics, Minnesota, Pergamon Press, 1963.

21. COON, R.F. and MERRITT, A.H., Predicting *In Situ* Modulus of Deformation Using Rock Quality Indexes, Determination of the *In Situ* Modulus of Deformation of Rock, ASTM STP 477, Am. Soc. Testing Mats., 1970.

22. BROCH, E. and FRANKLIN, J.A., The Point-Load Strength Test, International Journal of Rock Mechanics and Mining Sciences, Vol. 9, No. 6, 1972.

23. HEUZE, F.E., OHNISHI, Y., and GOODMAN, R.E., Borehole Jack Deformability Measurements and Strength Testing of Selected Rocks from the Auburn Dam Site, Report to U.S. Army Corps of Engineers, Omaha, Nebraska, 1971.

APPENDICES

APPENDIX 1

ANALYSIS OF STRAIN GAUGE CIRCUIT

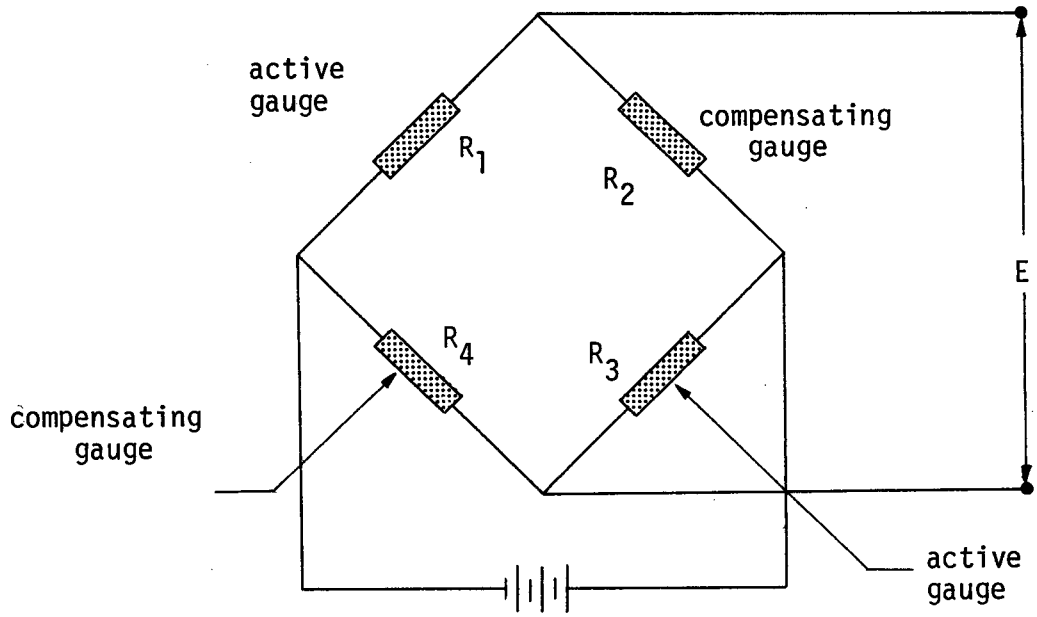

V = 1.5 volts R.M.S.

For the circuit configuration shown above Dally and Riley [4] have presented the following equation;

$$\Delta E = \frac{V\ r}{(1+r)^2}\left(\frac{\Delta R_1}{R_1} - \frac{\Delta R_2}{R_2} + \frac{\Delta R_3}{R_3} - \frac{\Delta R_4}{R_4}\right) \qquad \ldots .(1a)$$

where:

ΔE	voltage output from circuit
V	voltage applied to circuit
r	R_2/R_1
ΔR	resistance change of the strain gauges 1 through 4
R	initial resistance of strain gauges 1 through 4.

For the circuit above:

$$R_1 = R_2 = 120 \text{ ohms}, \quad \text{Therefore} \quad r = 1$$

When a strain is imposed on the test sample the resistance of the active gauges (R_1, R_3) will change while the compensating gauges (R_2,R_4) will show no change.

$$\text{Therefore} \quad \Delta R_2 = \Delta R_4 = 0$$

Therefore equation (1a) becomes:

$$\frac{\Delta E}{V} = \frac{1}{4}\left(\frac{\Delta R_1}{R_1} + \frac{\Delta R_3}{R_3}\right) \qquad \ldots . (2a)$$

Assuming $\Delta R_1 = \Delta R_3$ and $R_1 = R_3$ then (2a) becomes:

$$\frac{\Delta E}{V} = \frac{1}{2}\frac{\Delta R}{R} \qquad \ldots . (3a)$$

It is also known that:

$$\frac{\Delta R}{R} = (G.F.)\frac{\Delta \ell}{\ell} \quad \text{or} \quad \frac{\Delta R}{R} = (G.F.)\,\varepsilon \qquad \ldots . (4a)$$

where:

G.F. gauge factor

$\Delta \ell / \ell = \varepsilon$ = strain

Combining (4a) and (3a) yields:

$$\frac{\Delta E}{V} = \frac{1}{2}(G.F.)\,\varepsilon \qquad \text{or} \qquad \varepsilon = \frac{2}{(G.F.)}\left(\frac{\Delta E}{V}\right)$$

In other words, the full bridge circuit above indicates twice the correct strain values. The advantage of this circuit is that the sensitivity of strain measurement is increased by the factor of two.

APPENDIX 2

TIME STUDY OF LABORATORY TESTING PROGRAMME

	Operation	Time (min./sample)
1.	Cutting core with diamond saw	5
2.	Grinding core on surface grinder	
	2 1/2 hr./14 samples	11
3.	Measuring, weighing, logging	8
4.	Preparing sample for gauges	7
5.	Applying gauges, terminal tabs	10
6.	Soldering leads	10
7.	Testing continuity, coating with silicone rubber	2
8.	Deformation testing (2 cycles per sample)	50
	Total	103 min.
	(approximately 1 3/4 hr./sample)	

APPENDIX 3

RESULTS OF LABORATORY TESTS

APPENDIX 3A

QUARTZITE GNEISS (Values in psi x 10^6)

Sample Number	E_s 1st cycle	E_s 2nd cycle	E_w 1st cycle	E_w 2nd cycle	E_r 1st cycle	E_r 2nd cycle
N1	7.29	7.26	8.75	9.57	7.70	7.68
N4*	5.05	5.23	5.80	6.50	5.43	5.54
N5	7.63	7.60	10.3	9.47	6.94	
N6	7.70	7.64	8.97	9.63	8.22	8.23
N7	8.42	8.32	9.52	10.1	8.90	9.84
N8	6.45	7.09				
N9	5.48	5.60	6.86	7.53	5.83	6.11
N10	5.55	5.51	6.60	7.43	6.11	6.13
N11	6.69	6.93	8.28	9.09	7.10	7.37
N12	5.54	5.47	8.06	8.81	6.50	6.54
N13	7.08	7.03	8.98	9.56	7.59	7.58
N14	6.85	6.88	8.26	8.67	7.18	7.21
N15	6.22	8.19				
N16	6.32	6.24	7.39	8.21	7.01	6.97
N17	7.14	7.01	8.74	9.28	7.58	7.49
N18	6.82	6.76	8.09	8.63	7.14	7.11
N19	7.18	7.13	8.56	8.99	7.48	7.46
N22	6.02	5.99	7.13	7.79	6.46	6.48
N23	5.05	4.98	6.85	7.52	5.61	5.59
N26	4.61	4.58	6.77	7.25	4.94	4.95
N27	5.95	5.77	6.51	7.26	6.46	6.30
N38	5.61	5.71	7.10	7.79	6.15	6.28
N42	5.55	4.98	7.26	6.86	5.88	
N56	7.94	7.89	9.33	9.90	8.29	8.26
N57	6.26	6.21	7.19	8.03	6.71	6.70
N58	5.56	5.51	6.63	7.33	5.96	5.95

*Erroneous values due to faulty gauge.

APPENDIX 3A (continued)

Sample Number	E_s 1st cycle	E_s 2nd cycle	E_w 1st cycle	E_w 2nd cycle	E_r 1st cycle	E_r 2nd cycle
N66	6.49	6.42	7.61	8.23	6.92	6.93
N67	4.48	4.49	5.44	6.26	5.02	5.06
N74	7.33	7.28	8.17	8.79	7.67	7.63
N77	3.96		5.23			
N85	7.15	7.14	8.59	9.24	7.76	7.78
N93	5.89	5.74	7.79	8.22	6.26	6.14
N96	6.41	6.35	7.34	8.00	6.80	6.77
N	6.43	6.34	8.68	9.12	6.80	6.74
14	6.46	6.34	7.29	7.89	6.72	6.63
15	7.37	6.70	9.06	8.88	7.73	
16	5.86	6.12	6.95	7.82	6.27	6.55
24	8.42		9.56			
25	6.04	6.01	7.01	7.51	6.24	6.22
32*	3.57	3.47	4.42	5.22	3.99	3.94
33	7.09	7.02	8.05	8.79	7.56	7.53
39	7.64	7.60	8.68	9.35	7.92	7.91

*Erroneous values due to faulty gauge.

APPENDIX 3B

QUARTZ FELDSPAR SCHIST (Values in psi x 10^6)

(S = strike direction, D = dip direction)

Sample Number	E_s 1st cycle	E_s 2nd cycle	E_w 1st cycle	E_w 2nd cycle	E_r 1st cycle	E_r 2nd cycle
N40-S	1.04	1.04	2.27	2.69	1.14	1.17
N40-D	1.31	1.31	2.64	3.05	1.42	1.45
N44-S	2.97	2.96	2.81	3.36	3.38	3.38
N44-D	3.64	3.59	3.27	3.91	4.22	4.21
N52-S	1.09	1.09	2.71	3.19	1.34	1.37
N52-D	1.02	1.02	2.68	3.07	1.24	1.27
N54-S	0.99	1.00	2.42	2.87	1.22	1.25
N54-D	1.15	1.16	2.53	3.01	1.41	1.44
N55-S	1.52	1.49	3.20	3.68	1.91	1.91
N55-D	1.40	1.37	2.92	3.40	1.74	1.73
N61-S	2.62	2.60	2.42	3.33	3.23	3.21
N61-D	2.89	3.34	5.27	6.08	3.31	3.83
N69-S	2.04	2.04	4.03	4.42	2.38	2.40
N69-D	2.16	2.15	4.10	4.52	2.54	2.56
N70-S	10.5	10.5	9.61	11.5	12.1	12.1
N70-D	9.27	9.07	8.16	9.97	11.0	10.8
N71-S	3.41	3.36	3.15	4.01	4.08	4.07
N71-D	2.74	2.68	2.66	3.55	3.48	3.48
N75-S	1.57	1.43	1.83	2.57	2.08	1.96
N75-D	3.88	3.67	4.86	4.91	4.70	4.59
N79-S	7.36	7.26	7.24	8.56	8.38	8.34
N79-D	9.25	8.59	7.66	8.51	10.7	10.0
N89-S	1.44	1.41	1.79	2.15	1.66	1.64
N89-D	1.07	1.06	1.38	1.72	1.30	1.30
N91-S	8.27	8.20	7.09	9.03	9.94	9.86
N91-D	9.81	9.78	8.55	10.5	11.3	11.3

*Erroneous values due to faulty gauge.

APPENDIX 3B (continued)

Sample Number	E_s 1st cycle	E_s 2nd cycle	E_w 1st cycle	E_w 2nd cycle	E_r 1st cycle	E_r 2nd cycle
N99-S	2.71	2.70	4.02	4.39	2.93	2.93
N99-D	2.58	2.55	3.47	3.93	2.89	2.89
N100-S	1.19		2.46			
N100-D	0.86		1.78			
N101-S	1.72	1.72	2.94	3.11	1.86	1.87
N101-D	1.60	1.60	2.82	3.00	1.75	1.76
N102-S	1.25	1.24	2.55	2.77	1.38	1.39
N102-D	0.86	0.85	2.34	2.49	0.95	0.95
N103-S	0.92	0.90	2.67	2.98	1.07	1.07
N103-D	1.36	1.34	3.23	3.45	1.51	1.51
N201-S	0.92	0.81	0.74	1.32	1.27	1.20
N201-D*	1.55	1.56	4.61	4.24	2.11	2.36
N202-S	2.56	2.40	2.84	3.27	2.99	
N202-D	2.62	2.38	3.38	3.42	3.04	
N203-S	1.97	1.94	2.18	2.74	2.32	2.32
N203-D	4.18	4.09	3.66	4.12	4.60	4.50
N208-S	6.24	6.17	5.45	7.00	7.57	7.56
N208-D	8.49	8.29	7.38	9.92	10.9	10.8
N209-S	0.72	0.70	1.20	1.49	0.93	0.92
N209-D*	0.27	0.28	0.83	1.64	0.42	0.47

*Erroneous values due to faulty gauge.

APPENDIX 3C

PEGMATITE (Values in psi x 10^6)

Sample Number	E_s 1st cycle	E_s 2nd cycle	E_w 1st cycle	E_w 2nd cycle	E_r 1st cycle	E_r 2nd cycle
40*	8.45		12.7			
N20	4.39	4.30	5.01	5.91	4.73	4.64
N31	4.89	4.90	6.83	7.55	5.19	5.20
N33	4.32	4.26	5.76	7.09	4.87	4.88
N84	3.43	3.43	5.54	6.17	3.90	3.93
N92	2.43	2.42	3.88	4.64	2.91	2.94
Aluminum	10.4	10.4	10.4	10.4	10.4	10.4

*Premature failure, values disregarded.

APPENDIX 4

EXAMPLE OF STEREOGRAPHIC PROJECTION METHOD UTILIZED WITH THE GOODMAN JACK

The following data is used to illustrate the stereographic projection method for determining the spatial arrangement of loading directions and foliation planes:

1. Orientation of bore hole: strike 180 degrees, dip -4 degrees,
2. Angle between axis of core and foliation plane at the test location: 30 degrees,
3. Assumed strike of foliation at the test location: 025 degrees.

Referring to the stereonet below the data is processed in the following manner:

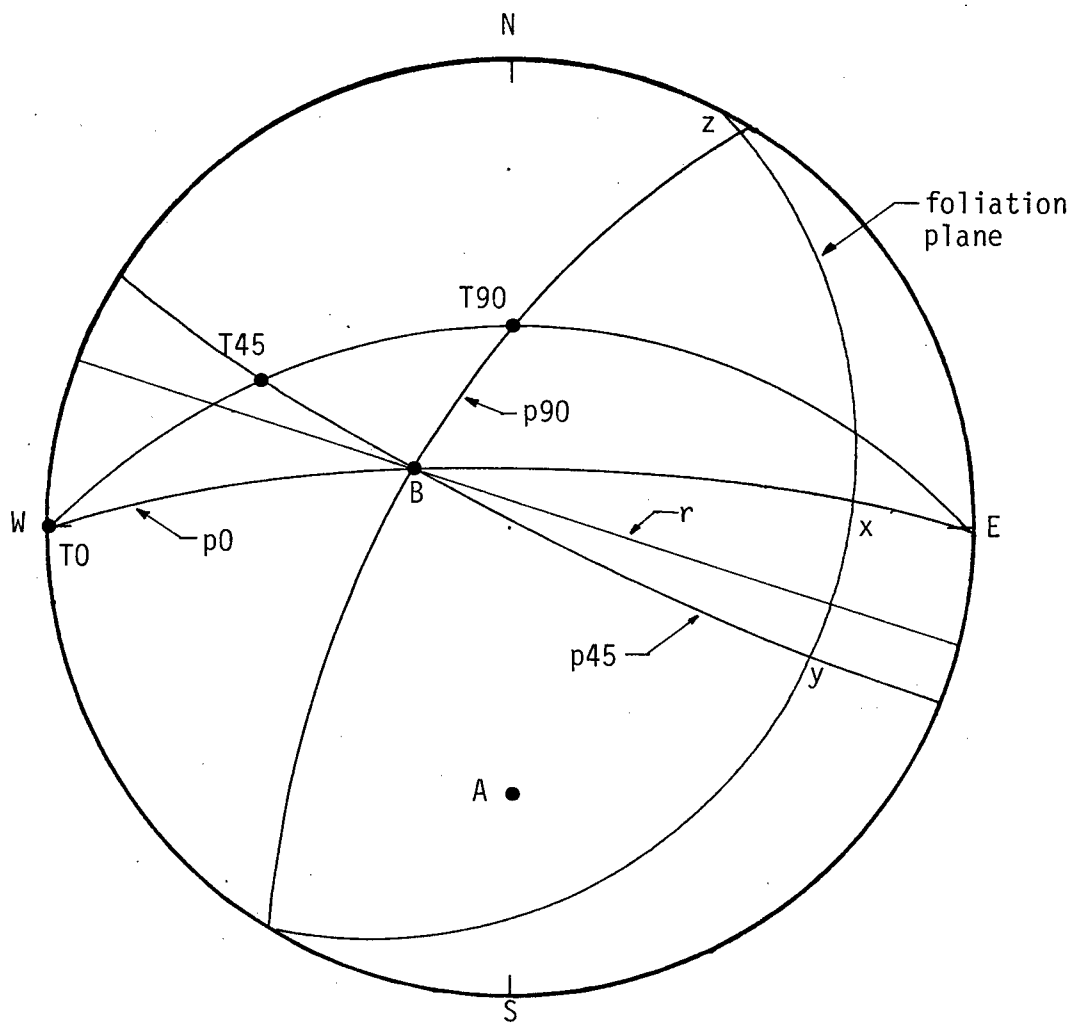

APPENDIX 4 (continued)

1. The hole is plotted, point A on the stereonet. This point represents not only the hole but also the pole to the plane containing the loading direction.
2. The strike of the foliation is then marked off. A plane perpendicular to this strike direction is plotted. (plane r) The pole to the foliation plane must be in plane r and is determined as follows. The known angle between the hole and the foliation is 30 degrees, thus the angle between the hole and the pole to the foliation is 60 degrees. The stereonet is thus rotated until the angle measured along a great circle between point A and the plane r is 60 degrees. The pole to the foliation is at this point. (point B)
3. The foliation plane is then plotted.
4. The plane perpendicular to the hole is plotted. By examining the orientation convention (see Figure 8) the loading directions for the three test orientations (0, 45, 90 degrees) are plotted within this plane. (See points T0, T45, T90 respectively).
5. The true angle between the foliation planes and particular loading direction can only be measured in the plane which is perpendicular to the foliation and also contains the loading direction. Also all planes perpendicular to the foliation plane must pass through the pole to that plane. Thus great circles are plotted through the pole and each loading direction. (See planes p0, p45, p90)
6. The desired angles are measured in the planes p0, p45, p90 from the loading direction to the point of intersection with the foliation plane. The results are as follows:

Test (Degrees)	Points Measured Between	Angle (Degrees)
0	T0 to x	22
45	T45 to y	56
90	T90 to z	55

7. In addition the inferred orientation of the foliation at the test location is 025 degrees strike with 23 degrees dip toward the southeast.

APPENDIX 5

GOODMAN JACK RESULTS

APPENDIX 5A

GOODMAN JACK RESULTS QUARTZITE GNEISS

(Modulus values in psi x 10^6)

Hole Number	Depth (ft.)	Orientation (Degrees)	E_s	E_w	E_r
NX-1	90	0	0.91	1.14	3.01
			0.84	2.13	2.92
		90	1.22	1.28	2.64
			1.17	2.17	2.57
		45	1.14	1.33	2.61
			1.07	2.03	2.30
NX-6	40	0	1.51	1.65	2.50
			1.46	2.18	2.43
			1.43	2.16	2.39
		90	1.33	1.46	2.26
			1.29	1.91	2.26
			1.27	1.97	2.26
		45	1.27	1.38	1.89
			1.23	1.64	1.85
			1.21	1.65	1.85
NX-6	55	0	2.07	2.30	3.74
			2.01	3.34	3.78
			2.00	3.59	4.07
		90	2.01	2.09	2.96
			1.96	2.52	2.93
			1.96	2.57	2.96
		45	2.00	2.03	3.16
			1.97	2.49	3.16
			1.95	2.74	3.10
NX-8	40	0	1.77	1.92	2.72
			1.76	2.38	2.79
			1.73	2.40	2.67
		90	1.78	1.92	2.90
			1.74	2.43	2.79
			1.72	2.40	2.75
		45	1.82	1.90	2.58
			1.79	2.24	2.58
			1.78	2.28	2.54
NX-8	50	0	1.74	1.89	2.61
			1.73	2.22	2.33
			1.76	2.05	2.69
		90	1.70	1.91	2.52
			1.68	2.28	2.43
			1.66	2.26	2.48

APPENDIX 5A (continued)

Hole Number	Depth (ft.)	Orientation (Degrees)	E_s	E_w	E_r
		45	1.90	1.94	2.55
			1.90	2.32	2.62
			1.88	2.30	2.60
NX-9	45	0	1.73	1.91	2.85
			1.68	2.39	2.78
			1.68	2.47	2.73
		90	1.87	2.14	2.73
			1.86	2.39	2.85
			1.84	2.47	2.58
		45	1.72	1.94	2.40
			1.65	2.07	2.50
			1.66	2.28	2.54
			1.65	2.26	2.46
NX-12	30	0	1.65	1.94	2.55
			1.61	2.32	2.52
			1.59	2.39	2.50
		90	2.00	2.28	3.07
			1.94	2.60	2.98
			1.94	2.60	3.01
		45	2.01	2.16	2.96
			1.96	2.49	2.83
			1.95	2.49	2.88
			1.80	2.42	2.76
NX-12	85	0	2.48	2.74	4.40
			2.39	3.70	4.34
			2.34	3.75	4.58
		90	2.02	2.30	3.01
			2.01	2.87	2.98
			1.98	2.90	3.16
		45	2.01	2.24	2.83
			1.98	2.65	2.76
			2.00	2.74	2.51
NX-12	95	0	1.76	2.24	3.35
			1.69	2.87	3.50
			1.68	3.09	3.42
		90	2.07	2.18	3.35
			1.97	2.74	3.13
			1.94	2.77	3.16
		45	1.69	2.03	3.29
			1.68	2.98	3.54
			1.66	3.25	3.58

APPENDIX 5A (continued)

Hole Number	Depth (ft.)	Orientation (Degrees)	E_s	E_w	E_r
NX-13	105	0	2.46	2.71	4.28
			2.32	3.59	4.12
			2.29	3.64	4.02
		90	1.40	1.60	2.20
			1.35	1.92	2.17
			1.34	1.97	2.17
		45	1.80	2.02	3.22
			1.72	2.71	2.94
			1.69	2.68	3.07

APPENDIX 5B

GOODMAN JACK RESULTS QUARTZ FELDSPAR SCHIST

(Modulus values in psi x 10^6)

Hole Number	Depth (ft.)	Orientation (Degrees)	E_s	E_w	E_r
NX-1	70	0	1.12	1.31	3.10
			1.06	2.41	
		90	1.13	1.36	2.30
			1.10	1.98	2.27
		45	1.00	1.34	3.14
			0.96	2.56	3.11
NX-2	50	0	1.33	1.55	2.09
			1.31	2.08	2.33
			1.20	2.04	2.92
		90	1.06	1.15	1.97
			1.03	1.59	1.98
			1.02	1.63	1.95
		45	1.50	1.65	2.01
			1.48	1.89	2.00
			1.46	1.89	1.92
NX-2	55	0	1.30	1.51	2.08
			1.27	1.92	1.97
			1.27	1.94	2.00
		90	1.10	1.24	1.91
			1.08	1.71	1.95
			1.06	1.74	1.93
		45	1.21	1.40	2.04
			1.17	1.69	1.92
			1.17	1.57	2.00
NX-2	75	0	1.24	1.20	2.17
			1.21	1.70	2.32
			1.19	1.87	2.31
		90	1.08	1.19	2.19
			1.03	1.72	2.16
		45	1.10	1.17	1.72
			1.09	1.56	1.67
			1.08	1.51	1.80
NX-2	80	0	1.71	1.83	2.01
			1.70	1.92	2.12
		90	1.07	1.26	1.76
		45	1.27	1.37	2.01
			1.25	1.66	1.98
			1.24	1.69	2.01

APPENDIX 5B (continued)

Hole Number	Depth (ft.)	Orientation (Degrees)	E_s	E_w	E_r
NX-3	70	0	1.13	1.31	2.32
			0.83	1.55	2.22
		90	0.62	0.68	1.50
			0.48	0.93	1.45
			0.39	0.93	1.47
		45	0.75	0.75	1.44
			0.55	0.87	1.37
NX-3	100	0	1.28	1.35	1.83
			1.23	1.67	1.80
		90	0.86	0.98	2.37
			0.71	1.52	2.37
		45	1.05	1.27	2.16
			0.89	1.72	2.15
NX-4	45	0	1.55	1.73	3.08
			1.49	2.65	3.02
			1.45	2.52	2.87
		90	1.30	1.39	2.36
			1.27	1.98	2.30
			1.25	1.98	2.34
		45	1.36	1.49	2.38
			1.32	2.04	2.34
			1.31	2.08	2.36
NX-4	50	0	1.58	1.60	2.88
			1.51	2.33	2.85
			1.49	2.43	2.70
		90	1.95	1.88	3.24
			1.89	2.70	3.32
			1.88	2.83	3.40
		45	1.33	1.48	2.50
			1.29	2.06	2.57
			1.27	2.13	2.62
NX-4	60	0	1.32	1.73	2.38
			1.24	2.16	2.28
			1.23	2.23	2.15
		90	1.13	1.39	2.19
			1.07	2.03	2.15
			1.04	2.03	2.16
		45	1.62	1.75	2.44
			1.55	2.15	2.40
			1.53	2.20	2.39

APPENDIX 5B (continued)

Hole Number	Depth (ft.)	Orientation (Degrees)	E_s	E_w	E_r
NX-5	30	0	1.33	1.45	1.98
			1.06	1.59	1.98
			0.87	1.58	1.96
		90	1.54	1.67	2.03
			1.30	1.77	2.14
			1.07	1.76	2.09
		45	1.49	1.65	2.02
			1.34	1.75	2.03
			1.13	1.75	2.06
NX-5	60	0	1.07	1.17	1.81
			1.03	1.44	1.71
			1.01	1.45	1.70
		90	1.08	1.13	1.36
			1.05	1.35	1.60
			1.03	1.39	1.56
		45	1.13	1.20	1.78
			1.11	1.55	1.78
			1.10	1.56	1.75
NX-5	78	0	1.42	1.43	1.77
			1.40	1.63	1.91
		90	1.38	1.45	1.93
			1.34	1.75	1.92
			1.33	1.79	1.89
		45	1.22	1.25	1.87
			1.19	1.61	1.84
			1.18	1.62	1.85
NX-8	60	0	1.58	1.68	2.57
			1.50	2.02	2.93
			1.48	2.48	2.79
			1.46	2.43	2.72
		90	1.46	1.61	2.56
			1.41	2.11	2.47
			1.38	2.11	2.42
		45	1.54	1.66	2.69
			1.51	2.24	2.63
			1.49	2.26	2.67
NX-11	30	0	1.20	1.40	2.11
			1.15	1.76	2.10
			1.14	1.76	2.13

APPENDIX 5B (continued)

Hole Number	Depth (ft.)	Orientation (Degrees)	E_s	E_w	E_r
		90	0.78	0.89	1.35
			0.76	1.25	1.38
			0.75	1.30	1.23
		45	0.91	1.12	1.51
			0.89	1.48	1.51
			0.88	1.52	1.50
NX-13	70	0	1.20	1.35	2.19
			1.17	1.97	2.19
			1.15	2.04	2.26
		90	1.46	1.97	2.56
			1.40	2.42	2.38
			1.38	2.56	2.36
		45	1.17	1.46	1.87
			1.15	1.68	2.50
			1.14	2.30	2.58
			1.14	2.38	2.58
NX-13	80	0	1.17	1.49	1.59
			1.15	1.80	1.66
			1.15	1.83	1.66
		90	2.56	2.53	3.31
			2.56	3.16	3.70
			2.52	3.34	3.49
		45	2.18	2.11	3.04
			2.15	2.53	3.04
			2.12	2.48	2.98
NX-14	60	0	0.70	1.13	2.58
			0.68	2.62	2.72
			0.68	2.95	3.10
		90	1.76	1.75	2.56
			1.73	2.22	2.60
			1.72	2.26	2.60
		45	1.34	1.62	2.33
			1.31	2.19	2.44
			1.30	2.33	2.42
NX-14	90	0	1.36	1.55	2.17
			1.31	1.85	2.17
			1.28	1.85	1.57
			1.30	1.77	2.21

APPENDIX 5B (continued)

Hole Number	Depth (ft.)	Orientation (Degrees)	E_s	E_w	E_r
		90	1.78	1.85	2.62
			1.73	2.22	2.60
			1.70	2.22	2.58
		45	1.40	1.73	2.20
			1.37	1.97	2.26
			2.85	2.03	3.31
NX-15	48	0	1.65	2.00	2.99
			1.55	2.66	2.86
		90	1.17	1.50	2.41
			1.14	2.15	2.22
		45	1.26	1.53	2.31
			1.21	2.02	2.24

APPENDIX 5C

GOODMAN JACK RESULTS PEGMATITE

(Modulus values in psi x 10^6)

Hole Number	Depth (ft.)	Orientation (Degrees)	E_s	E_w	E_r
NX-5	45	0	1.45	1.61	2.00
			1.43	1.83	2.01
			1.40	1.79	2.18
		90	1.76	1.88	2.32
			1.72	2.09	2.28
			1.65	2.09	2.29
		45	1.57	1.76	2.43
			1.56	2.09	2.50
			1.56	2.09	2.48
NX-7	30	0	0.84	0.90	1.52
			0.82	1.32	1.52
			0.85	1.50	1.70
		90	1.53	1.48	3.02
			1.46	2.40	2.92
			1.43	2.48	2.95
		45	1.04	1.03	2.12
			1.02	1.71	2.28
			1.03	1.89	2.33
NX-10	30	0	1.30	1.37	2.20
			1.23	1.49	2.05
			1.22	1.76	2.10
		90	1.60	1.53	2.56
			1.55	1.97	2.45
			1.52	1.97	2.48
		45	1.89	1.73	2.53
			1.85	2.16	2.57
			1.86	2.22	2.60
NX-15	60	0	1.56	1.71	3.29
			1.50	2.80	3.13
		90	1.45	1.97	2.55
			1.39	2.41	2.44
		45	1.42	1.81	2.48
			1.37	2.41	2.39